



University of
Strathclyde



swiss
space center

Website : iglunastrath.com

IGLUNA (Habitat in Ice) - Group Q

Final Report

Abstract :

Members:
Laetitia Petit (Sem I)
Jacob Kent
Jonathon Marshall
Pedro Corujo
Sarah Davidson

This project is delivered as part of an initiative proposed by the Swiss Space Centre (SSC) and European Space Agency (ESA), in order to develop technologies to sustain life in extreme conditions and beyond earth. Working as part of a larger team the members of this group made significant contributions across all areas. The proposed method of power generation was a solar array, where three varying solar tracking prototypes were designed and manufactured. Within the area of power harvesting, research and designs for piezo and triboelectric energy production has been completed along with simulations and analysis. An electrolyser has been designed and constructed as part of a larger hydrogen fuel cell storage solution. Finally, research has been conducted into the physical considerations involved in the implement of a power distribution system and recommendations have been presented.

Table of Contents

Cover Page	i
List of Tables and Figures.....	vi
List of Units and Nomenclature	viii
Units.....	viii
Nomenclature	ix
1. Introduction	1
2. Project Background.....	2
3. Technical Review.....	5
3.1. Distribution	5
3.1.1. Moon conditions.....	5
3.1.2. Terrestrial Power Distribution	10
3.1.3. DC Transmission.....	10
3.1.4. Wireless Power Transmission	10
3.1.5. Conductors.....	11
3.1.6. Insulators.....	12
3.1.7. System Hierarchy	12
3.1.8. Other areas of research	13
3.2. Generation	13
3.2.1. Generation Background	13
3.2.2. Helium-3.....	14
3.2.3. Solar Power Generation.....	14
3.2.4. Concentrated Solar Power	14
3.2.5. Passive Solar Energy.....	14
3.2.6. Photovoltaic Cells.....	15
3.2.7. Solar Tracking.....	15
3.2.8. Illumination Conditions at the Lunar South Pole	16
3.2.9. Single Axis Solar Tracker	18
3.2.10. Dual Axis Solar Tracker.....	18
3.3. Harvesting	18
3.3.1. Background	18
3.3.2. Literature Research.....	20
3.4. Storage	21

3.4.1. Literature Review	21
3.4.2. Pumped Hydro	22
3.4.3. Compressed Air Energy Storage.....	24
3.4.4. Flywheel	24
3.4.5. Supercapacitors.....	25
3.4.6. Batteries.....	25
3.4.7. Fuel Cells	27
4. Methodology.....	29
4.1. Distribution	29
4.2. Generation	31
4.2.1. Technical aims:.....	31
4.2.2. Concept 1: Stationary Solar Tracker.....	31
4.2.3. Concept 1: Construction	31
4.2.4. Concept 2: Single Axis Solar Tracker	33
4.2.5. Concept 2: Construction	34
4.2.6. Concept 2: Mechanism of Movement	34
4.2.7. Concept 2: Tracking Mechanism.....	35
4.2.8. Concept 3: Dual Axis Solar Tracking Farm.....	36
4.2.9. Concept 3: Construction	36
4.2.10. Concept 3: Mechanism of Movement	37
4.2.11. Concept 3: Tacking Mechanism	38
4.3. Harvesting	39
4.3.1 Arch-Shaped Generator	40
4.3.2. Cantilever Generator	46
4.4. Storage	48
4.4.1. Concept Generation.....	48
4.4.2. Construction.....	49
5. Results.....	53
5.1. Distribution	53
5.2. Generation	54
5.2.1. Concept 1	54
5.2.2. Concept 2	55
5.2.3. Lunar Solar Generation Estimate	56

5.2.4. Concept 3	59
5.3. Harvesting	60
5.3.1. Arch-Shaped Generator	60
5.3.2. Cantilever Generator	63
5.4. Storage	65
6. Discussion.....	66
6.1. Distribution	66
6.1.1. System Hierarchy and Power Calculations.....	66
6.1.2. Distribution system	66
6.1.3. Material choices.....	68
6.1.4. Future materials.....	70
6.1.5. Lunar Surface Positioning and cable length.....	71
6.2. Generation	72
6.3. Harvesting	73
6.4. Storage	75
6.4.1. Selection of Solution	75
6.4.2. Reflections.....	77
7. Project Management	80
7.1. Sub-Team Formation and Structure	80
7.1.1. Overview	80
7.1.2. Reflection	80
7.2. Communication.....	81
7.2.1. Overview	82
7.2.2. Reflection	82
7.3. Time management.....	83
7.3.1. Overview	83
7.3.2. Reflection	84
7.4. Financial Management.....	84
7.4.1. Overview	84
7.4.2. Reflection	84
7.5. Statement of Work Review	85
7.6. Final Reflection.....	85
8. Team Work.....	87

8.1. Overview	87
8.2. Departmental Team Dynamic	87
8.2.1. Overview	87
8.2.2. Reflection	87
8.3. Project Focus	88
8.3.1. Overview	88
8.3.2. Reflections	88
8.4. Communications	88
8.4.1. Overview	88
8.4.2. Reflection	89
8.5. Information Sharing	90
8.5.1. Overview	90
8.5.2. Reflection	90
8.6. Website	90
8.6.1. Overview	90
8.6.2. Reflection	91
8.7. Final Reflection	91
9. Conclusion	92
9.1. Distribution	92
9.2. Generation	92
9.3. Harvesting	93
9.4. Storage	94
9.5. Overall Project Conclusion	95
References	96
Appendix	102
Appendix 1: Arch-shaped and cantilever generators details	102
Appendix 2: Electrolyser Bill of Materials	104
Appendix 3: Arch-shaped generator output graphs	105
Appendix 4: Cantilever generator output graphs	106
Appendix 5: Electrolyser Drawings	107
Appendix 6: Prioritisation of IGLUNA Project Systems	108
Appendix 7: Statement of Work	110

List of Tables and Figures

Figure 1 - Project Team Structure	3
Figure 2: Elevation map of lunar south pole with names of various craters, [1]. Scale ranges from -8 to 8km.	5
Figure 3: Mosaic of lunar south pole, with relevant visible craters labelled, [6]; a – Shackleton; b – Sverdrup; c – Haworth; d – Shoemaker; e – Faustini.....	6
Figure 4: Permanently shadowed regions of the lunar south pole, [5]; a – Shackleton; b – Sverdrup; c – Haworth; d – Shoemaker; e – Faustini; f – Cabeus.....	6
Figure 5: Time-weighted lunar south pole illumination map, [8].	7
Figure 6: Severity of slopes at the lunar south pole up to 75 degrees south, [10].....	8
Figure 7: Percentage illumination of the lunar south pole on one day in the considered lunar seasons, in 2020.....	8
Figure 8: Lunar surface temperatures, [11]; Top left – daytime bolometric brightness temperatures; top right – night time bolometric brightness temperatures; bottom left – model-calculated annual average surface temperatures; bottom right – model-calculated depths at which ice lost by sublimation is below 2kgm^{-2} per billion years. The outer circle represents 80 degrees south latitude.	9
Figure 9: System diagram of a magnetic resonance wireless power transfer mechanism, [17].	11
Figure 10: Abrasion resistance test rig, an example of the procedures carried out to ensure cables are safe for utilisation in extra-terrestrial applications.	12
Figure 11: Cosine relation with incident solar radiation, [70]	16
Figure 12: Horizon mask with lunar topographic azimuth and elevation coordinates, showing annual solar movement from the Shackleton crater, [41]	17
Figure 13: Solar exposure distribution pattern showing Selenographic latitude and longitude ($^{\circ}$), [41].	17
Figure 14: Single axis solar trackers, horizontal axis (left) vertical axis azimuth (right), [42].	18
Figure 15: Dual axis solar tracker, [42]	18
Figure 16: Electric charges displacement [67]	20
Figure 17: Piezoelectric sensor [68]	20
Figure 18: Arch-shaped generator layers.....	21
Figure 19: Pumped Hydro Diagram [71]	23
Figure 20 : CAES Diagram [72]	24
Figure 21 - Concept 1 design render	31
Figure 22: Concept 1 part 1 render (left) prototype (right)	32
Figure 23: Concept 1 part 2, render (left) prototype (right)	32
Figure 24: Concept 1 part 3 render (top) prototype (bottom)	33
Figure 25: Concept 1, part 4.....	33
Figure 26 - Concept 2 design render.....	33
Figure 27: small outward gear (pinion) within inward facing gear (left) and small gear attached to motor (right)	34
Figure 28: Motor attached to the base plate of the structure	35
Figure 29: Oppositely facing solar panels (left) wiring connecting panels to motor in reverse polarity (right)	35

Figure 30: Concept 2 full structure facing the direction of maximal power output for the horizontal axis	36
Figure 31: Render of concept 3	37
Figure 33: Micro servo's attached to device 1 (sensory device).....	37
Figure 32: Underside of base part with vertical facing Arduino motors connected.....	37
Figure 34: 4 LDR'S separated by dividers.....	38
Figure 35: Arch-shaped generator	40
Figure 36: FEA geometry.....	41
Figure 37: Supports and load setup	42
Figure 38: Piezoelectric equations	43
Figure 39: <i>Piezoelectric references</i> [56]	44
Figure 40: Electric displacement [56].....	44
Figure 41: Simplified electric displacement, [56].....	45
Figure 42: Node calculations.....	46
Figure 43: Cantilever generator	46
Figure 44: Cantilever load	47
Figure 45: Cantilever harmonic analysis	48
Figure 46 : Single Cylinder Concept Sketches	49
Figure 47: Electrolyser Lid.....	50
Figure 48: Electrolyser Flange.....	51
Figure 49: Finished Electrolyser	52
Figure 50: Concept 1 3D printed prototype.....	54
Figure 51: Concept 1, all parts including additional components (mirrors).	54
Figure 52: Effect of mirrors inclined at varying degrees from perpendicular on output (V).....	55
Figure 53: Mirrors set perpendicular, 20° and 40° to the solar panel	55
Figure 54: Concept 2 Laser cut prototype.....	56
Figure 55: Concept 3 Dual axis solar tracking farm.....	59
Figure 56: Concept visualisation of a dual axis solar farm on the lunar surface	60
Figure 57: Bending polarisation, [64].....	61
Figure 58: Piezoelectric global charge	61
Figure 59: Arch-shaped mesh	62
Figure 60: <i>Relative permittivity</i> , [57]	62
Figure 61 : Electrolyser CAD Render	65
Figure 62: Potential layout for an early stage moon base, [3].....	67
Figure 63: Image of electrical resistivity and search regions of interest, [18].....	68
Figure 64: Insulator region of interest, [18].....	68
Figure 65: Conductor region of interest, [18].	69
Figure 66: Electrical resistivity against density, showing pareto front trade-off between the two, [18].....	70
Figure 67: Time-weighted lunar south pole illumination map showing regions of interest, [8].	71
Figure 68: Failed Connection Piece Housing.....	78
Figure 69: Steel Plate Supports.....	79
Figure 70 : Communication Structure	82

List of Units and Nomenclature

Units

Symbol	Name	Quality
A	Ampere	Current
mA	miliampere	Current
°C	Centigrade	Temperature
C	Coulomb	Electric charge
°	degree	Angle amplitude
F	Farad	Capacitance
g	gram	mass
kg	kilogram	mass
h	hour	Time
Hz	Hertz	Frequency
J	Joule	Energy
kJ	kilojoule	Energy
mJ	milijoule	Energy
K	Kelvin	Temperature
m	meter	Distance
km	kilometre	Distance
mm	millimetre	Distance
Km ²	Square meter	Surface
N	Newton	Force
Ω	Ohms	Resistance
μΩ	microohms	Resistance
Pa	Pascal	Pressure
W	Watt	Power
GW	Gigawatt	Power
MW	megawatt	power

Nomenclature

Symbol	Name	Unit
C_p	Capacitance	F
E	Energy Output	kWh/year
ε	permittivity	C^2 / Nm^2
H	Irradiance	W/m^2
i	Misalignment angle	°
PEG	Piezoelectric Generator	
PTEG	Piezo/triboelectric generator	
£	pound	
PR	Performance Ratio	
q	Electric charge	C
r	Conversion efficiency	
r_e	Electrical resistivity	Ωm
ref	Refined mesh	
t	time	seconds
TEG	Triboelectric generator	

1. Introduction

This Project is a European project proposed by the European Space Agency (ESA) and the Swiss Space Centre (SSC) where twenty student teams from nine different countries in Europe work together with the aim of designing a complete and functional human habitat on the Moon called IGLUNA. Inside this framework, the team formed by the University of Strathclyde has the role of designing a power system to provide power to the habitat. The power system should accommodate power generation, distribution, storage, harvesting and control; assuring the power required by the base and their inhabitants in extreme conditions as well as the experiments conducted inside of it and during explorations. One of the main difficulties that the habitat has is the availability of sunlight; the base will be placed in the south pole of the moon, where long dark periods are expected mainly produced by an eclipse. The teams aim to develop and produce scaled prototypes and models to demonstrate the viability of the designs as well as their implementation along with other teams' designs that could be interacting with them. A field demonstration involving all project teams will take place in the month of June. As said, the scope of the project encompasses the design of a full power system, capable of meeting the energy demand of the moon base and other teams' experiments. As well as the deadlines imposed by the University of Strathclyde, the team will adhere to the requirements and deadlines of the ESA, allowing them to track the progress of the project, fulfilling a midterm review (16/01/2019) and the field demonstration (17/06/2019) [1].

2. Project Background

IGLUNA is a collaborative project, in which participating teams aim to develop technologies to sustain life in extreme conditions, as well as conduct space-based experimentation. The moon base to be designed in the IGLUNA project is to be located at the lunar South Pole, in one of the six craters located there, under the surface in lava tubes. The Moon is a natural satellite of Earth, accomplishing its orbit in 30 days. The moon is the most accessible place for scientific expeditions with a relatively short travel distance, but it is not a welcoming place. Gases are tenuously held to the moon surface; however, the atmosphere can effectively be considered non-existent. The moon's surface is also unprotected from meteorite impacts and incident solar radiation. Due to the lack of liquid water and extreme temperatures, life as it is on Earth is impossible on the moon. At the chosen location, there should be water ice accessible which is essential for life and could also be a source of fuel and oxygen. A subsurface base provides protection from radiation and micrometeorites, and a more stable temperature compared with the surface. It could also permit a synergy between mining and building, [1].

The project is developed by a group formed by twelve fourth-and fifth-year students from Mechanical and Aerospace Engineering (MAE) and Electrical and Mechanical Engineering (EME) departments (Figure 1). Within this main group, a smaller sub-group of MAE students (four annual students and a midterm student) will produce a specific internal project, where the goals, achievements and working structure will be discussed further within the project management and team work sections.

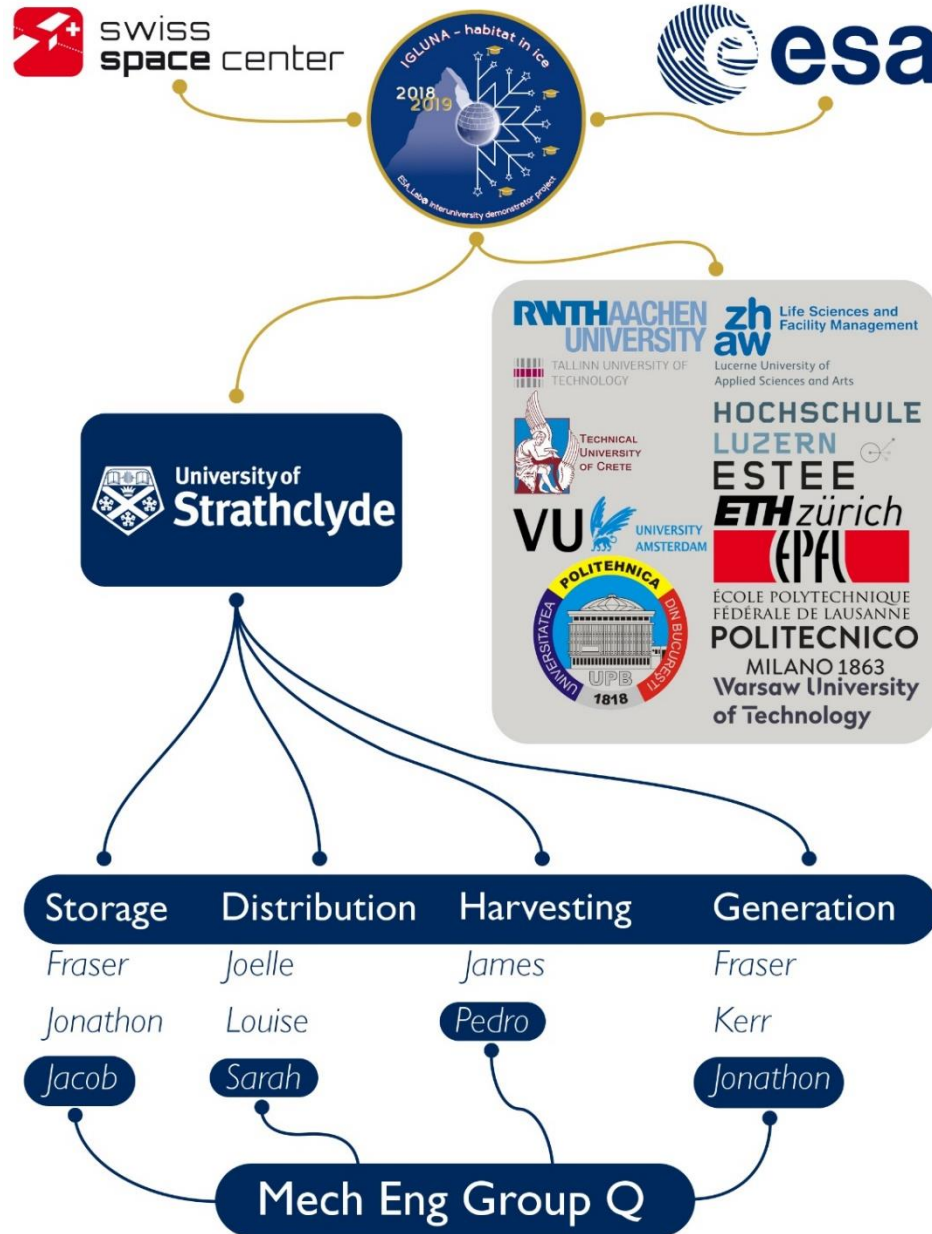


Figure 1 - Project Team Structure

Due to the extreme conditions previously described, all the technology designed and developed should be compatible with the environment it would face when working on the moon base. The main challenges affecting the power systems are the low

temperatures, the long darkness periods, the topography of the lunar surface and the low gravity. These facts reduce the range of possible technologies selected to solve the generation, distribution, storage, harvesting and control of power. The lunar environment is not the only complication; solutions for each system sub-section must be reached in agreement, as each project will have some effect on the others.

Following the improvement of green technologies, the problems faced in each aspect of the project can be based on clean technologies. This decision has three main advantages:

- The use of renewable energies is not dependent on the availability of a fuel to power the energy systems that in most cases will be exhausted in coming years.
- Non-renewable energies will need either the transportation of fuels from the Earth to power the plants located in the moon or began the moon mining and exploitation of the moon. Renewable energies could be powered by means of resources available on the moon.
- Finally, non-renewable energies will obviously lead to moon contamination.

With these ideas in mind, the technologies chosen by this group (thoroughly explained in this report) are solar energy as generation source, hydrogen fuel cells for energy storing and a piezo and triboelectric generator to harvest energy. This selection (as mentioned before) is inter-dependent; the solar energy would not be available at all time, nor at solar eclipse periods, so a high capacity energy storage system is needed. This need is fulfilled by the hydrogen fuel cells, able to provide energy to the moon base. The energy harvesters will take advantage of wasted energy, minimizing the energy needs when solar panels are not available.

3. Technical Review

3.1. Distribution

3.1.1. Moon conditions

The surface of the moon could be described loosely as maintaining an atmosphere; strictly speaking, these are drifting atoms held by the moon's gravity, [2]. For general engineering purposes it can be considered a vacuum. The lunar regolith, dust covering the solid rock beneath the surface, has very low electrical conductivity meaning that dust particles retain charge for a long period, [3].

The region of interest is the southern pole of the moon, as mentioned. This is the region most likely to contain high volumes of water because of the permanently shadowed regions (PSR) of the southern craters. The craters of interest are Cabeus, Haworth, Shoemaker, Faustini, Shackleton, and Sverdrup, [1]. Shackleton crater is approximately 21km in diameter, [4].

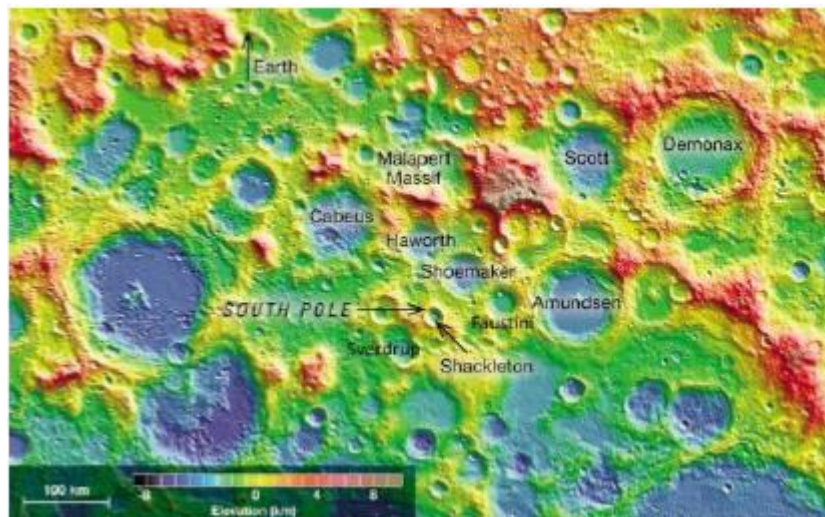


Figure 2: Elevation map of lunar south pole with names of various craters, [1]. Scale ranges from -8 to 8km.

It is clear from Figure 2 that there are regions of significant elevation (red) surrounding the depressions (blue/purple).

A more focussed view of the southern pole is given in Figure 4, Figure 3, and Figure 5. These images were captured by NASA's Lunar Reconnaissance Orbiter (LRO).

Figure 4 shows the permanently shadowed regions, with appropriate labels for the crater basins, [5].

Figure 3 is a high definition mosaic of the south pole, again with appropriate labels, [6]. In the original image, one pixel represents 1m, [6]. It can be seen from this image the severe effects of shadowing due to the low sun. The sun will be close to the horizon throughout the year, [7].

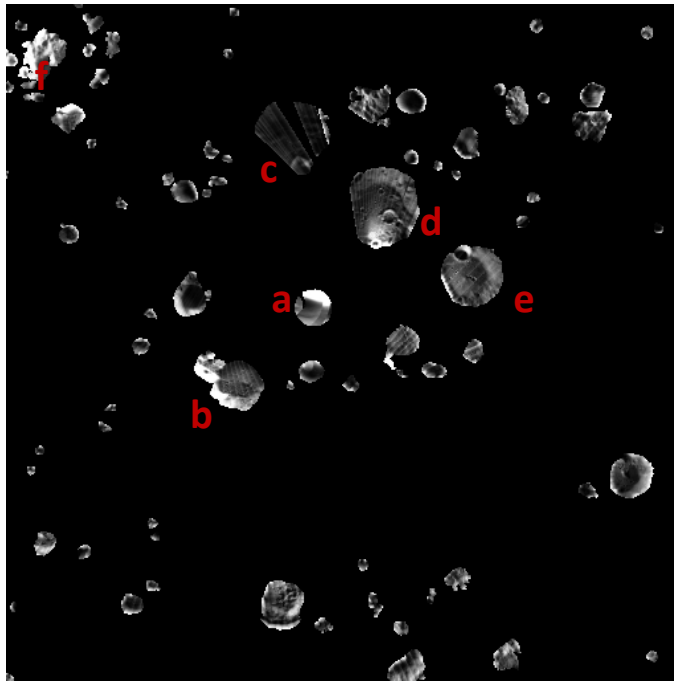


Figure 4: Permanently shadowed regions of the lunar south pole, [5]; a – Shackleton; b – Sverdrup; c – Haworth; d – Shoemaker; e – Faustini; f – Cabeus.

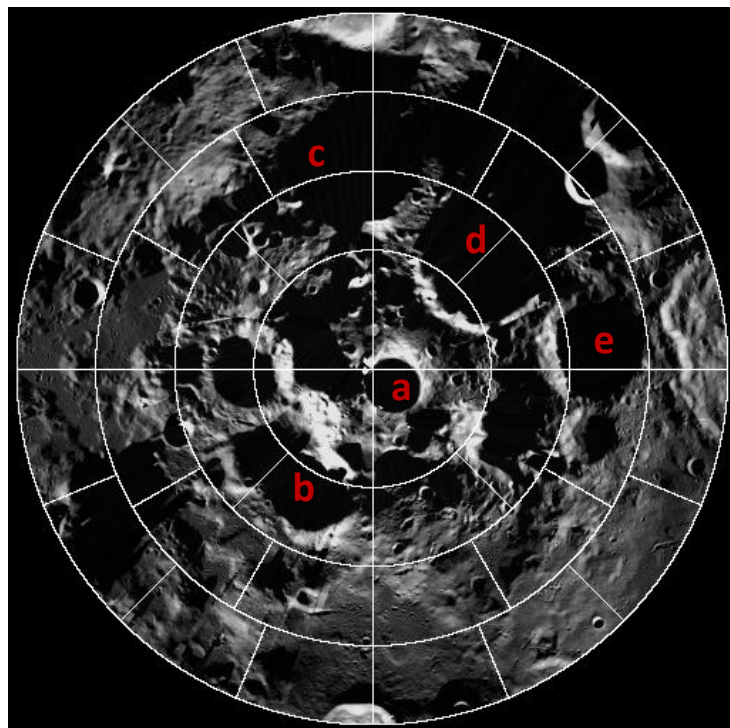


Figure 3: Mosaic of lunar south pole, with relevant visible craters labelled, [6]; a – Shackleton; b – Sverdrup; c – Haworth; d – Shoemaker; e – Faustini.

Figure 5 shows the time-weighted illumination of the pole around the Shackleton crater, a crucial consideration for solar panel positioning, [8]. The moon takes 30 days to rotate upon its axis fully, [7]. The South Pole will experience prolonged periods of sunlight and darkness.

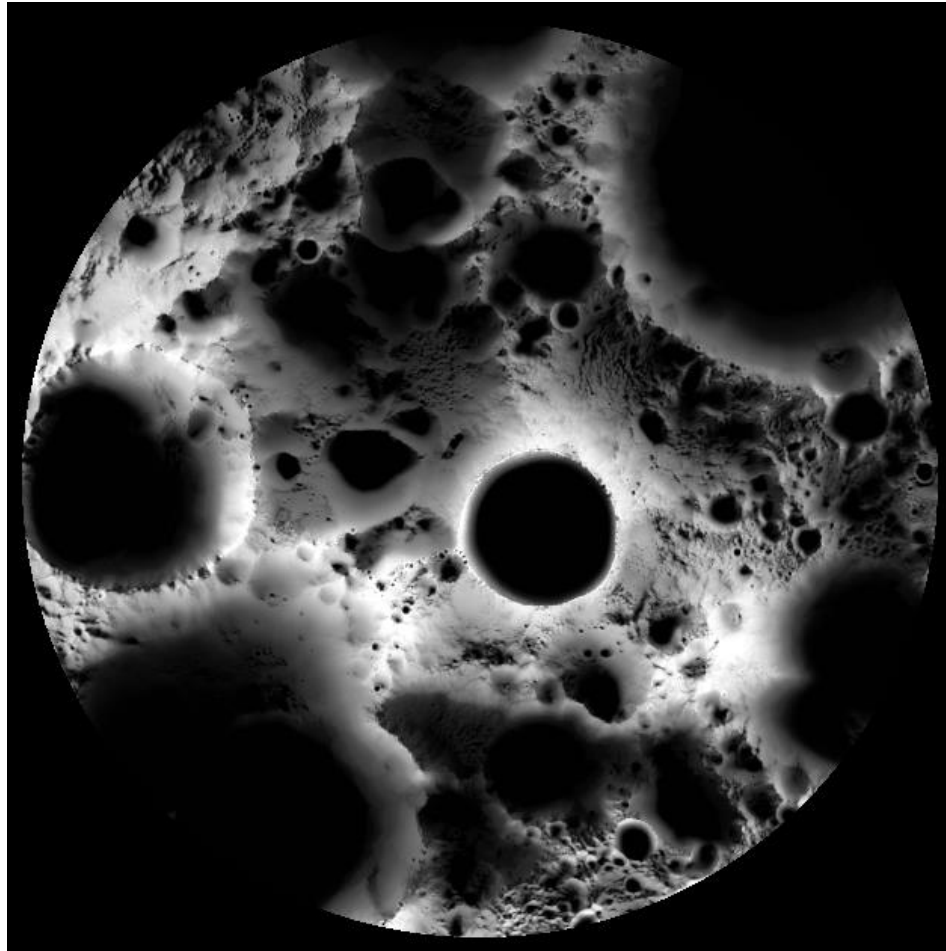


Figure 5: Time-weighted lunar south pole illumination map, [8].

Figure 7 shows the predicted illumination of the south pole during lunar summer, autumn and winter in 2020, [9]. The study predicted lighting conditions based on available topography data collected from the region by the Japanese SELENE lunar orbiter. It was predicted that an area on the rim of the Shackleton crater would receive light for 86% of the year in 2020.

Figure 6 shows the severity of surface gradients at the south pole of the moon. The image was captured using the Lunar Orbiter Laser Altimeter (LOLA) aboard the LRO, [10]. The steepest slopes are shown in red and white, at 25 degrees or above. Green represents slopes between 10 and 20 degrees approximately. The flattest terrain is shown in blue, with a slope of 5 degrees or less.

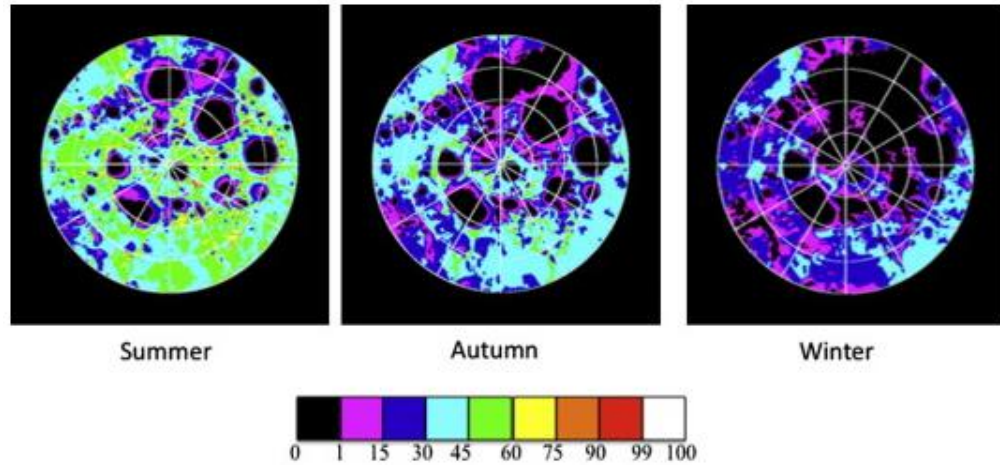


Figure 7: Percentage illumination of the lunar south pole on one day in the considered lunar seasons, in 2020.

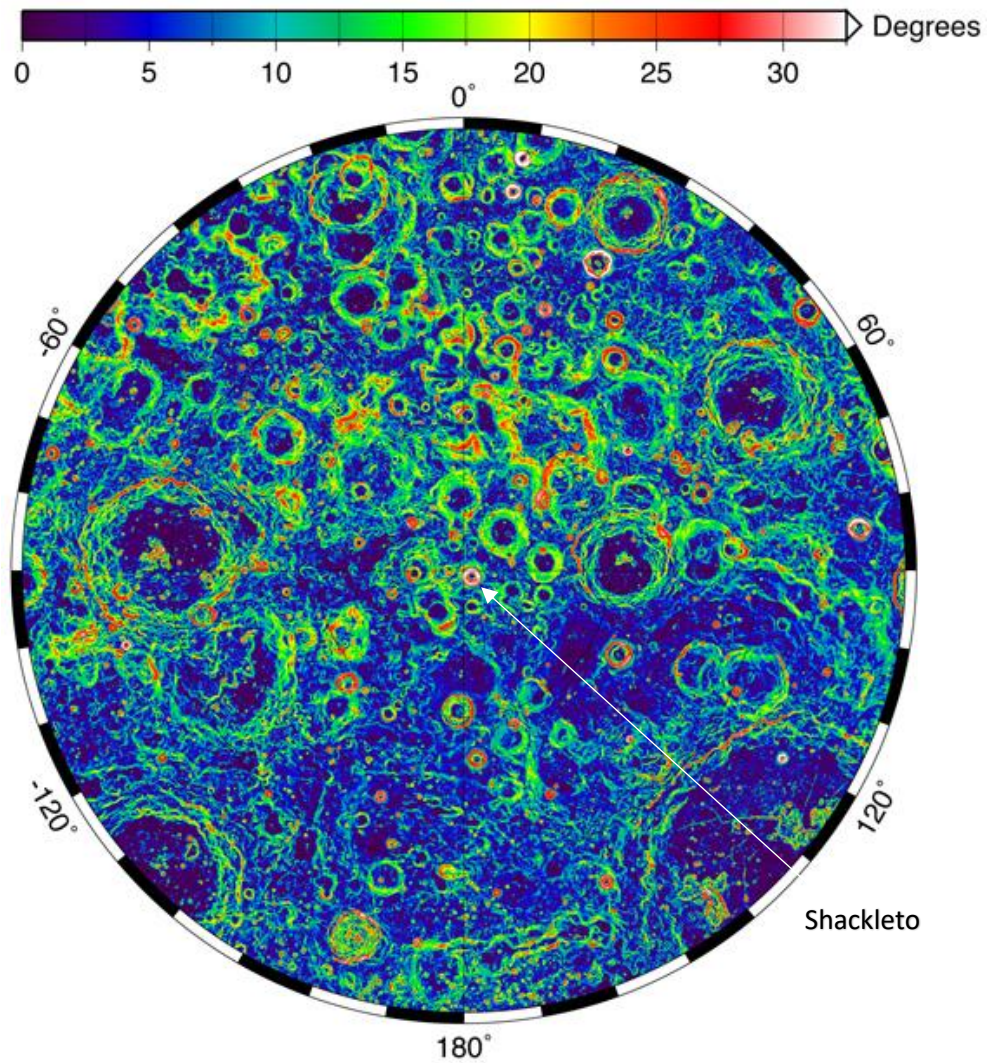


Figure 6: Severity of slopes at the lunar south pole up to 75 degrees south, [10].

Prediction of moon surface temperatures varies between sources. It is estimated that

at the south pole, near the Shackleton crater, the temperature is approximately 40K in shadowed regions and 220K elsewhere. There is a monthly fluctuation in temperature of around 10K, [3]. The Diviner lunar radiometer experiment upon NASA's LRO captured images showing surface temperatures between 6 September and 3 October 2009, the period running up to the southern solstice of the moon, [11]. The observed

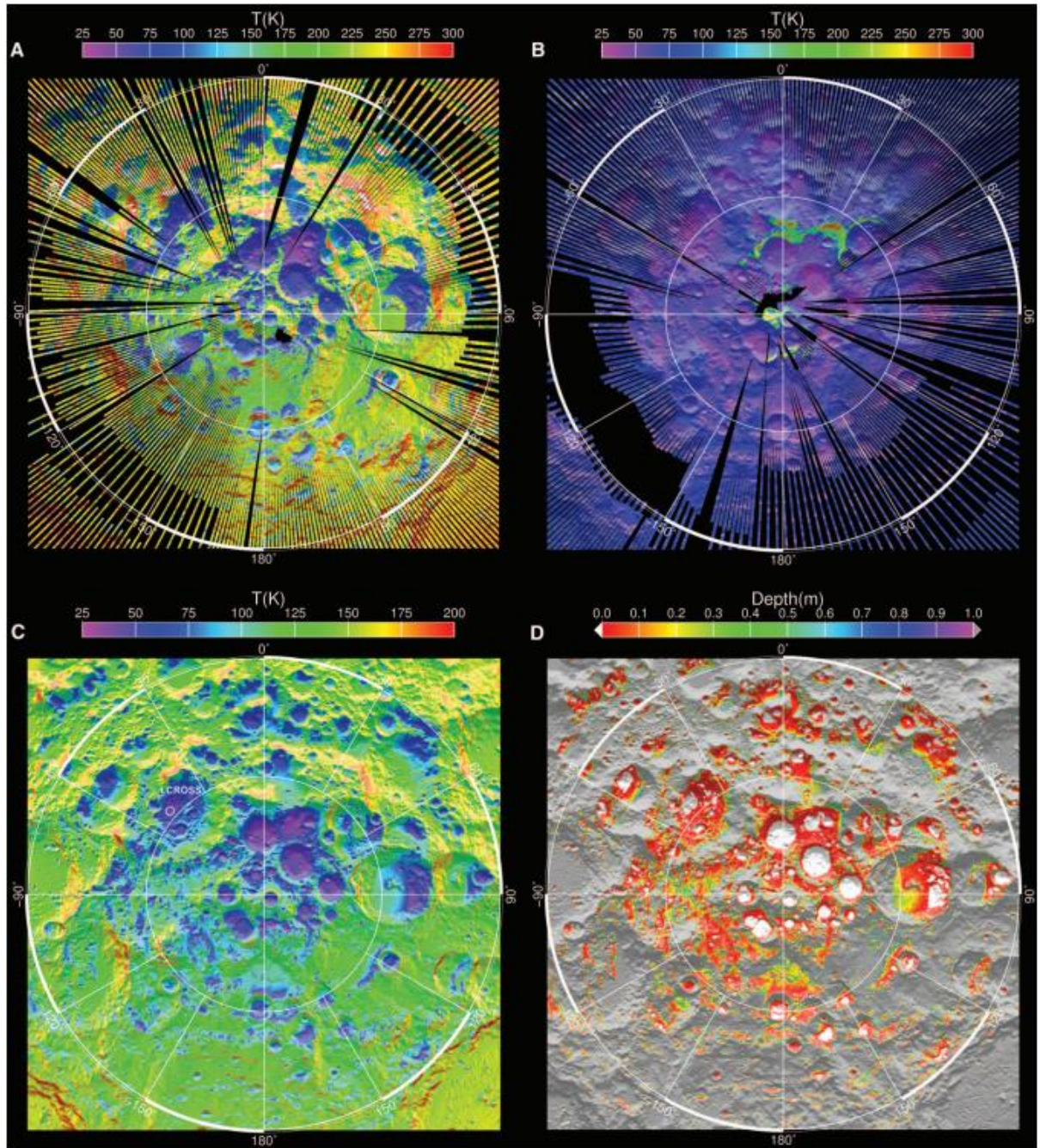


Figure 8: Lunar surface temperatures, [11]; Top left – daytime bolometric brightness temperatures; top right – night time bolometric brightness temperatures; bottom left – model-calculated annual average surface temperatures; bottom right – model-calculated depths at which ice lost by sublimation is below 2kgm^{-2} per billion years. The outer circle represents 80 degrees south latitude.

temperature ranges can be seen in Figure 8, with a corrected maximum of 300K at peaks and minimum of around 25K in the lowest regions.

3.1.2. Terrestrial Power Distribution

Power transmission systems on earth carry high voltage alternating current (AC) over large distances. For terrestrial applications, copper tends to be used for current carrying conductors, due to its high electrical and thermal conductivity, [12].

Generation on earth takes many forms, for example coal fired plants, thermal nuclear plants, and the small-scale generation of roof-mounted solar panels. Consumers are numerous and distribution widespread, with various power components required to ensure the frequency and rated voltage are maintained. Supply and demand are flexible; supply alters to meet demand. Transformers are positioned to step down the higher transmission voltages to those required by consumers.

3.1.3. DC Transmission

DC transmission is uncommon on earth for large scale power systems but is used on the International Space Station, [13]. The solar arrays generate a DC voltage, and this is maintained at 160V for transmission on the primary power circuit. Via DC-to-DC conversion it is lowered to 124V DC for the secondary power lines, [14].

US power generation was up to 31kW initially from each of the solar cell blankets on the solar array wings (SAW). Each SAW has 2 blankets of 32800 solar cells. The cells are 14% efficient, [14].

3.1.4. Wireless Power Transmission

Research into microwave wireless power transmission is ongoing. Microwaves are electromagnetic radiation, with wavelength of 0.1mm to 100mm. A current area of research is to use a satellite of solar arrays to capture energy and beam it to the surface of the moon using microwaves, [15].

Geostationary terrestrial satellites orbit 36000km above the earth's surface. It is estimated that a 1GW system would require a pointing accuracy of 0.001 degrees (allowing deviation of a few hundred metres) and a signal receiving site of 2km diameter, [15]. With no atmosphere to speak of, at least in comparison to Earth, lunar satellites could be much closer to the moon surface than Earth's satellites. Thus, with a similar accuracy, an area of fewer receiver antenna would be required. A low orbit would be approximately 100km. There is the issue with maintaining an orbit around the moon, due to regions of significant density fluctuation causing varying gravitational pull, [16], and the gravitational pull of the earth. It is possible to choose an orbital inclination which will allow the satellite to orbit indefinitely; stable inclinations are 27°, 50°, 76° and 86°, [16]. The latter is over the lunar poles.

Magnetic resonance wireless power transfer (WPT) may also be applied. The basis for this is the generation of a time varying signal in the primary winding (e.g. sinusoidal, square), which induces a transient current in the secondary. The primary and secondary circuits are tuned to the same frequency. The signal is then rectified and filtered to give a DC current, [17]. A system diagram is shown in Figure 9.

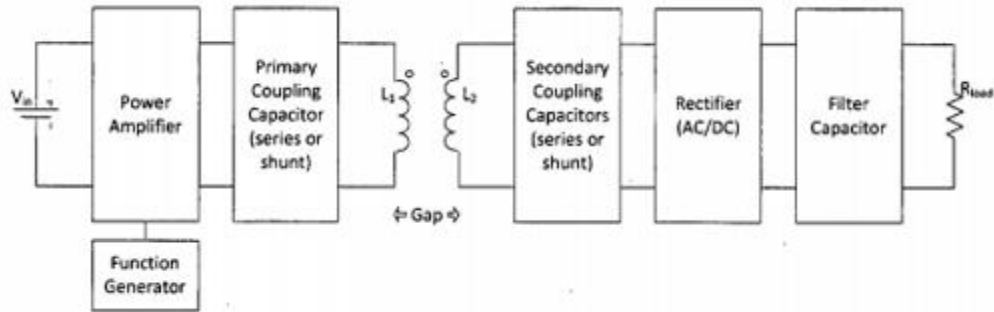


Figure 9: System diagram of a magnetic resonance wireless power transfer mechanism, [17]

3.1.5. Conductors

Pure copper tends to be used as electrons have a large mean free path, ensuring little resistance to current flow, [12]. Of all metals, silver has the highest conductivity, followed by copper, gold and aluminium. Silver is immediately discounted for extensive cabling use due to the prohibitively high cost. In cases where mass must be reduced aluminium is used, [12].

Various statistics are taken from CES EduPack [18]:

Material	Density (kg/m ³)	Resistivity (μΩ·cm)	Coefficient of thermal expansion (μstrain/°C)	Cost (£/kg)
Aluminium (non-age hardening, wrought alloy)	2.5x10 ³ – 2.9x10 ³	2.5 – 6	22 – 25	1.51 – 1.62
Copper	8.93x10 ³ – 8.94x10 ³	1.74 – 5.01	16.9 – 18	4.17 – 4.48
Gold	1.93x10 ⁴ – 3.33x10 ⁴	2 – 3	13.5 – 14.5	2.75x10 ⁴ – 3.33x10 ⁴
Silver	1.05x10 ⁴ – 1.06x10 ⁴	1.67 – 1.81	19.5 – 19.9	383 – 505

Table 1: Various properties for conductor materials

3.1.6. Insulators

The ESA aims to have increased standardisation within the space industry. There are many safety standards and regulations which must be met and increasing standardisation of components can help with this. Insulation must conform to many of these safety standards, for example working temperature, shielding requirements, and volume and composition of gases produced if burned. Consideration must also be given to susceptibility to radiation effects, acceptability of insulation to prevent arcing, twisting of long cable lengths, and temperature increase due to current flow in the wire, [19] [20]. A range of tests must be carried out to ensure materials are safe to use, and that the constructed cabling is up to the required quality. These include a shrinkage test due to prolonged temperature, bending tests to ensure no cracks are found in the insulation, and 'scrape abrasion resistance' testing (Figure 10), [21].

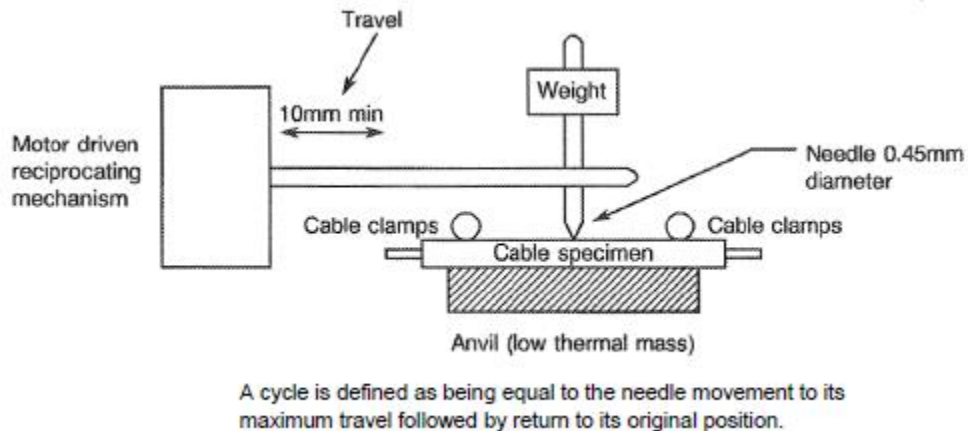


Figure 10: Abrasion resistance test rig, an example of the procedures carried out to ensure cables are safe for utilisation in extra-terrestrial applications.

Commonly mentioned materials in the specifications are polyimide and polytetrafluoroethylene (PTFE). Both have excellent temperature performance and ultraviolet radiation resistance. Polyimide has inherent fire-retardance and low smoke emission, as well as good resistance to both creep and wear. The material is fatigue resistant from -240C to +260C in air, [18]. PTFE has outstanding chemical resistance, good low temperature toughness, and also does not easily burn. Operational temperature for PTFE is -270 to +250C, [18]. Both polyimide and PTFE have drawbacks however, such as high cost and density respectively.

There will be significant resistance in the line if transmission voltages are relatively low for safety, which may vary from location to location if the wire is at a different temperature. Thus, good insulation is crucial.

3.1.7. System Hierarchy

Establishment of a system hierarchy is a crucial part of safe habitat operation. Control is needed in the case that there is a fault and for periods of eclipse, where a large

proportion of power for the base would come from storage, harvesting, and back-up generation sources. Control system hierarchies are based primarily upon maintaining life support, an example is that on the International Space Station (ISS).

On the ISS, the flight systems ensure that the environment is habitable and safe, [22].

The flight systems consist of:

- Crew Health Care System (CHeCS)
- Computers and Data Management
- Guidance, Navigation and Control
- Thermal Control System (TCS)
- Extravehicular Activity (EVA)
- Propulsion
- Communications
- Electrical Power System (EPS)
- Environmental Control and Life Support System (ECLSS)

The ECLSS provides clean air and water to the crew and is one of the top priorities, [23].

3.1.8. Other areas of research

Other areas of research important to the sub-team included:

- Smart grids
- Grounding
- Requirements for safe control

These were considered by other sub-team members.

3.2. Generation

3.2.1. Generation Background

The generation team aimed to develop a system that will accommodate the energy demands necessary to support life within the IGLUNA habitat. The supply of energy would be required to maintain life support systems, as well as support additional experimentation within the lunar environment.

Traditional means of energy generation would be less feasible for the purpose of the IGLUNA project, due to the high transportation costs of fossil fuels from earth to the lunar South Pole. This meant that a sustainable energy generation system would be required, where maximising in situ available resource utilisation, for immediate and long-term usage, would impact the energy system design. In order to optimise the energy output of the system, with limited transportable raw materials, the generation team focussed on increasing the power output to device weight ratio and potential scalability of the system. Areas of focus also included reduced design complexity for improved system operating lifetime, suitability to the lunar environment and improved methods of control.

3.2.2. Helium-3

During the Apollo 17 lunar mission, samples of the moon's upper crust were observed to contain helium-3; a non-radioactive isotope of hydrogen, [24]. This resource can act as a powerful fuel for nuclear fusion, in which electrical power can be generated with almost no radioactive waste. It's estimated that 1 million tonnes of He-3 is available on the lunar surface, with the capability of providing earth with energy for over 1,000 years, [25] [26]. Preliminary investigation by the Fusion Technology Institute and Wisconsin Centre for Space Automation and Robotics showed He-3 mining was both technically and economically viable, however substantial advancements in technology would be required to do so effectively, [27] [28].

3.2.3. Solar Power Generation

The sun acts as a natural fusion reactor, releasing around 3.86×10^{26} Watts of energy at any given moment through the consumption of approximately 4 million tonnes of hydrogen per second. The consumption of hydrogen mass is converted into helium and energy, due to large pressures and temperatures at the sun's core, [29]. Electromagnetic is also released in this process, where it travels through space reaching the lunar surface. The generation team looked to harness this emitted energy for use in the IGLUNA project, by developing a system suitable for the lunar environment.

3.2.4. Concentrated Solar Power

Concentrated Solar Power (CSP) utilises mirrors arranged in a satellite structure to concentrate incident solar radiation from a large surface area towards a single point. The energy is converted to heat, which powers a turbine using steam in turn powering a generator, or it can heat molten salt which in turn heats a boiler.

This method has been proven to be effective, where it has been utilised terrestrially in large-scale projects such as the Ivanpah Solar Power Facility within the United States, [30] [31]. Within the IGLUNA project a CSP system could be used as a catalyst for thermochemistry to produce hydrogen from water, aiding in project experimentation. Despite its utility, a distinct rise in the cost effectiveness and power efficiency of silicon photovoltaic cells makes CSP uncompetitive.

3.2.5. Passive Solar Energy

Passive solar energy converts direct sunlight into heat energy to be used in lighting and heating. Trombe walls, consisting of a heat absorbent black material combined with a transparent panel for trapping heat energy, can effectively be used as radiator when sunlight isn't available. This could allow for reduced power consumption within the base, however it does not effectively meet the complex energy demands of the IGLUNA project. The generation team therefore looked towards a solar system that could output energy, with photovoltaic cells offering a practical solution.

3.2.6. Photovoltaic Cells

Photovoltaic cells (PV) utilise the photovoltaic effect, where sunlight is converted to electricity using small packets of energy in the form of photons. Each photon contains a level of energy depending on its wavelength, which strikes a PV cell and is absorbed by a semiconductor material. This generates electricity by the dislodging of an electron within the semiconductor material, where the negatively charged electron moves to a side of the material, which is treated so that it is more receptive to electrons. This promotes movement of negatively charged electrons towards the receptive side creating an electrical imbalance; voltage potential, which when connected to an external load creates a circuit. The current generated is DC, which requires a converter to supply AC electricity.

Since Edmond Becquerel discovered the photovoltaic effect (1839), it has been used in a range of commercial applications such as the Longyangxia Dam Solar Park in China, where it has been proven to be highly effective in generating power. Spread over 25 km² 4 million solar panels generate 220-gigawatt house of electricity annually, [32]. Within a space context, NASA has developed advanced solar cell and array technologies, which have been demonstrated on the International Space Station where 2,500 square meters of solar array, generating 120 kilowatts of electricity, [33] [34]. The Glenn Research Centre's high-efficiency multi-junction solar cells were of particular interest to the generation team where silicon wafer support substrate combined with a selenium semiconductor provides a low cost, robust PV cell, suited for application in space and the lunar environment, [35].

Multi-junction (cascade) cells, offer greater efficiency than single-junction PV cells as a greater portion of the light's spectrum is utilised, allowing for more energy to be used in the photoelectric effect. NASA's selenium interlayer multi-junction cell, uses three junctions each with a different absorption wavelength, offering a doubling in the electricity conversion compared with single-junction cells. A strong factor limiting the effectiveness of a PV cell is the loss in efficiency that occurs when a panel is not directly facing incident solar radiation, which the generation team aims to address using a solar tracking system.

3.2.7. Solar Tracking

Sunlight can be separated into "direct beam" and "diffuse sunlight", with around 90% of the solar energy carried within "direct beam", [36]. Energy contained within diffuse light can increase with varying weather conditions, however this will not be applicable within the lunar environment. It is therefore a core component of the generation team's aims to maximise the duration solar cells are exposed to direct beam radiation; in order to maximise energy output.

The energy contribution of direct beam radiation is impacted by the cosine of the angle between incident perpendicular solar radiation and the solar panel, [37]. The angle of

misalignment between the solar panel and direct beam radiation should be minimised, where power loss due can be approximated by, [38]:

Direct power loss (%) due to misalignment angle (i)

$$\text{Power Loss (\%)} = 1 - \cos (i)$$

Misalignment angle (i)	Loss
0°	0%
3°	0.14%
15°	3.4%
30°	13.4%
45°	30%
60°	>50%
75°	>75%

Table 2: Showing power loss (%) compared with the misalignment angle (i)

The sun maintains an angular speed across the lunar sky, meaning the incident angle is constantly varying relative to the solar panel. Optimal positioning is found when the angle of misalignment is 0°.

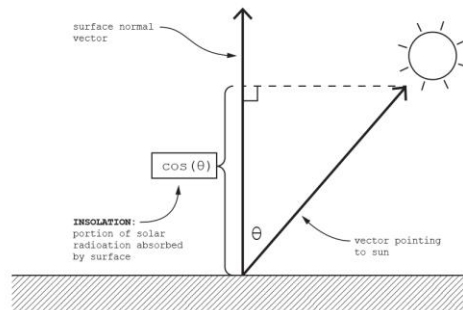


Figure 11: Cosine relation with incident solar radiation, [70]

The reflectance of the solar material can have a drastic impact on solar power output at angles above 56° (Brewster’s angle), varying with wavelength, [39] [40]. In order to minimise the drastic losses incurred from misalignment and reflectance at high angles of incidence, it was crucial that the generation team developed an accurate and adaptable tracking system.

3.2.8. Illumination Conditions at the Lunar South Pole

Illumination condition were covered in part in section 3.1.1.; information in this section focusses more on conditions affecting power generation.

The moon’s axial tilt of 1.5° compared with earth’s tilt of 23.5°, means that the South Pole is almost perpendicular to the ecliptic plane enabling regions of almost constant illumination from the sun (varying with season).

Selenographic coordinates are used to express the sun’s motion through the lunar sky, in which illumination metrics are accurately tracked from the Shackleton ridge. A horizon mask, topographic azimuth and elevation coordinates show the extent of the sun’s vertical and horizontal movements (Figure 12), [41].

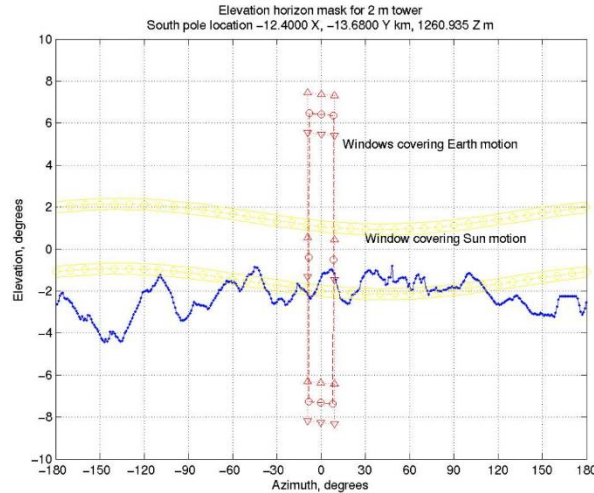


Figure 12: Horizon mask with lunar topographic azimuth and elevation coordinates, showing annual solar movement from the Shackleton crater, [41]

It can be observed that the sun is almost visible throughout 360° of its motion horizontally (azimuth angle) with a mean variation in vertical tilt of ± 1.54 degrees Selenographic latitude (Figure 13). This can be seen more clearly using a solar exposure distribution pattern, taken over a 19-year period, [41]. It is therefore crucial that a solar tracker be able to rotate horizontally (azimuth) to accommodate 360° of motion, as well as address the $\pm 1.54^\circ$ variation in vertical movement.

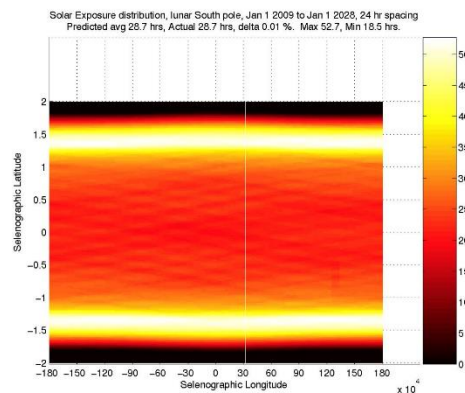


Figure 13: Solar exposure distribution pattern showing Selenographic latitude and longitude ($^\circ$), [41].

3.2.9. Single Axis Solar Tracker

A single axis solar tracker aims to maximise solar output by adjusting its direction relative to the sun's positioning within one axis of movement. Single axis trackers can be categorised as horizontal (azimuth) or vertical axis (zenith) and are used depending on the sun's movement (Figure 14, [42]). Horizontal trackers rotate from east to west whereas vertical trackers rotate from north to south, and can each be effective depending on latitude. Horizontal (azimuth) trackers perform well following the sun's movement in a low arc in the sky, which can be found at the lunar South Pole. The generation team decided to develop an autonomous horizontal solar tracker, to maximise the 360° sweep of the sun whilst incurring the relatively lower vertical losses.

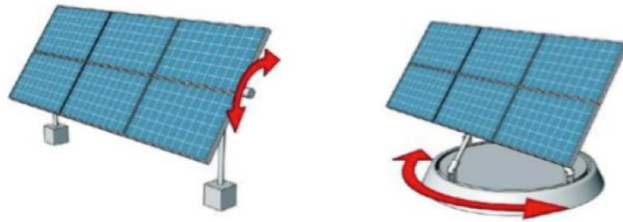


Figure 14: Single axis solar trackers, horizontal axis (left) vertical axis azimuth (right), [42].

3.2.10. Dual Axis Solar Tracker

Dual axis solar trackers have two planes of movement, allowing for the PV panel to maintain a perpendicular angle of incidence to the sun as it moves in both horizontal and vertical axis. This allows for the optimal acquisition of solar radiation in any direction for a longer duration of time, by means of adjusting the azimuth and zenith angles simultaneously (Figure 15).

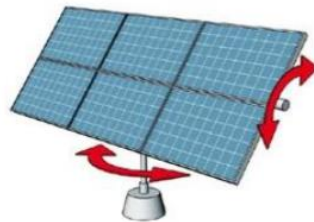


Figure 15: Dual axis solar tracker, [42]

3.3. Harvesting

3.3.1. Background

The IGLUNA project is based on the future, using a self-sustainable philosophy and working with clean technologies. From that point of view, energy harvesting is needed to optimise the energy inside of the human habitat. This kind of generator is powered by wasted energy that could not be used by other means, creating a more efficient

energy system. Another positive point for energy harvesting in this project is the assistance delivered to energy generation when the solar panels are not in use, which also has an impact on energy storage. Energy harvesting will reduce the direct demand from the energy storing systems during night and solar eclipse. With that purpose, two harvesting systems have been developed based on thermoelectric and piezo/triboelectric generators.

- Thermoelectric: This part has been developed by a fourth year student from the wider Strathclyde team.
- Piezo/triboelectric generator: This is the harvesting system developed by the MAE group. Piezoelectricity is based on the generation of electricity by converting mechanical energy into electrical energy, meaning that when a piezoelectric material is deformed it can produce electricity. This behaviour is produced by the arrangement of the electric charges of the atoms that constitute the material. When at rest, the electric charges of the atoms are perfectly balanced; however, when the material is deformed, interaction between the atoms and its charges takes place, producing the orientation and movement of positive and negative charges [43]. This process occurs throughout the structure creating a voltage difference between each face of the material (Figure 16). It also takes place in the opposite sense, when an electric current is applied on a piezoelectric material, it will undergo a mechanical stress and so a deformation. Triboelectricity is also based on the transformation of mechanical energy into electrical energy, but in this case the process is different. Triboelectric materials become electrically charged when a different material is in contact with them and then separated. An example of triboelectric behaviour takes place when a balloon is rubbed against the hair. These two kinds of materials can be used together in order to obtain better energy output as triboelectric materials produce relatively high voltages and piezoelectric materials generates relatively high currents. The implementation of the generators developed in this project would take place under the floor, producing electric energy from human steps and movements.

Piezoelectric Effect in Quartz

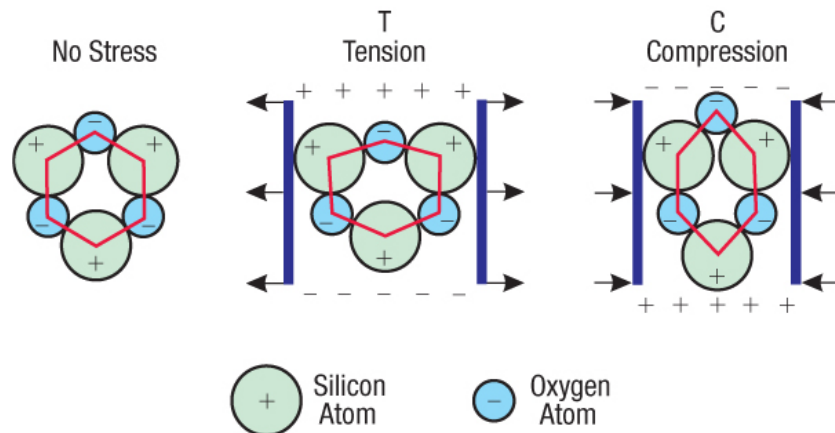


Figure 16: Electric charges displacement [67]

3.3.2. Literature Research

Although piezo and triboelectric materials are not widely used in energy generation, they are used for some specific applications, with piezoelectric materials are more commonly used. Research was carried out to find the applications of these materials. Their main application is the manufacture of sensors and actuators and as said before, most of them are made of piezoelectric materials. By applying a small current, the material will change in size, allowing it to be used as an actuator.

The piezoelectric based sensors and generators are almost equal, both are based in the generation of an electrical output although sensors are focused on the sensitivity of the signal and the generators on obtaining a high output. Due to this difference in preferences of each device, the layout of the generators is usually different from the sensors (Figure 17) in order to maximize the output power. Generators are normally based on bending deformations instead of axial pressure and have higher electrical output values.

When designing the generator, the combined action of the piezoelectric and the triboelectric materials should be considered, creating a device capable of use

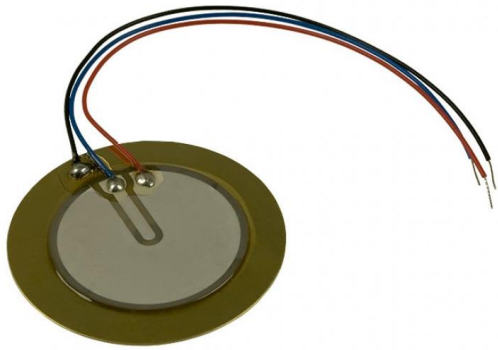


Figure 17: Piezoelectric sensor [68]

simultaneously. Taking this fact into account as well as the main actuation process (human steps), an arch shaped generator was selected as main generator.

The arch shaped generators are based on the deformation by bending of a piezoelectric material layer, producing the contact with the triboelectric material. The piezoelectric layer is situated in the upper part of the generator (Figure 18), covered by two electrodes while the triboelectric layer is in the lower part, with an electrode below it. When the upper part is pressed, the PE material produces electrical energy until it reaches the TE material which will also generate electricity, where it shares the lower PE electrode. The PE part is covered by a polymer that enhances the output values, returning the generator to its initial position after actuation.



Figure 18: Arch-shaped generator layers

3.4. Storage

3.4.1. Literature Review

Little research has been conducted thus far which focuses on requirements of a lunar outpost and fully explores power storage options. There have been a few papers based around this topic but do not fulfil the aims that this work sets out to achieve. The first of which is a paper produced by NASA back in 1990.

Written by Hickman et al and titled “Design Consideration for Lunar Base Photovoltaic Power Systems” [44] it explores the harsh environment experienced on the moon and potential loads that could be experienced. It notes the inadequacy of Nickel-Hydrogen batteries due to the ‘large power requirements’ and the developmental infancy of flywheels and storage coils. Suggestions are made that regenerative fuel cells (RFC’s) are the most promising option to fulfil the requirements [44]. The report only mentions five potential storage options and three of these just in passing. Significant focus is also shifted to the reduction of power use through times when power generation is not possible. While this paper is focused on a similar area there is only a small section dedicated to storage and therefore cannot provide a comprehensive review. It was also published over 25 years ago and simply cannot take into account recent advancements in storage technology.

A second paper also published by NASA and written by Khan et al [45] in 2006 takes a fresh look at the topic but draws many of the same conclusions with regards to energy storage. The main suggestion again is the use of RFC's but this time with the addition of batteries. The insufficient capacity of Nickel-Hydrogen batteries is pointed out and Lithium-ion types are suggested, instead, due to their high specific energy (energy per unit mass) [45]. Gravitational based storage, supercapacitors, thermal reservoirs and flywheel are disregarded due to their mass inefficiency. This paper shares many of the same shortcomings of the previous paper, most notably its lack of exploration into other options. It holds more weight regarding recent technological advancements but 13 years is still a substantial period of time especially in the technology industry.

In the year 2000 a paper was written by Gietl et al which outlined 'The Electrical Power System of the International Space Station' [46]. While this isn't lunar based it is the only case of the design, development and practical implication of an off-earth power system which supports life. The paper gives a thorough review of the system in place on the ISS and provides substantial useful data. The ISS makes use of nickel-hydrogen batteries to store energy and explains the mentions of this particular battery in previous NASA papers. This battery has been tried and tested and therefore is the first suggestion when off-earth storage is proposed but is ill-suited for a lunar outpost [46]. Although this paper is informative and provides a good basis to build upon for other aspects of the power system, its lack of relevancy means the information is not applicable to the design of power storage.

In order to determine what storage route should be pursued, a thorough review of currently available technology was conducted. This was to determine the characteristics of all developed options which will aid in selection. If no obvious candidate presented itself, substantial knowledge will have been attained to allow a new design to be made based on available technology.

3.4.2. Pumped Hydro

Though it may seem an unlikely option, pumped hydro accounts 99% [47] of bulk energy storage worldwide and there are many benefits to its usage. In principal, this is simply transferring electrical energy to potential energy and back again. This is typically achieved with a low reservoir, pump, high reservoir and turbine. When surplus energy is created a pump is powered to move water from the lower reservoir to its higher counterpart, increasing its potential energy along the way. When the demand for energy

exceeds supply, water can be released from the higher reservoir through a turbine, creating electricity, back down to the lower lake. Systems are also found to use a linear

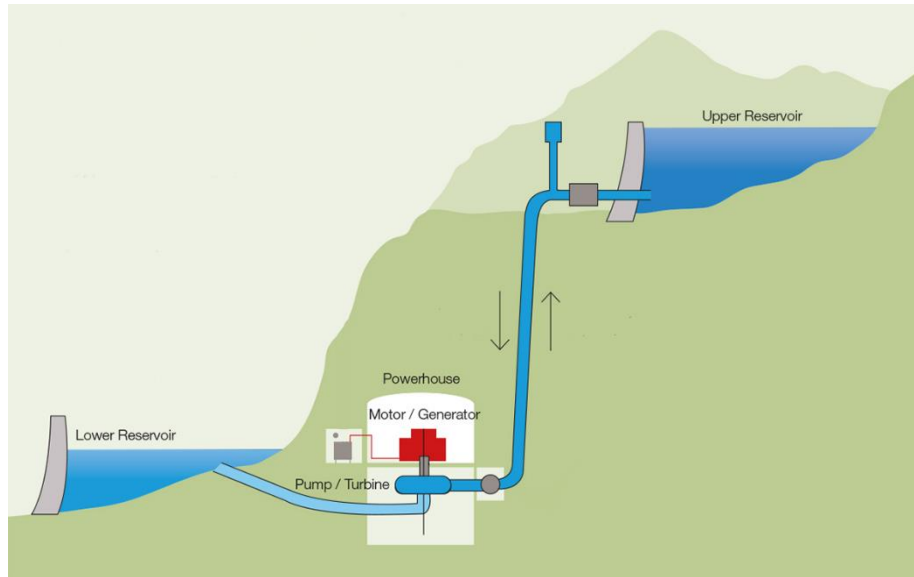


Figure 19: Pumped Hydro Diagram [71]

system as oppose to a loop which employs a combined turbine/pump unit. This decreases complexity and the number of moving parts and required infrastructure. With energy efficiencies of between 70% and 80% being achieved it is easy to understand the popularity of the system [47]. It can also be scaled to meet a variety of needs with ‘pico’ systems operating at less than 5 KW to large systems exceeding 1500 MW [47]. When compared to other storage options pumped hydro has a significantly longer lifespan, although this is often balanced with larger initial capital costs. There are also no losses during energy storage provided there are no leaks and evaporation and rain balance the effects of one another. However, in order to install a system such as this many geographic conditions need to be met which requires extensive research and assessment. When looking to implement a system on a moon base many additional issues also arise which make this a less attractive option. While there is water on the moon, the sub-zero temperatures meaning it exists as ice. Though this isn’t an issue regarding the storage of energy, it does when it needs to be transferred from one height to another. Heating the ice is an option but this would result in large reductions in efficiencies. The location of the habitat will have boundaries and the chances of finding a suitable geographic location within reasonable vicinity would be slim. A reduction in gravity also leads to greater elevation changes or greater volumes to achieve the equivalent energy storage on Earth. Though in an ideal system this wouldn’t matter, larger distances and more volumes will incur greater friction losses which will further reduce efficiency. The difficulty dealing with temperatures, reduced efficiency and geographic dependency of pumped hydro limits its potential in a lunar environment. This

form of storage has been created utilising specific characteristics of Earth and thus doesn't transfer well to other environments.

3.4.3. Compressed Air Energy Storage

Compressed air energy storage (CAES) is another form of storage which uses geographical characteristics to store potential energy. With the use of a compressor, when there is an overproduction of electricity the air is compressed and then stored underground. Large airtight natural caverns are used to store air between 40 and 70 bar [48]. When the energy is to be released, it is diverted through to three turbines of decreasing pressure with burners which are used to increase efficiency [48]. The use of staged turbines and fuel to power the generator is not entirely necessary but it significantly increases the efficiency of the process. Smaller capacity clean CAES that don't burn fossil fuel have been theorised but have yet to be put into practise on a large scale. Efficiency of these systems are expected to peak at 50% while larger systems making use of burners can reach 70% [48]. A feasibility study into clean CAES systems used in conjunction with solar panels theorised efficiencies of around 46% [49]. A beneficial characteristic of CAES is that no stored energy loss over time if a fully leak-free space is maintained. While there is a significant geographical aspect to this option, the 'lava tubes' discovered on the moon could pose as an ideal underground space. The addition of burners would not be suitable for a lunar version of the system as there is no supply of fuel. With regards to longevity, a compressor/generator relies heavily on mechanical components and thus fatigue will likely become an issue for long-term use. The decreased gravity does mean substantially less gas on the surface of the moon. Theoretically, this shouldn't result in any issues provided the compressor can still compress the gas into the chamber.

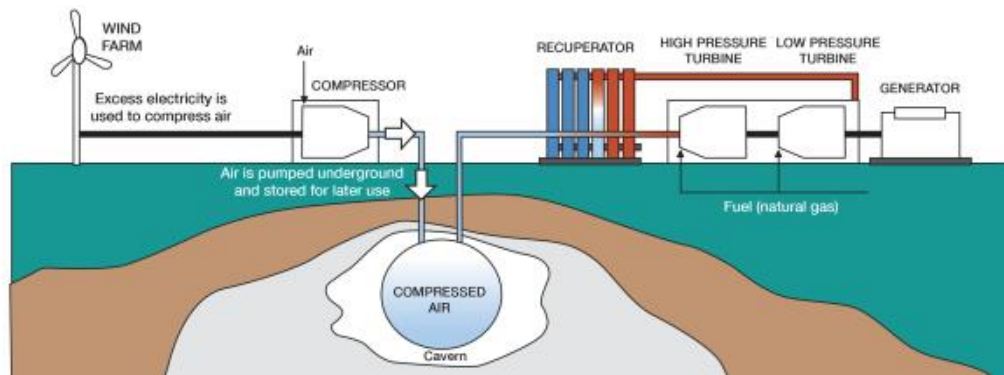


Figure 20 : CAES Diagram [72]

3.4.4. Flywheel

The introduction of new technologies isn't always through the discovery of new concepts but occasionally is through the continual development of old concepts. This is true for the flywheel, and in recent years has crossed the threshold of potential viability for energy storage. For many years, the primary use of the flywheel was to smooth out the

operation of machinery. Its large mass could absorb large mechanical energy fluxes and dissipate them smoothly. As development progressed, the efficiency of the system increased. The chosen method for facilitating the rotational motion evolved from a shaft and hole to ball bearings and finally to magnetic bearings. It was this final change coupled with increasing machining accuracy that made the flywheel a competitive storage option. To store energy, a motor/generator spins a heavy mass converting electrical energy to rotational kinetic. When the energy is to be released, the motor switches to generation mode and the spinning mass rotates the generator and outputs electricity. The magnetic bearing and vacuum chamber in which the mass is housed creates a near frictionless system. This system also benefits from a fixed size, where an increase in storage comes simply by increasing the rotational velocity of the mass. Due to its mechanical form of storage, there is zero deterioration in capacity or efficiency over time while not in use. It is a relatively energy dense form of storage peaking at 1.28 MJ/kg [50] (flywheel only) for high grade composite flywheels. The use of this storage form also doesn't change from earth to the moon and can be used the same in reduced gravity and in different atmospheres. There are still small frictional losses in modern flywheels due to connection between motor/generator and the mass. During long-term energy storage the system will be continually losing energy making the flywheel more suitable for shorter periods of storage. [50]

3.4.5. Supercapacitors

A lot of interest has gathered around the topic of supercapacitors in recent years and the potential applications of the technology are vast. The charge/discharge rates are the most astounding characteristic of the supercapacitor along with its minimal performance degradation over time. Capacitors work by storing electrical energy between two plates and supercapacitors operate under the same principle. Materials and design advancements have greatly increased the capacity in recent years and these new 'high-capacity' variations have been branded supercapacitors. The downside to capacitors is the discharge rate of stored energy and this problem has yet to be resolved. Although the energy density is increased over time it still falls short of current battery technologies. With up to 95% efficiency levels [51], limited performance degradation and quick charge/discharge rates, supercapacitors have the potential to rule the future of energy storage if the prevailing issues can be eliminated. In the current state, however, the drawbacks make this storage format unusable for lunar applications. [51]

3.4.6. Batteries

Batteries have become the only option for small-scale energy storage due to their convenience, size and ease of operation. They become less attractive when compared to other options after scaling up but still prove very competitive. Batteries store energy chemically with an energy output from ions which flow from positive to negative electrodes through an electrolyte. While there are a wide variety of battery technologies, this will be a restricted review of the most relevant types. The first of which

is one that has been used in multiple satellites including the Hubble telescope and the ISS.

The nickel-hydrogen battery, as the name suggests, uses nickel as one electrode and hydrogen as the other and is unique in its composition. Where batteries typically have two similar halves, the NiH₂ battery has a Nickel-Cadmium regular half-cell and a hydrogen-oxygen fuel cell on the opposing half. High specific energy (0.216 KJ/kg) [52] and extensive cycle life (40000 cycles) [52] make this battery type well-suited to use in space missions. However, the gases used in this battery are required to be heavily pressurized and thus requires each cell to contain its own individual pressure vessel. The system is also sensitive to temperature changes and needs to operate within a small temperature window. The pressure requirements and limited application outside aerospace drives up capital costs of this battery type.

Flow batteries are an emerging battery type which has created interest in the industry in recent years, the most promising of which is the Vanadium Redox Flow Battery (VRB) [53]. This battery type differentiates itself from the traditional kind by carrying the ions (the medium by which the energy is stored) in the electrolyte not the electrodes. Two electrolytes travel through two independent circuits and the transfer of ions occurs through a membrane. Redox flow batteries boast a virtually indefinite cycle life [53] although mechanical components such as the pumps will require replacement over time. Output of flow batteries are still limited to below what is considered useful for most applications and the system can only achieve realistic efficiencies on a large scale [53]. At this stage of development flow batteries, much like supercapacitors, exhibit exceptional benefits in one area but fail to reach basic standards in many others.

Lithium-Ion batteries are a sub-category of batteries which are named after the transferred ion as oppose the electrodes used. They have increased in popularity over the last two decades due to many favourable characteristics. [52] Quick charge time, compact design and high energy density have caused Li-ion batteries to dominate the small electronics sector. Wide-scale use of the technology has also drastically reduced costs and expedited the optimisation as a result of the highly competitive consumer market. Li-ion has been the planned replacement of the Ni-H₂ battery on the ISS and all other applications of the older battery will likely follow suit. A higher specific energy, larger operating temperature window and comparable cycle life in addition to the previously mentioned benefits makes the switch an obvious choice. The Li-ion battery is not without its drawbacks, with cases of thermal runaway and capacity degradation over time (even when not in use) compromising the technology in many applications, [52]. Entirely sealed packaging, while convenient, makes repairs impossible leaving battery replacement the only option in the event of a malfunction. [52]

3.4.7. Fuel Cells

Much like batteries, fuel cells have many variations which differ in their operation and constituent components and materials. The principle which separated fuel cells and batteries is the supply of fuel. Where a battery is fully self-contained, a fuel cell requires a constant supply of fuel in order to produce electricity. The presence of many designs, comes different benefits (and drawbacks) that will lend themselves to different applications.

Alkaline Fuel cells (AFC) has been the fuel cell of choice for the space industry and was used in the well-regarded Apollo program. The alkaline description comes from the use of potassium hydroxide as the electrolyte for transfer of ions [54]. Hydrogen and oxygen are the two fuels required for this system and the combination of which produces electricity and water. A low operating temperature, low cost and high efficiencies (up to 60%) [54] makes this an attractive option. The sensitivity of the electrolyte (to carbon oxides) is one of the largest disadvantages of this system and requires pure oxygen otherwise the potassium hydroxide can become compromised. Systems within the fuel cell can help combat this issue but stringent tolerances must be applied to the storage and generation of oxygen which, in turn, can increase costs.

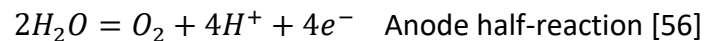
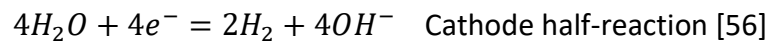
A different fuel cell design has been developed to run at very high temperatures and bring with it a number of advantages. The Molten Carbonate Fuel Cell (MCFC) [54] is not at risk of carbon dioxide (or monoxide) contamination and uniquely has some flexibility with its fuel input. This solves the problems found in the AFC but in doing so has created more issues of its own. The high temperatures increase the rate of breakdown of internal components and thus reducing the lifetime of the system. Special consideration must also be taken with regards to construction to deal with the hostile conditions. It also suffers from prolonged start up times which means it cannot be used to create electricity when a fluctuating output is needed. Its poor power density is also a disadvantage, but it has been proven to operate at high power outputs of up to 3 MW [55]. The long list of drawbacks makes the use of this cell type suitable for only a small number of applications.

Eliminating the need for a liquid electrolyte is an interesting modification successfully carried out by the proton exchange membrane or polymer electrolyte membrane (PEMFC). This has a variety of practical benefits including eliminating the need for maintenance of a liquid electrolyte and any moving parts involved with the circulation of the it. Reduction of space and a weight reduction are further advantages. The PEMFC also operates at low temperatures (between 50-100°C) [54] increasing the longevity of components. Short start-up times gives greater flexibility for electricity production and can, therefore, accommodate more applications. The solid membrane electrode assembly (MEA) that replaces the electrolyte is sensitive to impurities within the fuel and the components which make up the assembly consists of expensive materials. A

catalyst is also necessary to facilitate the transfer of ions and is typically made of platinum which adds to costs.

It was then decided within the storage team to progress on to the next stage of the project with the a PEMFC as a primary storage option and flywheel as the secondary. The requirements of a storage solution dictate that electricity is the format for both the input and the output. It was then necessary to develop an electrolyser which would have electricity as an input and produce the fuels required for the PEMFC (which can combine the fuels to produce electricity). When dividing responsibilities across the team both the flywheel and PEMFC acquisition along with gas storage fell out with the scope of the mechanical engineering team. Therefore, the focus for the methodology section within the storage team will lie solely on the design and construction of the electrolyser.

An electrolyser uses electricity from a DC source connected to an anode and cathode to split water molecules into their constituent elements – hydrogen and oxygen. Electrons from the cathode allow the separation of H^+ atoms from water molecules to produce hydrogen gas and OH^- ions in one half reaction. In the other half reaction, water molecules split to produce oxygen along with electrons and H^+ ions at the positive anode.



4. Methodology

4.1. Distribution

The distribution sub-team took the critical role of connecting power generation and storage with the loads and demands of the moon base. The approach began with the research of high-level concepts, and then focussed into areas of interest.

Initially, research was carried out by the group as a whole in order to gather a good database of general information regarding the moon environment, potential challenges and thoroughly review the literature regarding lunar outposts. Potential areas for innovation were also discussed for the four main sub-teams, for example potential harvesting solutions.

Following the division of members into sub-teams, individuals focussed on sub-team specific research to generate solutions to the challenges at hand. Research remained reasonably high-level. The initial investigation was carried out into:

- a. Power distribution network possibilities/examples
 - i. International Space Station (ISS). The International Space Station has been considered extensively as a case study as it represents the only case of long-term human survival away from earth.
 - ii. Smart grids
 - iii. Wireless power transmission
 - iv. Existing cabling solutions
 - v. Challenges which may be faced in the lunar environment (e.g. high temperature fluctuation thus need a wide range of operation temperatures, lunar dust)
- b. Safety
 - i. Batteries/storage
 - ii. Power sink
 - iii. Fail-safes
 - iv. Regulations
- c. Location of solar panels
 - i. Satellite
 - ii. Moving/rotating panel field
 - iii. Distance to the habitation
- d. Sources and loads
 - i. For example; Solar power generation; Nuclear generation; Hydrogen fuel cells; communications; scientific experiments; life-support; harvesting
- e. Proof-of-concept prototype
 - i. Creation of a user interface (UI)
 - ii. Simulation of the average day/week

iii. Potential for real-time solar generation power measurement and distribution throughout a system at the field test

The team then worked to determine which ideas were feasible, in terms primarily of the conceptual moon base, but also in terms of creating a relevant demonstrator project. Assessment of benefits and drawbacks were used to decide upon final solutions.

Work was then divided into individual areas of interest or speciality to ensure that skills were utilised effectively. The subjects were split into more mechanically based and more electrically/electronically based. Importantly, regulation was considered a separate sub-team (though contained within and working closely with distribution).

Outreach to other IGLUNA projects was carried out to establish the power requirements for the moon base, and was an ongoing task as concurrent projects updated their power requirement estimations. Relaying of relevant information to the generation, harvesting and storage teams was subsequently carried out as required.

An important initial step was the establishment of a system hierarchy composed of standard systems contained within a lunar base, giving special consideration to the current ongoing projects in the extended IGLUNA program. Again, this was ongoing as IGLUNA projects altered and updated.

Distribution strategies (cabling) for the extended distribution network were applied, and their applicability to the lunar environment assessed. Consideration was also made to potential future solutions, to be used after moon base inception.

Appropriate material choices for the harsh environment of operation were found, for insulators, connectors and conductors. Future possible material choices were considered. Optimal solutions for both insulators and conductors were dependant on electrical resistivity (r_e): $R = r_e \frac{L}{A}$. It was assumed that the length (estimated using positioning) and area (estimated using current) of cabling would be known. The secondary objective was to minimise density. Insulator materials were screened on service temperature; a minimum of 30K. Forming ability was also considered. CES EduPack was used for investigation.

Optimal locations for power network components on the moon were assessed, for example the solar arrays, with consideration to safety.

EME team members carried out an assessment of necessary safety measures and grounding required and created the electrical system diagram for distribution network. Development of the distribution field-test prototype is also being carried out by EME team members, along with specification of experiments to be carried out during the July field-test.

4.2. Generation

The generation team aimed to develop a single axis and dual axis solar tracking system in order to maximise the effective output of highly efficient photovoltaic cells to meet the energy demands of the IGLUNA project. The task of developing a robust energy system was addressed with three concept designs, which aimed to meet the technical and project aims set by the generation team. These concepts included a stationary solar device, a single axis (azimuth) solar tracker and a dual axis solar tracking farm.

4.2.1. Technical aims:

- Develop an autonomous solar tracking system which would improve solar panel efficiency and output
- Improve tracking capabilities, accuracy and adaptability
- Compare the energy output of single axis and dual axis solar tracking systems with a stationary panel
- Ensure the suitability of the system within the lunar environment
- Test the use of mirrors in improving solar panel output
- Allow for ease of transportation and scalability through minimised design complexity, shape, control and device weight
- Meet the design requirements set by IGLUNA project

4.2.2. Concept 1: Stationary Solar Tracker

Concept 1 (Figure 21) aimed to address a number of IGLUNA design requirements including the display of key measurements, as well as providing a suitable control to compare the effectiveness of tracking system against a fixed stationary panel.



Figure 21 - Concept 1 design render

4.2.3. Concept 1: Construction

The device was developed using Solidworks, where files were converted to be 3D printed at Strathclyde's FabLab facility. The device was made up of 3 main components which when attached, allowed for manual adjustment in the vertical and horizontal axis.

A summary of concept 1's technical design requirements are shown:

- Support a stationary solar panel

- Manual adjustment of azimuth and zenith angles
- Sustain life support and experimentation
- Deliver key measurements of its surroundings and output
- Facilitate additional mirror testing

A wide base provided the device with stability, as well as the ability to accommodate life support and experimentation. The design offered improved heat insulation, whilst paying homage to the lunar igloo component of the IGLUNA project name.



Figure 22: Concept 1 part 1 render (left) prototype (right)

The electronics embedded into the structure of part 1 included a voltmeter, humidity sensor, temperature sensor, USB power delivery and positive/negative output, meeting the requirements set by the IGLUNA project (Figure 22).

Part 2 (Figure 23) connected to part 1 allowing for a full range of motion horizontally, with the curvature of the design seamlessly matching part 1 allowing for protection against dust and temperature.

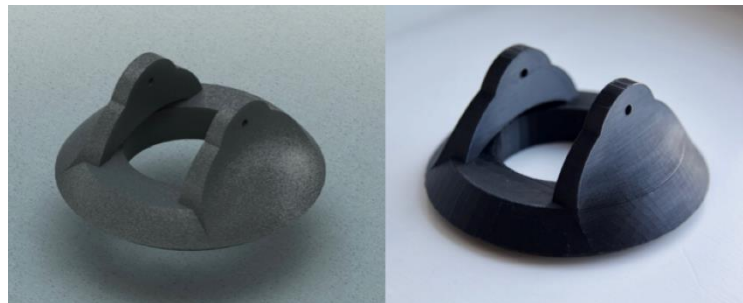


Figure 23: Concept 1 part 2, render (left) prototype (right)

Attaching to part 2, part 3 held the 6V 200mA solar panel with a surface area of 110 x 85 mm² (Figure 24). The design allowed for 180° of motion in the vertical axis.

Part 4 attached to part 3, allowing the addition of beam-focussing mirrors (Figure 25).

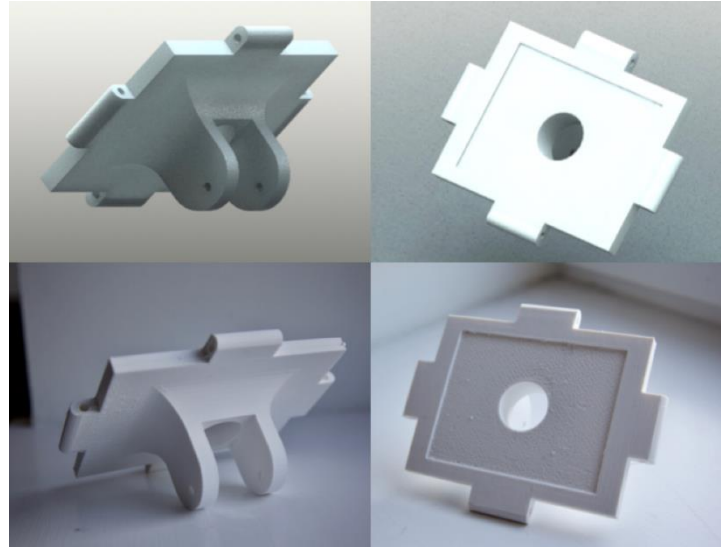


Figure 24: Concept 1 part 3 render (top) prototype (bottom)



Figure 25: Concept 1, part 4

4.2.4. Concept 2: Single Axis Solar Tracker

The generation team aimed to address the aim of developing an autonomous horizontal (azimuth) single axis solar tracking system (Figure 26).

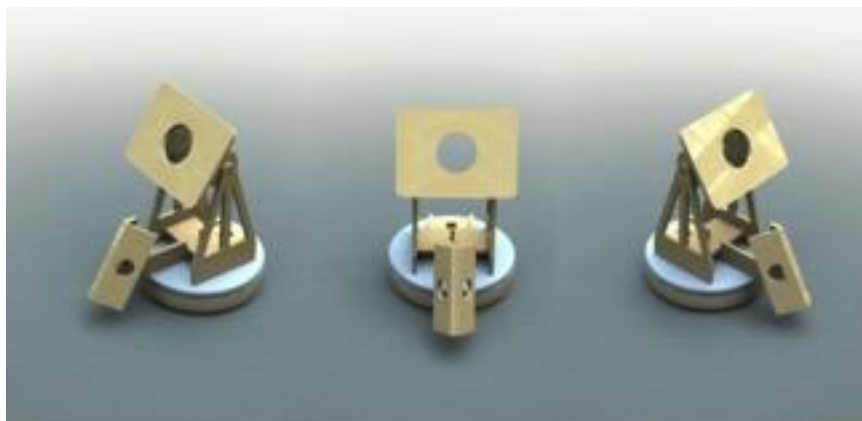


Figure 26 - Concept 2 design render

4.2.5. Concept 2: Construction

The device was designed using Solidworks, where it was converted into DRW files to be laser cut from 6mm plywood at Strathclyde's FabLab facility. A summary of the technical design requirements of concept 2 are shown:

- Autonomous single axis (azimuth) solar tracking capabilities
- Ability to support a 6V 200mA solar panel
- Reduced design complexity to reduce maintenance
- Self-sufficient movement
- Reduced overall weight and size through a flat packed design for transportation

4.2.6. Concept 2: Mechanism of Movement

Movement was generated using a small motor attached to a pinion gear, which rotated within the teeth of a larger internally facing gear ring (Figure 27). The motor was fixed to the structure's base plate, Figure 28, meaning its rotational movement was converted into rotation of the solar panel around a central pole, allowing for 360° of rotation in the horizontal axis.

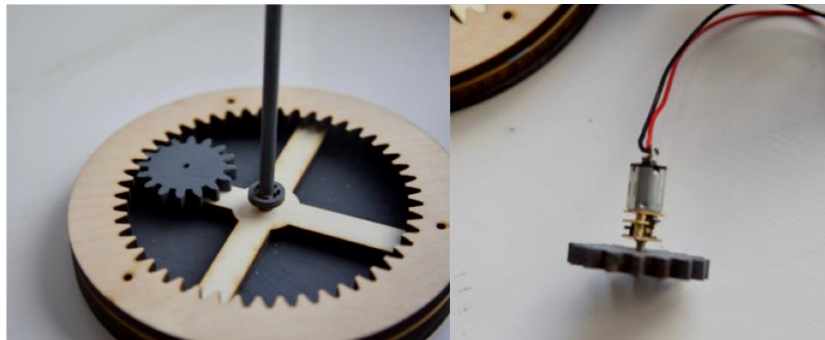


Figure 27: small outward gear (pinion) within inward facing gear (left) and small gear attached to motor (right)

4.2.7. Concept 2: Tracking Mechanism

The method for tracking the sun's movement was two opposite facing solar panels connected to a motor with reverse polarity (Figure 29). The positive (+) and negative (-) outputs of the solar panel on one side of the opposing panels would be connected to the positive (+) and negative (-) inputs for the motor. Conversely the positive (+) and negative (-) outputs of the other solar panel were connected to the negative (-) and positive (+) inputs of the motor.

Sunlight hitting the left solar panel would generate a clockwise movement of the gear, which turned the structure in the direction of the left panel. Sunlight hitting the right

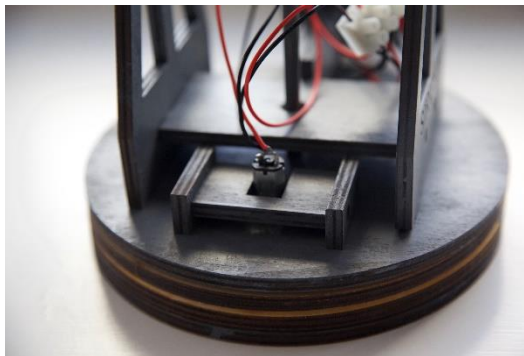


Figure 28: Motor attached to the base plate of the structure

panel would cause the motor to turn anti-clockwise towards the right panel.

When the device has rotated so that the sun is directly between two oppositely facing solar panels, each will receive an equal voltage leading to the motor not moving in either direction (Figure 30). Since the solar panel is positioned perpendicular to the opposing solar panel structure, this position of no movement which will mean the main solar panel is directly facing the sun in the horizontal axis.



Figure 29: Oppositely facing solar panels (left) wiring connecting panels to motor in reverse polarity (right)



Figure 30: Concept 2 full structure facing the direction of maximal power output for the horizontal axis

4.2.8. Concept 3: Dual Axis Solar Tracking Farm

The generation team aimed to develop a dual axis solar tracking system, using an improved weight saving design with programmable control. The improvements made to both the control and weight minimisation, allow for improved scalability with a farm offering increased power output to weight ratio. The main design requirements for concept 3 are shown:

- Improved solar tracking accuracy and control
- Power output to device weight ratio
- Reduced complexity of design
- Enable scalability

The dual axis system improved tracking capabilities by eliminating losses in the vertical direction, with more accurate controllable sensors. The improvements in design allowed for an optimisation of weight, whilst still supporting a 6V 200mA solar panel, improving its power to weight ratio. The improvements to design and control allowed for increased scalability.

4.2.9. Concept 3: Construction

Concept 3 was designed using Solidworks, to be laser cut from 3mm plywood, which dramatically reduced overall weight. An Arduino board, 4 LDR'S and 2 micro servos were used for device control and movement, offering much higher levels of control.

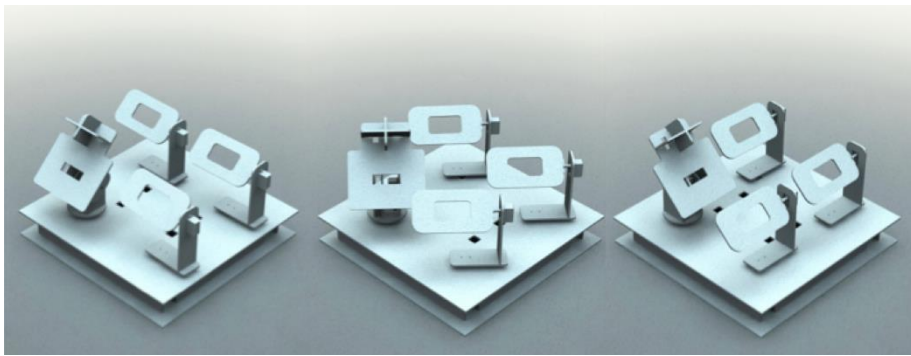


Figure 31: Render of concept 3

Construction involved super-gluing components together, for both the directional sensing device, the clones, and the base part (Figure 31).

The base part was built to allow for the vertical facing bottom motor to protrude from its surface, as well as providing each device with adequate stability. The electronics of each device were stored within the base part structure (Figure 33). Motors were held with screws under the upper surface of the base part.

4.2.10. Concept 3: Mechanism of Movement

Micro-servos located at the base (directed vertically) and at the intersect point (directed horizontally), provided movement in dual axes (Figure 32).

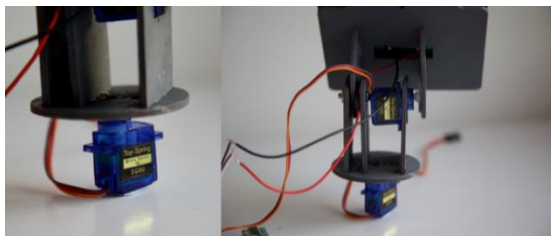


Figure 32: Micro servo's attached to device 1 (sensory device)

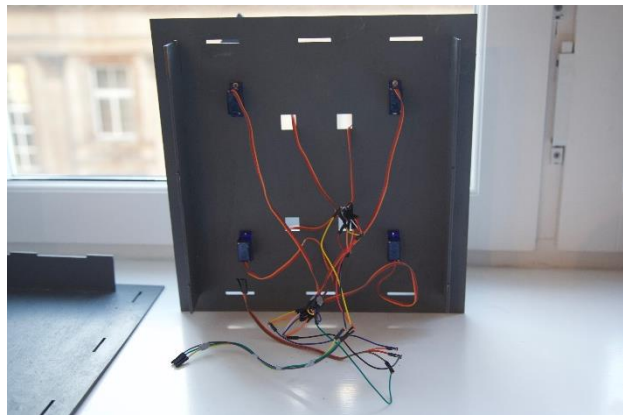


Figure 33: Underside of base part with vertical facing Arduino motors connected

The clone part does not have any sensory capabilities. Instead it receives the signal return for device 1, allowing it to follow its movements in unison. Three clone devices move using the signal from device 1, displaying scalable capabilities, reducing overall design complexity and reducing maintenance issues. The lack of sensory equipment allowed the device to be optimised further with regard to weight achieving less than half the weight (12g) compared with device 1 (29g).

4.2.11. Concept 3: Tacking Mechanism

4 LDR's separated by dividers (Figure 34), detected slight variations in light allowing for a voltage difference to be generated between each LDR; controlled by the Arduino.

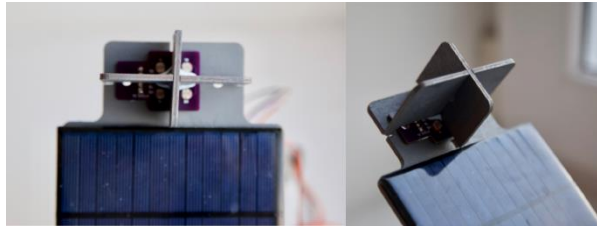


Figure 34: 4 LDR'S separated by dividers

Pseudo code for Arduinio dual axis solar tracking algorithm is shown in Table 3. The board is programmed to take input readings and calculate the following:

$$\text{Average top} = (\text{top left} + \text{top right}) / 2$$

$$\text{Average bottom} = (\text{bottom left} + \text{bottom right}) / 2$$

$$\text{Average left} = (\text{top left} + \text{bottom left}) / 2$$

$$\text{Average right} = (\text{top right} + \text{bottom right}) / 2$$

Using these averages, the differences were calculated where the (average top – average bottom) controlled vertical movement and the (average left – average right) controlled horizontal movement. The Arduino checked if the voltage differences exceeded its tolerance, which will lead to movement of the motors.

1. Include Servo library
2. Initiate Servo 1 in horizontal direction (90°)
3. Initiate Servo 2 in vertical direction (90°)
4. Set servo upper and lower limits (120° , 15°)
5. Initiate LDR pin connections (top left, top right, bottom left, bottom right)
6. Read sensor information (top left, top right, bottom left, bottom right)
7. Take average values for top $((\text{top left} + \text{top right}) / 2)$
8. Take average value for bottom $((\text{bottom left} + \text{bottom right}) / 2)$
9. Take average value for left $((\text{top left} + \text{bottom left}) / 2)$
10. Take average value for right $((\text{top right} + \text{bottom right}) / 2)$
11. Check difference between top and bottom (average top – average bottom)
12. Check difference between left and right (average left – average right)
13. If average left > average right (turn anticlockwise)
14. If average left < average right (turn clockwise)
15. If average left = average right then (do nothing)
16. If average top > average bottom (turn anticlockwise)
17. If average top < average bottom (turn clockwise)
18. If average top = average bottom then (do nothing)

Table 3: pseudo code for Arduino used in Concept 3

4.3. Harvesting

This subproject will be based on the development, analysis and comparison of different PTEG option in order to obtain the most suitable implementation for the moon base, taking the arch-shaped generator as reference. The analysis will be carried out with the FEA software ANSYS where the behaviour of the devices will be simulated.

During the simulations, changes have been made to geometry to improve the generator or avoid possible errors. After the simulation, the data was extracted to perform calculations that allowed the estimation of the output power for each option and for comparisons to be made. Future work that could be carried out to improve the virtual prototype was then discussed. A virtual model was chosen due to the high price of the PE materials and the very specific shape characteristics required. For clarification, the aim of this project was to develop a virtual model similar to reality, giving only approximate results. This allowed comparison of different generator layouts and the

optimisation of these, providing an approximation of the output energy values for the moon base. The assumptions considered will be explained in the report when needed.

4.3.1 Arch-Shaped Generator

The first step in the development of the harvesting generator was the design of the floor structure which must be able to allow the complete movement of the generator, allowing it to return to its initial position at rest and be comfortable for the users. With these guidelines, the structure could now be designed. In this case the layout chosen is shown in Figure 35. The working principle is really basic, the layers composing the generator are located inside a steel frame that prevents them from being displaced and assures the perfect alignment between the two parts of the generator. In the upper part of the frame, a spongy material is placed; it is the interface between the users and the generator, being the material making up the floor. With this idea in mind the shape was developed, creating shallow corners on its sides. Although the floor is relative thick in comparison with the rest of the structure, to avoid disturbances while walking, the lack of material on the sides allows its deformation and the contact with the generator. The material used for the floor is a flexible polyurethane with a low Young's modulus. For the generator, the materials chosen were copper for the electrodes, polytetrafluoroethylene for the TEG, PVDF for the PEG and nylon 66 for the protector

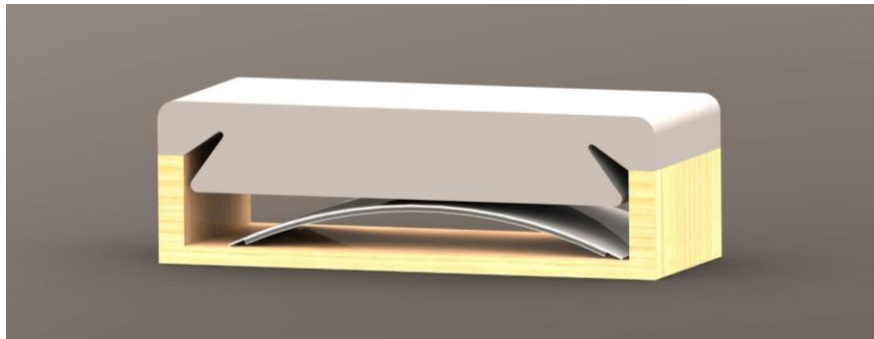


Figure 35: Arch-shaped generator

layer. The reasons for choosing these materials will be later discussed. The thicknesses of the PVDF and Nylon films are 1 and 0.5 mm each. The arch lengths are 100 mm for the PVDF and 110 mm for the nylon, being both 50 mm wide. The dimensions of the frame are slightly bigger, being the total high less than 60 mm. The floor of the moon base would be formed by these structures. The reason for using relative small generators is the comfort of the users; bigger generators mean bigger deformations, leading to an uncomfortable layout due to the small moon gravity. To check the complete dimensions, refer to the technical drawings in appendix 1.

Once the design is decided and the materials chosen, the virtual model can be generated. To do so, SolidWorks software was used to create the model geometry. A complete model with all the components was created as well as a simpler model for the FEA software. The second model only contained the base of the structure, the piezoelectric material and the nylon layer; as the rigidity of the rest of the components is negligible. When studying the interaction between the shape, the deformation and

the output power of the generator, only the piezoelectric component is important, the triboelectric material output will only depend on the area in contact with a different material.

The final model is slightly different from the previous shown due to some working problems in the first analysis related with the placement of the generator. The change performed on the generator was the fastening of one of the ends of the generator to avoid the irregular displacement of the layers (in the real model it would be done with a flexible silicone allowing the rotation of the fixed edge) and the enlargement of the nylon film to protect the PE material during the sliding (image).

The material chosen for the base is steel, due to its resistance that will minimize the amount of material used in the frame, maximizing the number of generators in the floor of the base. The reasons for choosing the nylon 66 as protector film are the resistance and flexibility of the material, allowing it to withstand the force and deformation produced on it and return to its initial position even with only a millimeter in thickness. Finally, the material for the PE generator film is PVDF, an inert polymer. The reason for choosing this material even when others have better piezoelectric properties (ceramics) is its flexibility, something needed if large deflection is expected; the common piezoelectric materials are usually ceramics and minerals, which are strong but brittle.

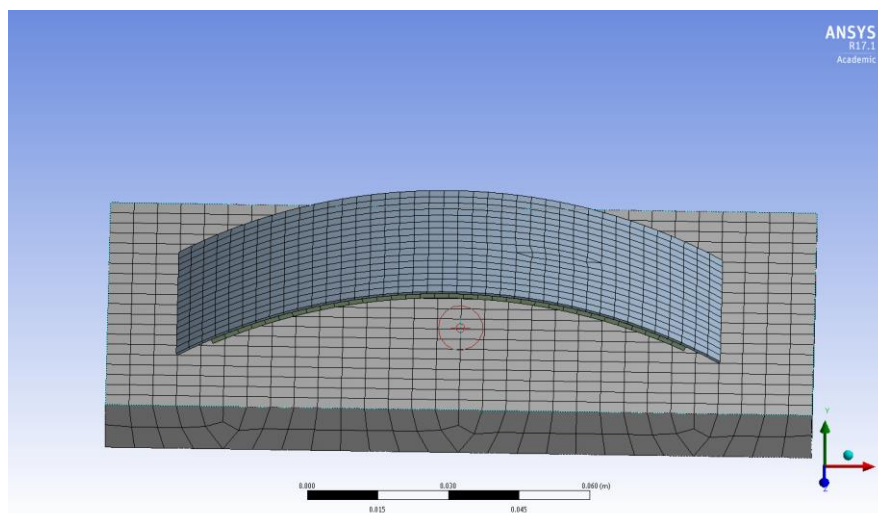


Figure 36: FEA geometry

The ANSYS analysis carried is a static structural shell elements analysis, the nylon and PVDF films are considered as shell elements (Figure 36). Shell elements are a good option when the thickness of the object is small in comparison with its total shape as it is in this case. Large deformations are expected in the analysis, so the large deflection option must be selected for the solution; to avoid errors during the solution (due to the big deformations) progressive load increments are applied from 0 to 110 [N] (weight of a 70 kg person in the Moon) in the y direction. The stepping of the loads is selected by trial and error; a force step is applied checking that the program is able to reach a solution

by a remote displacement allowing only the rotation in the z axis, as would happen with the silicone fastening commented before. The force is applied on the whole surface of the nylon film, assuming a perfect contact between the floor material and the upper part of the generator.

Once these settings are defined, the calculation of the desired data can begin, being the stresses the most important. But before the data obtained can be trusted, the mesh convergence should be performed to validate the data. To do so, different meshing options are applied, and the results obtained in each case compared. Table 4 shows stresses obtained (in Pa) for different meshes, the base is always set to 5 mm.

Mesh	X Stress	Y Stress	Z Stress
General 5mm	1.11e7	1.16e5	3.47e6
General 3mm	1.12e7	1.15e5	3.6e6
General 2 mm	1.16e7	1.15e5	3.56 e6
General 2mm + ref	1.13e7	1.15e5	3.56e6

Table 4: Arch-shaped mesh convergence

As can be seen the difference between the *general 2mm*, the finer refined mesh and the *general 5mm* is relatively small, is less than 3% in the worst case. To choose the best option for the calculations, two main aspects should be considered; the difference in the computational time, around 5 minutes for the 5 mm mesh and more than an hour for the *2mm + ref* one. Apart from that, divergence could occur in the small mesh due to large stress values in small elements of the mesh but this is not the case. Considering the efficiency of the process, the difference in the stress values is not remarkable in comparison with the time needed in each case, so the 5 mm element size mesh is chosen.

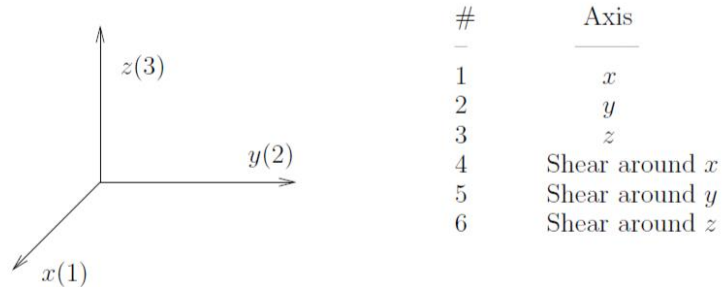
The results can now be analysed and extracted for future calculations. The behaviour of the deformations and stresses are the expected. However, if the y direction stresses are analysed, there is a regressive progress of the stresses. This could seem strange, but as the stresses in the x and z direction are growing with the load, the reduction in the y stresses is produced by the interaction of the other stresses.

$$\begin{aligned} \varepsilon_i &= S_{ij}^E \sigma_j + d_{mi} E_m \\ D_m &= d_{mi} \sigma_i + \xi_{ik}^\sigma E_k \end{aligned}$$

Figure 38: Piezoelectric equations

These are the equations that relate the mechanical and electrical behaviour of a piezoelectric material [57]. The first one allows the calculation of the strain produced by the stress and electrical field applied, whereas the second one is used for the calculation of the electric displacement depending on the stress and the electric field applied. For

the calculations performed from now on, the second equation will be used. The meaning of each term in the equation is shown in Figure 38 along with the convention used for the matrix calculations.



- σ ... stress vector (N/m^2)
- ε ... strain vector (m/m)
- E ... vector of applied electric field (V/m)
- ξ ... permittivity (F/m)
- d ... matrix of piezoelectric strain constants (m/V)
- S ... matrix of compliance coefficients (m^2/N)
- D ... vector of electric displacement (C/m^2)
- g ... matrix of piezoelectric constants (m^2/C)
- β ... impermittivity component (m/F)

Figure 39: Piezoelectric references [56]

As shown in Figure 39, the coordinate system is different from the one used until now in ANSYS, to solve this issue, an auxiliary coordinate system was created allowing the data to be interpreted as in the equations. The calculation is performed in matrix form, considering the properties of the materials in the different directions and relating each term Figure 40.

$$\begin{bmatrix} D_1 \\ D_2 \\ D_3 \end{bmatrix} = \begin{bmatrix} d_{11} & d_{12} & d_{13} & d_{14} & d_{15} & d_{16} \\ d_{21} & d_{22} & d_{23} & d_{24} & d_{25} & d_{26} \\ d_{31} & d_{32} & d_{33} & d_{34} & d_{35} & d_{36} \end{bmatrix} \begin{bmatrix} \sigma_1 \\ \sigma_2 \\ \sigma_3 \\ \sigma_4 \\ \sigma_5 \\ \sigma_6 \end{bmatrix} + \begin{bmatrix} e_{11}^\sigma & e_{12}^\sigma & e_{13}^\sigma \\ e_{21}^\sigma & e_{22}^\sigma & e_{23}^\sigma \\ e_{31}^\sigma & e_{32}^\sigma & e_{33}^\sigma \end{bmatrix} \begin{bmatrix} E_1 \\ E_2 \\ E_3 \end{bmatrix} .$$

Figure 40: Electric displacement [56]

Due to the properties of the materials, the matrices can be simplified as in Figure 41. In the model developed in this project the direction of polarization chosen, and where the electrodes will be placed to obtain the electricity generated is the z axis, so the rest of the terms can be neglected as they will not affect the behaviour of the generator, [58].

$$\begin{bmatrix} D_1 \\ D_2 \\ D_3 \end{bmatrix} = \begin{bmatrix} 0 & 0 & 0 & 0 & d_{15} & 0 \\ 0 & 0 & 0 & d_{15} & 0 & 0 \\ d_{31} & d_{31} & d_{33} & 0 & 0 & 0 \end{bmatrix} \begin{bmatrix} \sigma_1 \\ \sigma_2 \\ \sigma_3 \\ \sigma_4 \\ \sigma_5 \\ \sigma_6 \end{bmatrix} + \begin{bmatrix} e_{11}^\sigma & 0 & 0 \\ 0 & e_{11}^\sigma & 0 \\ 0 & 0 & e_{33}^\sigma \end{bmatrix} \begin{bmatrix} E_1 \\ E_2 \\ E_3 \end{bmatrix}.$$

Figure 41: Simplified electric displacement, [56]

In addition, there are no expected electric fields while working, so the simplifications lead to the formula to calculate the electric displacement:

$$D_3 = d_{31} \times \sigma_x + d_{32} \times \sigma_y + d_{33} \times \sigma_z$$

The matrixes below are used for ceramic piezoelectric materials, when using PVDF as in this case, the second d_{31} should be changed by d_{32} .

Piezoelectric properties of PVDF can be found in Table 5.

Piezo Strain Constant (shear mode direction 1)	d_{31}	Uniaxial Film: 22 pC/N Bi-axial Film: 6 pC/N Copolymer: 7-8 pC/N
Piezo Strain Constant (shear mode direction 2)	d_{32}	Uniaxial Film: 3 pC/N Bi-axial Film: 5 pC/N Copolymer: 7-8 pC/N
Piezo Strain Constant (thickness mode)	d_{33}	Uniaxial Film -30 pC/N Bi-axial Film: -30 pC/N Copolymer: -33/34 pC/N
Maximum usable temperature		Uniaxial Film: 75-80 deg C Bi-axial Film: 75-80 deg C Copolymer : 110 deg C

Table 5: Dielectric properties, [69]

In order to calculate the output electric displacement for the stress values obtained in the model, the data of the three principal stresses should be exported from ANSYS. In this case, the calculations were performed in Excel. The data exported from ANSYS correspond to the value of the stresses in the PVDF film for each node of the model. As shown in Figure 42 the location of each node seems to be repeated, this is produced by the shell element analysis; the body is considered as a plane but data on each surface of the body is calculated, leading to that repeated location values that correspond with the nodes in the upper and lower surface for a shell element point.

Node Num	X Location	Y Location	Z Location	Normal Stress x (Pa)	Normal Stress y (Pa)	Normal Stress z (Pa)	D3 no abs	D3 avg	qint	
7	3547	0,10199	8,11E-02	9,48E-02	-37793	1,21E+05	21947	-1,13E-06	1,03E-06	4,32E-12
8	3547	0,10199	8,11E-02	9,48E-02	27751	-1,32E+05	-23962	9,34E-07		
9	3548	0,10199	8,11E-02	0,1448	-39637	1,21E+05	21988	-1,17E-06	1,07E-06	4,47E-12
10	3548	0,10199	8,11E-02	0,1448	29292	-1,32E+05	-24053	9,69E-07		
11	3549	0,10199	8,11E-02	9,77E-02	-63363	1,24E+05	22629	-1,70E-06	1,46E-06	6,1E-12
12	3549	0,10199	8,11E-02	9,77E-02	41076	-1,27E+05	-23157	1,22E-06		
13	3550	0,10199	8,11E-02	0,10069	-87435	1,24E+05	22533	-2,23E-06	1,69E-06	7,08E-12
14	3550	0,10199	8,11E-02	0,10069	38895	-1,22E+05	-22219	1,16E-06		
15	3551	0,10199	8,11E-02	0,10363	-71134	1,24E+05	22595	-1,87E-06	1,08E-06	4,54E-12
16	3551	0,10199	8,11E-02	0,10363	-67,667	-1,22E+05	-22137	2,98E-07		
17	3552	0,10199	8,11E-02	0,10657	-45884	1,24E+05	22616	-1,32E-06	9,14E-07	3,83E-12
18	3552	0,10199	8,11E-02	0,10657	-36966	-1,22E+05	-22242	-5,12E-07		

Figure 42: Node calculations

4.3.2. Cantilever Generator

The output data for the arch-shaped generator was compared to that of another model, discussing advantages and disadvantages for each model and selecting the optimal one. The second layout selected is based on developed sensors and generators. In this case the generator is a cantilever structure formed by a steel layer, two electrodes and the PVDF films. The structure is almost the same as in the arch-shaped generator; the floor material shape is different to apply the force in the desired part of the generator. The cantilever generator works in two different situations, the common bending deformation as the arch shaped one and a vibration when allowed. The layout of the cantilever generator is shown in Figure 43. In this case, the triboelectric material is not used.

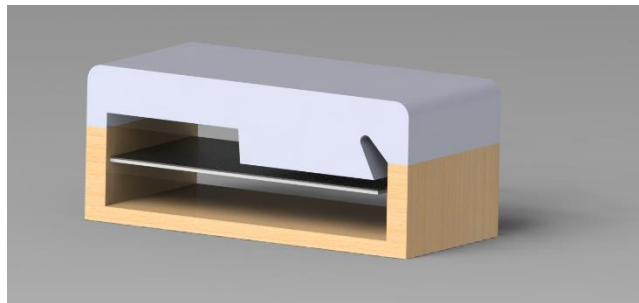


Figure 43: Cantilever generator

The model simulation was like the one performed in the arch-shaped generator. The geometry design was carried out in SolidWorks using a simplified geometry where only the support, the steel plate and the PE material were taken into account. Again, shell elements were used, and the same force magnitude was applied but in this case, distribution was only on half the surface. The load distribution chosen, and the thickness of the steel sheet is determined by the behaviour of the structure, considering the limit stress on the steel plate to avoid plastic deformation. The final load distribution is displayed in Figure 44 and the plate thickness is set to be 2 mm (the PVDF layer thickness is again 1mm as the new results must be compared to those of the previous model). Progressive loads were applied following the same procedure explained in the arch-shaped generator. As supposed for a cantilever analysis, the support selected was a fixed support. The surfaces of the shell elements were divided in two, to allow independent movements but for the analysis, it will be considered as a whole. The size of the layers were 100x50 mm², similar to the arch-shaped case. The complete technical drawing is displayed in the appendix 1.

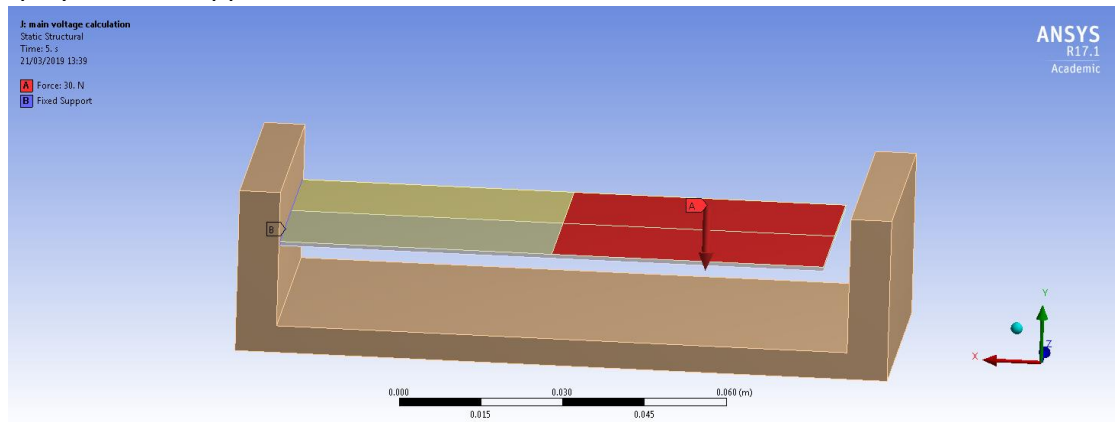


Figure 44: Cantilever load

Mesh convergence should be performed to find the best model for the analysis. In Table 6 the values of the principal stresses are displayed (in Pa). The coordinate system used is the one set for the piezoelectric calculations.

Mesh	X stress	Y stress	Z stress
General 5mm	4.1e5	1.42e6	734.3
General 3mm	3.99e5	1.38e6	728.1
General 1mm	4.07e5	1.40e6	733.7

Table 6: Cantilever mesh convergence

With these results a small difference between the 5mm mesh and the 2mm one is obtained but the calculation time was halved, so the 5mm mesh was chosen. This mesh will reduce the calculation time when small steps are needed ; in a calculation like the one performed in the arch shaped generator to obtain the current.

As mentioned, a voltage and current calculation was performed as in the previous model but for this generator the movement of the system studied is different. The interesting behaviour in this case is the vibration, so although the formulas used are the same as the ones described in the previous section, the time calculations were different. The movement of a cantilever beam is like the that of a spring and both vibrations can be computed in a similar way, a harmonic movement described by:

$$\omega = \sqrt{\frac{k}{m}}$$

$$z = Z \times \cos(\omega t)$$

The beam has a stiffness as springs do, and the movement when vibrating is also cyclic. The behaviour of the generator was considered to be a vibration caused by a step and freely moving; the floor system used to produce the behaviour described here will be described later. In order to calculate the variation of the deformation with time, and so the voltage and current generated, the harmonic frequency of the system should be found. To do so, a harmonic analysis was performed using ANSYS. Once the analysis was done, it was found that the first harmonic of the structure, coinciding with the movement desired was 156.79 Hz (Figure 45).

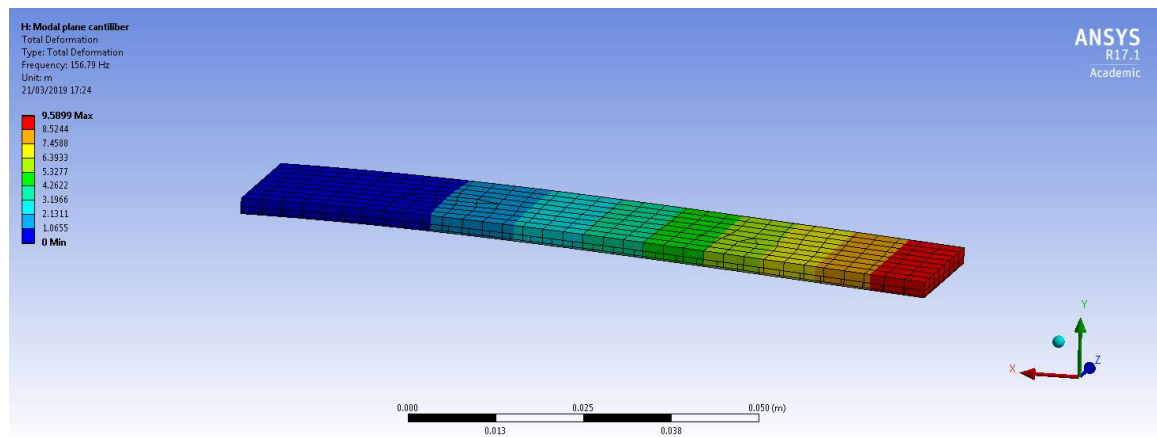


Figure 45: Cantilever harmonic analysis

4.4. Storage

(Note: This section will be limited to a description of the actions which took place during the design and construction of the electrolyser. Explanation of choices, along with elaboration on design features will be found in the discussion section)

4.4.1. Concept Generation

A variety of concepts were sketched early on in the design stages with a focus on both single and dual cylinder designs. The single cylinder design consisted of an acrylic tube

with a plastic sheet separator down the middle (Figure 46). Electrodes are situated on either side of the separator protruding through the tube to produce exposed connection points. On top is a removable lid with valves and hoses. A slight variation on the single cylinder design had electrodes on separate small side housings. The dual cylinder designs are primarily two larger tubes connected by a smaller cylinder. Each tube houses electrodes with openings in the lid of each cylinder. A second major variation of the two-cylinder design was given serious consideration. The design proposed a much smaller (both in height and diameter) second cylinder that would allow for storage inside the larger unit when not in use. After much trial and error, the solution was finalised.

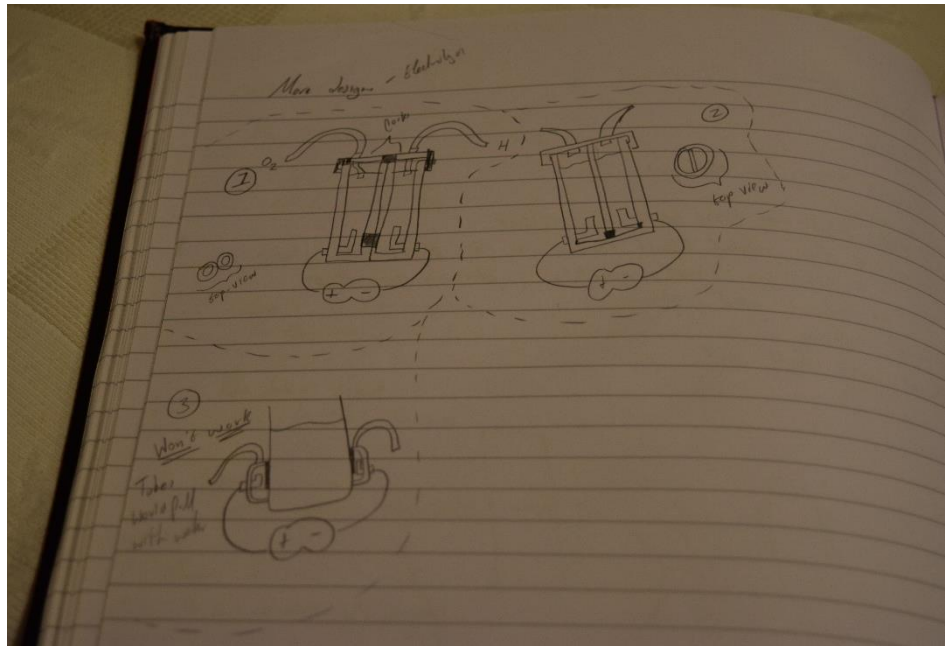


Figure 46 : Single Cylinder Concept Sketches

4.4.2. Construction

Note: A Bill of Materials can be found in Appendix 2

The construction of the design started with the cylinder walls. Cylindrical tubes of 150mm (outside) diameter and 3mm thickness purchased online were cut into one 125mm length and a second 140mm length using a standard wood saw. Edges cut using the saw were sanded down to dull any sharp edges and to remove any height disparity across the end.

One of the ten stainless steel plates was secured and a 6mm hole was drilled 10 mm from the centre of one edge. As opposed to drilling holes in either side of each plate, central holes were drilled into all plates and marks the first variation from the CAD model design. A large semi-circle (32mm diameter) was drilled into the top of a one of the plates. Threaded rods were then cut to into 150mm lengths.

Two 144mm diameter discs of 5mm thickness were pre-cut by the technicians at Strathclyde University. A 14mm hole was drilled through the centre of both, and the circumference was continually sanded until they could fit comfortably within the large cylinders with no additional force. Two larger 150mm diameter discs of 15mm thickness were purchased online and holes were again drilled into the centre of them this time measuring 20mm. Once the centres were aligned, one 144mm disc was glued to the

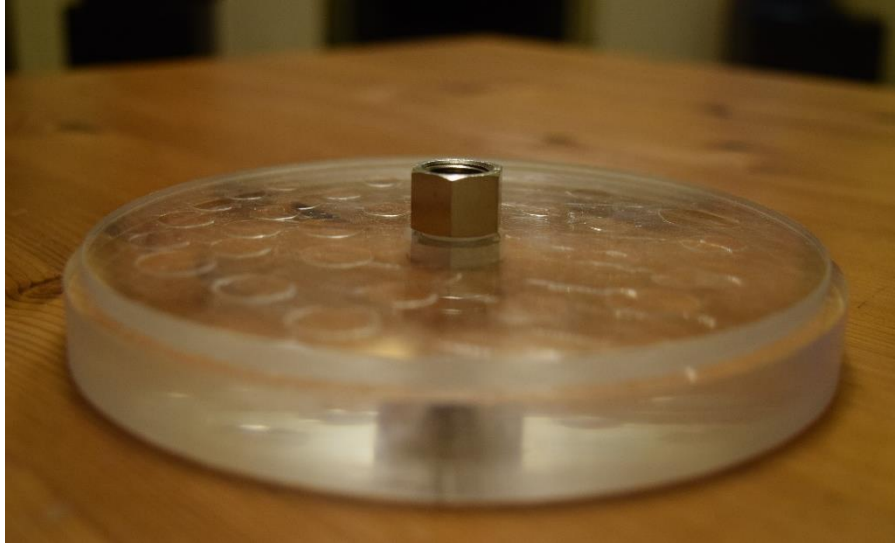


Figure 47: Electrolyser Lid

150mm disc with the use of a hybrid sealant and adhesive. The two bulkhead fittings were pushed through the centre holes and secured with a nut (Figure 47).

The bottom of the cylindrical tubes were warmed allowing the two remaining 144mm discs to be pushed into the end of each without the need for sanding. The hybrid adhesive and sealant was applied to the connection between the two pieces from inside.

The two 60 x 60 blocks were drilled with 34mm hole through the centre and a larger diameter 52mm hole cut to a depth of 10mm around this. The remaining materials had



Figure 48: Electrolyser Flange

to be removed by heating with a naked flame and removing the more pliable plastic with pliers.

The 34mm diameter acrylic tubing was cut to two 25mm lengths. Two 52mm diameter disk were drilled through with a 34mm diameter hole cutter drill attachment. Around 4mm in from the circumference ten 5mm holes were drilled and a neodymium magnet was placed in each. The hybrid sealant was used to secure all the magnets in position and to connect one disc to an end of each of the tubes (Figure 48). A rubber gasket was then cut and glued onto one of the flanges.

The rubber gasket rings were cut to have an inner diameter of 144mm and were attached to the lid section.

A hole of 34mm diameter was then drilled in the each of the cylinders and equal heights. The two tubes with the magnet flanges were inserted into the holes and glued with the hybrid sealant. A 6mm hole was drilled into the cylinder around 10mm above the bottom disc.

A section of the smaller diameter tubing was cut to a 60mm length and cuts were made along its length to create 120° profiles. Further cuts were made to allow them to support the stainless-steel plates. Final cuts across its length created four supports each of which with an incision to accommodate the plates.

The final section in the assembly process starts by inserting the threaded rod through the 6mm hole in both tubes and screwing a washer followed by a plate followed by another washer. This is repeated four more times and the supports can then be placed on the final plate. The 6mm hole where the threaded rod is placed can then be sealed with the hybrid sealant and concludes the construction of the electrolyser (Figure 49).



Figure 49: Finished Electrolyser

5. Results

5.1. Distribution

The table presents current estimations of key parameters for the lunar base power system, including power demand, cable materials, cabling requirements, and positioning of components.

Estimated moon base power requirement	67kW
Estimated moon base power requirement with electrolysis production	104kW
AC/DC transmission	DC
Distribution system	Primarily over-surface cabling, working toward a wireless system.
Estimated max line voltage	380V DC
Estimated secondary transmission voltage	48V DC
Estimated cabling material	Aluminium
Estimated connector material	Copper/ Silver/ specialist engineered alternative
Estimated insulation material	PTFE/ polyimide/ PE
Estimated length of cabling	10s of km
Location of solar arrays	Various locations, on elevated areas surrounding Shackleton crater
Location of fuel-cell (storage)	Within the base, in temperature-controlled environment (safe distance from personnel)
Location harvesting techniques	Under the floor of the habitat
Potential source of back-up power	Located safe distance from the base in protective environment

Table 7: Summary of distribution final results

Development of the prototype was taken on by 2 individuals from the EME side of the project. The intention is to create a small model indicating loads and supply and to test a number of different failure scenarios to identify how it will control power, utilising a simplified system hierarchy. A computational simulation may also be carried out to analyse the power requirements for the lunar base over a standard week/month, as well as during periods of eclipse or power loss.

5.2. Generation

5.2.1. Concept 1

The final prototype is shown in Figure 51 and Figure 50. Analysis of the design was carried out following the assembly.

Variations of misalignment were tested, with six repetitions, over the course of 60 seconds to calculate the average, which was tested against the expected outputs. The equations represent power loss and expected output:

$$\text{Power Loss (\%)} = 1 - \cos(i)$$

$$\text{Expected output} = V * (1 - (1 - \cos(i)))$$



Figure 51: Concept 1 3D printed prototype

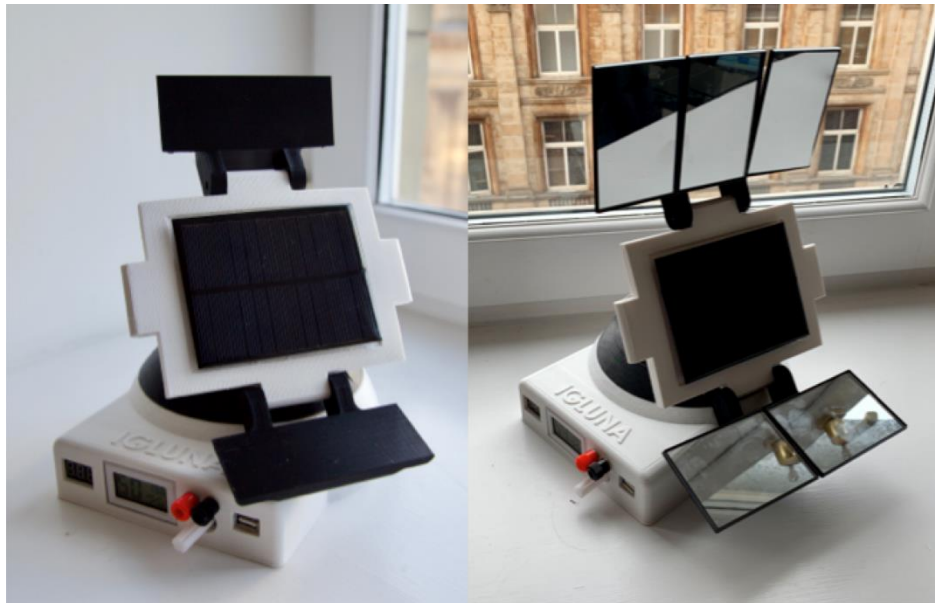


Figure 50: Concept 1, all parts including additional components (mirrors).

Results are summarised in Table 8.

Table 8: Power loss (%) varying with misalignment angle (degrees)

Misalignment angle (°)	Power loss (%)	Expected Output (V)
0	0	5.6
20	6.03	5.26
40	23.4	4.29
60	50	2.8
80	82.6	0.9744
100	100	0
120	100	0
140	100	0

By increasing the misalignment angle in increments of 10°, a graph was created (Figure 53).

5.2.2. Concept 2

The final assembly of concept 2, the single axis solar tracker, is shown in Figure 54.

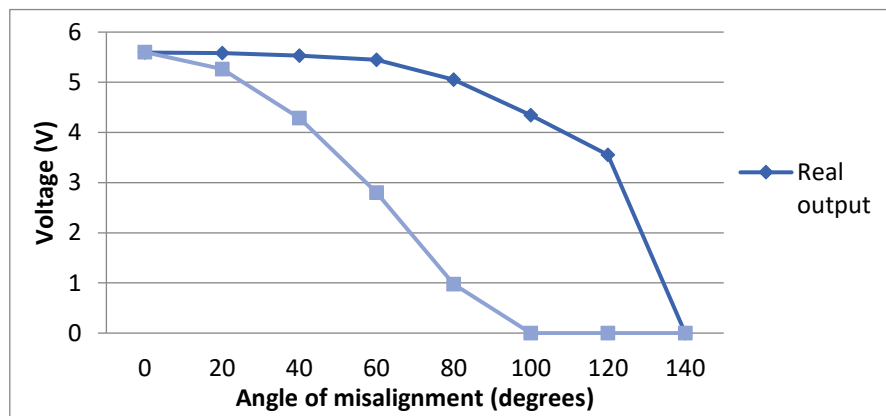


Figure 53: Mirrors set perpendicular, 20° and 40° to the solar panel

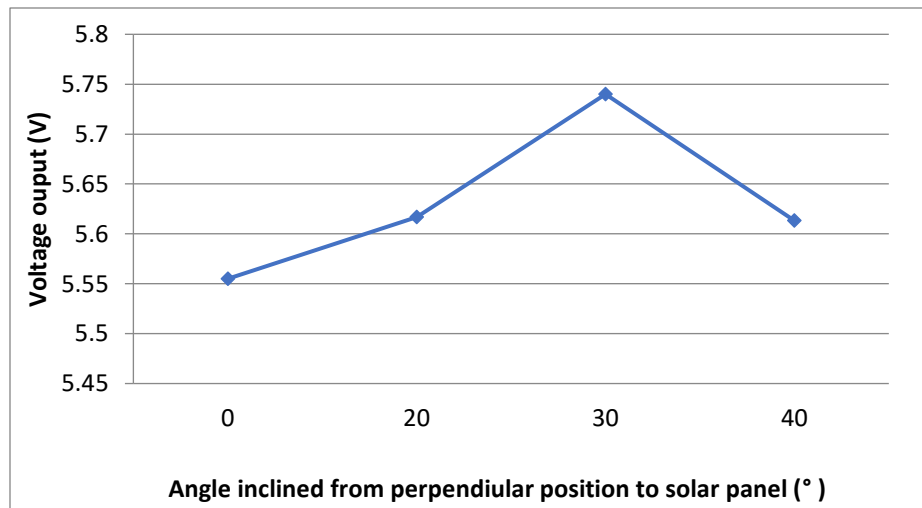


Figure 52: Effect of mirrors inclined at varying degrees from perpendicular on output (V)

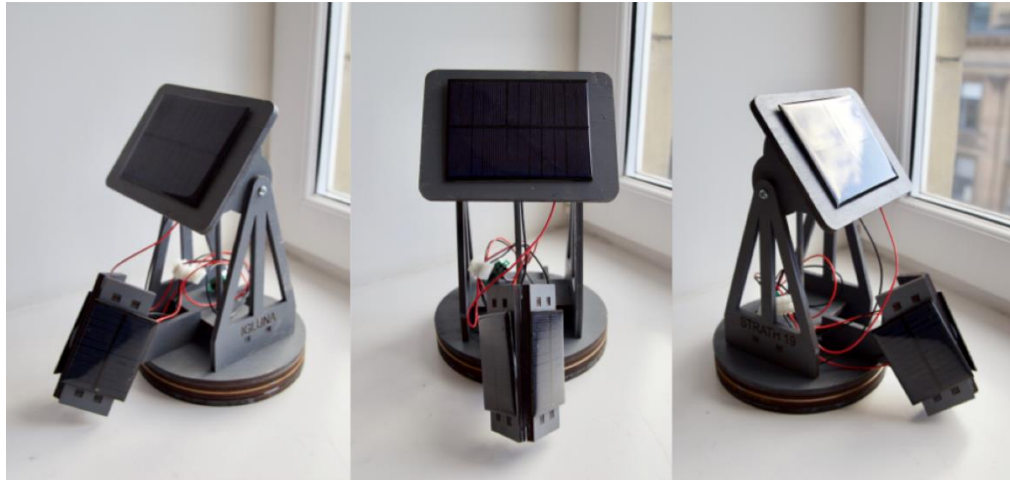


Figure 54: Concept 2 Laser cut prototype

5.2.3. Lunar Solar Generation Estimate

In order to calculate the energy output (E) of a photovoltaic system, the following equation is used:

$$E = A * r * H * PR$$

Values were estimated in order to calculate the energy output of the solar device, where NASA's selenium interlayer multi-junction solar cell was used, [59] [60]. An average solar irradiance (H) (as recorded at the lunar south pole) of 1367.3 W/m² (1.367.3 kW/m²) will be used, [61]. The lunar South Pole, specifically the Shackleton crater, receives light on average 86% of the year, providing irradiance for 313.9 days (7533.6 hours). A performance ratio of 0.75 will be applied, to accommodate losses due to DC cables, temperature and dust; where high performance terrestrial PV plants attain a performance ratio (PR) of 0.8, [62]. Results are summarised in Table 9.

Conversion efficiency (r)	40%
Panel surface area (A)	10 m ²
Solar irradiance (H)	1367.3 W/m ²
Performance ratio (PR)	0.8

Table 9: Important values for lunar-based panel

Total estimated

energy (E)

generated by a solar power system:

$$E = A * r * H * PR$$

$$E = 10 * 0.4 * 10300.691 * 0.8$$

$$E = 32962.211 \text{ kWh/year}$$

Power loss from single axis system with max vertical misalignment 2°:

$$\text{Power Loss (\%)} = 1 - \cos (i) = 1 - \cos (2)$$

$$= 6.09172 \times 10^{-4} = 0.0609\%$$

$$E (\text{Power Loss}) = E * 6.09172 \times 10^{-4} = 20.07 \text{ kWh}$$

Yearly output of 10m2 solar panel (single axis):

$$E - (E * \text{Power Loss (\%)}) = 32962.211 - (32962.211 * 6.09172 \times 10^{-4})$$

$$= 32942.131$$

The International Space Station utilises a solar array of 2500 m², suggesting a lunar base (IGLUNA project) may feasibly host up to 5000 m², [63]. New E is calculated by replacing A=10 with A=5000:

$$E1 (\text{max}) = A * r * H * PR = 5,000 * 0.4 * 10300.691 * 0.8 = 16481105.6 \text{ kWh/year}$$

$$= 1.648 \times 10^7 \text{ kWh/year}$$

The power loss of the system due to misalignment:

$$\text{Power Loss (\%)} = 1 - \cos (i) = 1 - \cos (2) = 6.09172 \times 10^{-4} = 0.0609\%$$

$$\text{Power Loss} = 1.648 \times 10^7 * 6.09172 \times 10^{-4} = 10039.1545 \text{ kWh/year}$$

$$= 1.004 \times 10^4 \text{ kWh/year}$$

Effective Solar Panel Output:

$$E (\text{effective}) = E - E (\text{power loss}) = 16481105.6 - 10039.1545 = 16471066.45 = 1.647106 \times 10^7 \text{ kWh/year}$$

Estimations can be made with regards to the losses a stationary solar panel will incur due to misalignment in both the vertical and horizontal axes. It is observed that solar panel output dramatically degrades above angles of 60°, meaning a stationary solar panel will incur severe output losses above a 120° sweep in the horizontal axes, [64].

Assuming output out with the 120° are zero, the panel will only receive solar radiation for 1/3 the duration of a system with horizontal solar tracking capabilities. The stationary panel will incur the same vertical losses as the single axis system.

Stationary solar panel maximum solar output:

$$\begin{aligned} \text{Horizontal loss} &= \frac{2}{3} * E \text{ (max)} \\ &= \frac{2}{3} * 16481105.6 \\ &= 10987403.73 \\ &= 1.099 \times 10^7 \text{ kWh/year} \end{aligned}$$

Vertical power loss (stationary) = Vertical power loss (single axis tracker)

$$= 1.004 \times 10^4 \text{ kWh/year}$$

Effective energy output stationary

$$\begin{aligned} \text{Effective output stationary} &= \frac{1}{3} * \text{effective output single axis} \\ &= \frac{1}{3} * 1.647106 \times 10^7 \\ &= 5490353.33 \text{ kWh/year} \\ &= 5.490 \times 10^6 \text{ kWh/year} \\ \text{Loss} &= \frac{2}{3} * 1.647 \times 10^7 \\ &= 1.098 \times 10^7 \text{ kWh/year} \end{aligned}$$

Dual axis solar tracking will not incur losses due to misalignment, receiving the full 1.648 x10⁷ kWh/year of direct beam radiation. A comparison of the three tracker mechanisms is shown in Table 10.

Device	Loss (Horizontal) kWh/year	Loss (Vertical) kWh/year	Total Loss kWh/year	Effective output kWh/year	Improvement kWh/year
Stationary	1.099×10^7	1.004×10^4	1.1×10^7	5490353.33	0
Single axis	0	1.004×10^4	1.004×10^4	16471066.45	$10980713.12 = 1.098 \times 10^7$
Dual axis	0	0	0	16481105.6	$10990752.27 = 1.099 \times 10^7$

Table 10: Variations in loss and output for different devices with a 5000m² solar panel surface area

5.2.4. Concept 3

The final assembly of the farm concept is shown in Figure 55.

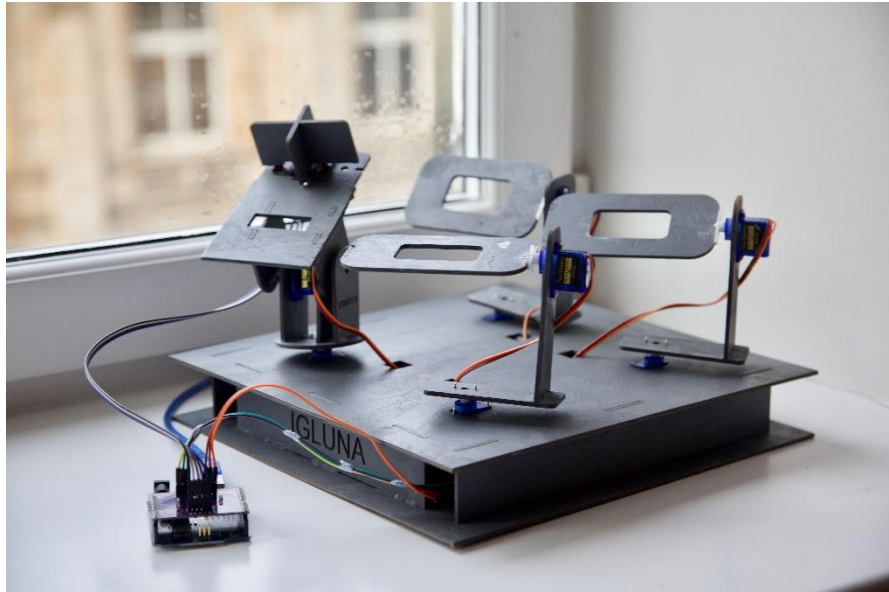


Figure 55: Concept 3 Dual axis solar tracking farm

A visualisation of a lunar solar farm is shown in Figure 56.

The generation team successfully developed a dual-axis solar tracking system, able to follow light sources with a high degree of flexibility and accuracy. The device can track in both the horizontal and vertical axes; ensuring that incident “direct beam” solar radiation is constantly perpendicular to the solar panel, maximising output and minimising losses.

The reduction in design complexity allowed for a decrease in weight whilst maintaining the stability to support solar panels used in concept 1 and 2. This gave it a high-power output to weight ratio. The lightweight design and nature of control gave the system scalability, in which devices could move in unison using a single detection source. This

would be required to accommodate the proposed 5000m² solar panel area, in order to effectively meet the energy demands of the IGLUNA project.

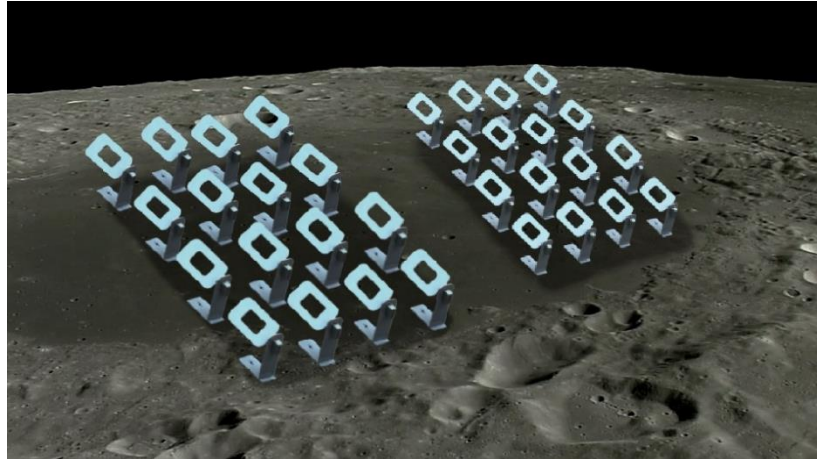


Figure 56: Concept visualisation of a dual axis solar farm on the lunar surface

5.3. Harvesting

5.3.1. Arch-Shaped Generator

The calculation of the total electric displacement was carried out for each node. At this point, it is important to understand the behaviour of the piezoelectric materials. When a stress is applied to this kind of material, electric charges are displaced in a preferred direction as previously mentioned. The direction or sign of the polarization of the materials is opposite depending on the kind of stress induced on it (tension or compression). When bending stresses are produced, both tension and compression stresses appear on the material. This situation will lead to a complex behaviour where the final direction of polarization is uncertain as the compressive stresses will “push” the charges in one sense and the tensile stresses in the opposite. To avoid this kind of behaviour, instead of using one layer of piezoelectric material, two half thickness layers are used, placing them together but in opposite polarization direction, allowing the lower and upper part of the material to produce a potential difference in its preferred

direction. This solution leads to a situation where each stress produces a voltage difference in the desired direction. This process is displayed in Figure 57 [65].

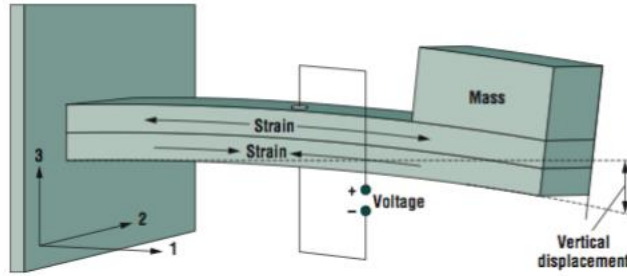


Figure 57: Bending polarisation, [65]

Taking this into account, the total electric displacement across the thickness of the material at each node pair can be calculated as the average of the value produced in the upper and lower surfaces, as both will produce a potential difference equally in the same direction (due to the two opposed layers). For each pair of nodes, this calculation was performed. Once the electric displacement was computed, the charge on the PVDF faces can be calculated through the expression in Figure 58.

$$q = \int \int [D_1 \ D_2 \ D_3] \begin{bmatrix} dA_1 \\ dA_2 \\ dA_3 \end{bmatrix}$$

Figure 58: Piezoelectric global charge

The procedure for the calculation was similar to a numerical integration; the value of the electric displacement on each point calculated was multiplied by the differential of the area, the amount of area associated to each pair of nodes. In this case, this calculation was relatively simple as the elements in the film model are all the same size (Figure 59) so the term dA_3 (the rest are not needed because the generation is in the 3rd direction) is the total film area divided by the pair of nodes. The total charge is equal to the sum of all these terms.

The total voltage was then calculated with the following expressions [57] as the piezoelectric materials behave as a capacitor, accumulating charges on each face and producing a potential difference.

$$V = \frac{q}{C_p}$$

$$C_p = \frac{A \times \epsilon_{33} \times \epsilon_0}{t}$$

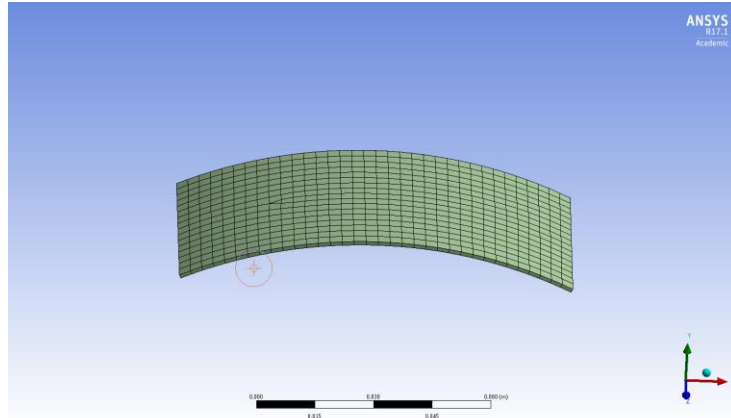


Figure 59: Arch-shaped mesh

Where A and t are the total area and thickness of the piezoelectric material respectively.

$$\frac{\epsilon_{33}^T}{\epsilon_0} \quad 7.6^d$$

Figure 60: Relative permittivity, [57]

The voltage output calculated was that generated when the generator is fully pressed. However, the electric production along its deformation should be considered as well, in order to calculate the output current. The current in a capacitor is the capacitance multiplied by the differential of the voltage with respect to time, and this is how it has been calculated in the model.

To calculate the different time positions, the velocity of a step was measured. According to recent tests, [66] the velocity of a person walking on the moon is 5 km/h so this speed will be assumed for the step. With that velocity and the distance covered by the generator before being completely pressed the generation time is calculated.

$$time = \frac{distance}{velocity}$$

$$I = C \times \frac{dV}{dt}$$

The time is then divided in different steps and the total deformation in the z direction at each instant is calculated as in Table 11.

t	z
0.0000	0.0000
0.0010	0.0014
0.0020	0.0028
0.0030	0.0042
0.0040	0.0056
0.0050	0.0070
0.0060	0.0084
0.0070	0.0098

0.0080	0.0112
0.0090	0.0126
0.0103	0.0144

Table 11: Arch-shaped calculation points

The next step was the calculation of the stresses at the times calculated. The process was the following:

- The number of calculation sub-steps in ANSYS was increased to obtain more values during the simulation.
- For each deformation position calculated before, a similar value was found in ANSYS sub-steps.
- For each sub-step the principal stresses were obtained, and the output voltage calculated as described before.
- The output current and power was calculated at each position.

The result is the table shown in Table 12.

t	z	sub-step	V	I	W
0	0	0	0	0	0
0,001036	0,00145	17	688,9901	2,238E-05	0,007710603
0,001957	0,00274	23	525,565	-5,97E-06	-0,00156814
0,003093	0,00433	30	2069,304	4,573E-05	0,047318539
0,004114	0,00576	31	2718,664	2,139E-05	0,029076053
0,005193	0,00727	32	3009,011	9,057E-06	0,013626824
0,007	0,0098	33	4050,814	1,94E-05	0,039286014
0,008	0,0112	34	4189,119	4,653E-06	0,009746771
0,009071	0,0127	37	4342,955	4,831E-06	0,010490163
0,0103	0,01442	last	4464,737	3,335E-06	0,007445271

Table 12: Arch shaped results

The graphs representing the voltage, current and power with respect to time are shown in appendix 3.

5.3.2. Cantilever Generator

With the harmonic frequency, the total displacement before release, and the necessary equation, the time steps can be calculated, obtaining the points in Table 13.

t	z
0	-3,426
0,00025	-3,32262
0,0005	-3,01872
0,00075	-2,53264
0,001	-1,89371
0,00125	-1,1405
0,0015	-0,31845
0,00175	0,522808

Table 13: Cantilever calculation points

As in the previous model, the values obtained in the Table 14 are just a guideline and close values should be found in the ANSYS sub-steps in order to describe the behaviour of the generator in an appropriate way. To do so, only values from the maximum displacement (t=0) to the 0-displacement position are needed because the movement of the generator is supposed to be symmetric. Once the sub-steps were obtained, the process was the same, calculate the voltage, the current (capacitance times variation of voltage with time) and power.

t	Y	V	I	W
0,0000000	-3,426	628,22	0	0
0,0002556	-3,318	608,42	-0,00026	-0,079302747
0,0005171	-2,991	548,9	-0,00077	-0,210141298
0,0007401	-2,555	469,32	-0,0012	-0,281743502
0,0010084	-1,870	341,42	-0,0016	-0,273806232
0,0012508	-1,138	209,34	-0,00183	-0,191910708
0,0014983	-0,324	59,68	-0,00203	-0,060694222
0,0015652	-0,099	18,36	-0,00208	-0,019104237
0,0015945	0,000	0	-0,00211	0
0,0016238	0,099	-18,36	-0,00211	0,019330244
0,0016906	0,324	-59,68	-0,00208	0,062099175
0,0019382	1,138	-209,34	-0,00203	0,212897595
0,0021806	1,870	-341,42	-0,00183	0,312993951
0,0024489	2,555	-469,32	-0,0016	0,376377309
0,0026719	2,991	-548,9	-0,0012	0,329517191
0,0029334	3,318	-608,42	-0,00077	0,232927981
0,0031890	3,426	-628,22	-0,00026	0,081883521

Table 14: Cantilever results

Graphs containing the evolution of the voltage current and power with time are in the appendix 4.

5.4. Storage

The final dual-cylinder design (Appendix 5)(Figure 61) was much the same as the initial sketch with two separate cylinders connected by a third piece. Both cathode and anode took the form of five stainless steel plates connected via two steel threaded rods. Steel washers either side of the steel plates would hold the plates and provide connection from the rods to the plates. A third threaded rod will protrude through the tube and connect to the first plate. Plastic triangular supports placed on the bottom of the cylinder provided structural support for the electrodes. The connection piece between the cylinders was designed to act as a water tight magnetic fluid coupling. The connection piece is an acrylic tube with a flange at either end, with small holes in the flange to accommodate neodymium magnets. Within the larger cylinder would be an acrylic block with a circular recess with equal dimensions to the flange. Small holes are also present on the opposing side of this block in corresponding positions for the placement of more magnets. A rubber gasket was designed to be placed on the connection piece to ensure a water-tight seal. Various revisions of the connection piece were made throughout the design process as forethought was given to the manufacturing of the component. The lid of each cylinder was simply a large acrylic disc with a lip to allow placement onto the cylinder. A gasket was designed to fit around this lip to produce a gas-tight seal around the top of the device. In the centre of the lid, a metallic fitting was secured by a threaded section and nut. In order to secure the lid a simple latching mechanism was designed and fitted to the side of each cylinder and lid. Given the symmetrical nature of the design only one half of the entire device was modelled on the Solidworks software. In reality the designs required one cylinder to be around 60 mm taller than the other but all other design features remained identical.

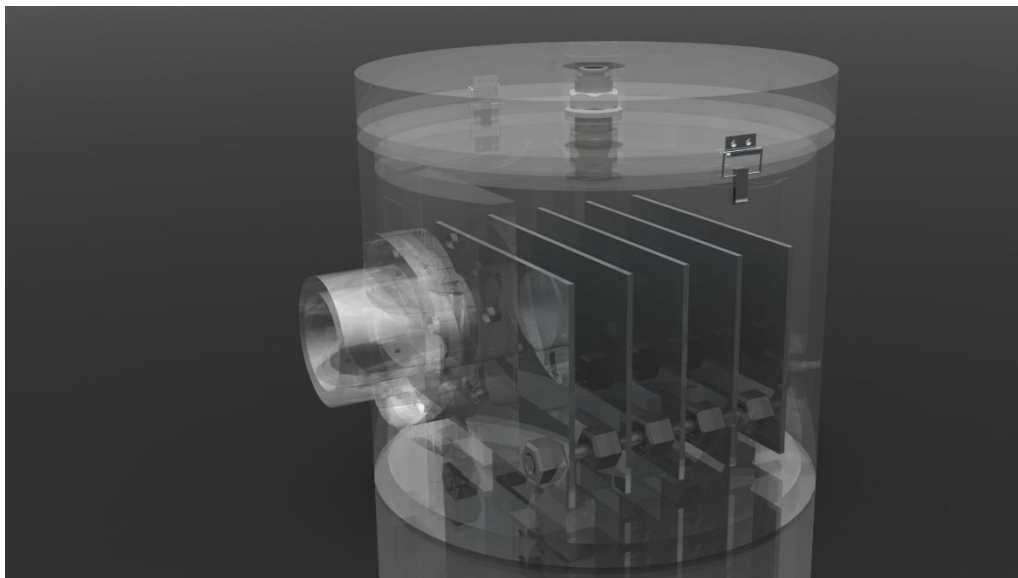


Figure 61 : Electrolyser CAD Render

6. Discussion

6.1. Distribution

6.1.1. System Hierarchy and Power Calculations

The estimated power required was calculated by considering the IGLUNA Systems with known power requirements, estimating those without known values, and considering supplementary equipment not specified within any particular project. It was assumed that there were ten connected lunar base modules. Loads were split into 3 categories (critical, non-critical, loads which can be shed) based upon the established system hierarchy. A ranking system was used, from high to low importance. Priority was of course given to life support systems; these include maintenance of atmospheric temperature and pressure, and the relevant projects which generate oxygen, water, and food. Disposal of waste, communication, health monitoring, and emergency lights were also of high importance. The hierarchy of IGLUNA systems is presented in Appendix 6. Transmission voltages were then estimated by other team members, dictating requirements for the mechanical side of the project.

6.1.2. Distribution system

Wireless transmission was considered both from a satellite to the moon surface, and site-to-site on the moon.

Wireless transmission of power on the surface would be beneficial to reduce the effect of wear on power components; it may eradicate connector deterioration due to contact with lunar regolith, [17]. The charged particles on the lunar surface may adversely affect outside electrical components and solar arrays, potentially coating them. The regolith is also undesirable for electrical grounding due to the poor conductivity. Magnetic resonance may be usefully applied for smaller scale applications, like charging phones and robotics.

An orbiting satellite array of solar panels would have benefits, namely a predictable generation cycle without interference from conditions on the surface. Power could be beamed to the surface during periods of surface darkness. The irregular gravitational pull of the moon may be an issue, however there is a stable inclination path which passes over the poles, where a receiver could be conveniently placed. It may be impractical to have a large receiving antenna placed on the moon, and there would be the need for some redundancy in case of damage to the receiver or satellite. Careful transport of the delicate equipment would be required, but this has been the case in many space missions.

In all, it was decided that research and development was still required and so the idea was deemed currently infeasible. It was decided that the worst-case start up condition, involving cables running on the moon surface, should be what is designed for, with the intention to upgrade.

There were several topics of interest for cabling:

- AC or DC transmission
- Transmission voltages
- Material for conductor
- Material for insulation
- Length required (depends on location of various power system components)

The latter three were considered in the mechanical part of the project.

Cables could be over ground, underground, or suspended in some way above the surface. Suspended cabling could be used as it is on earth, but with multiple solar array locations it would be ideal to consider wireless power transfer across the surface. Thus, avoiding the need for cable supports and vast lengths of cables running along the steep terrain. As mentioned, it was decided to choose over ground cabling, as this would likely be needed during the initial stages of habitat construction.

Whilst surface cables may present the greatest danger to personnel and experience the greatest temperature fluctuation, underground cabling would require significant robotic labour. The ground is rocky and would be difficult to excavate. Even with over ground cabling, robotics would likely be needed to lay the cables. This should ultimately be considered during cabling and robotics design. Cabling dimensions and materials are determined by the voltage and current requirements/limits and the environment surrounding the cable.

- Cross-sectional size of conductor – determined by the current in the cable
- Thickness of insulation – determined by the voltage carried by the conductor
- Composition of the outer jacket – determined by environmental conditions (temperature; exposure to water, sunlight, etc)

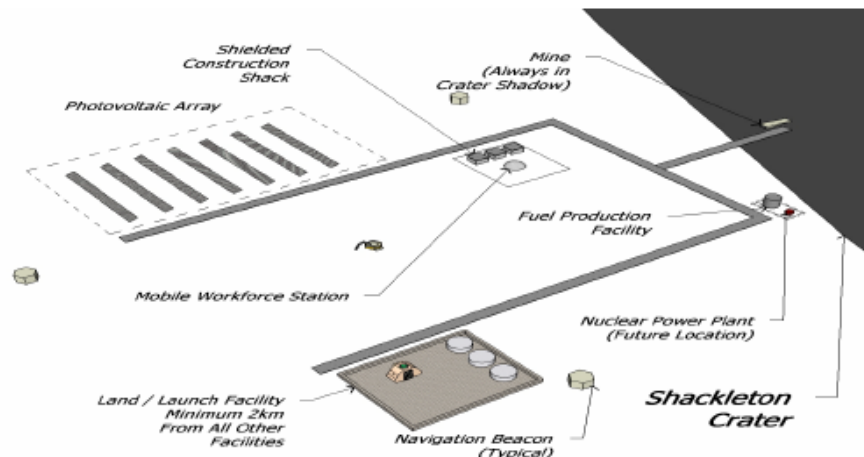


Figure 62: Potential layout for an early stage moon base, [3].

6.1.3. Material choices

For conductors and insulators, the property of utmost concern is electrical resistivity; it must be low and high respectively. Additionally, low density, appropriate temperatures of operation, processability, durability, and flexibility were required. Figure 63 shows the regions of interest for insulators and conductor search, with different colours representing different classes of materials.

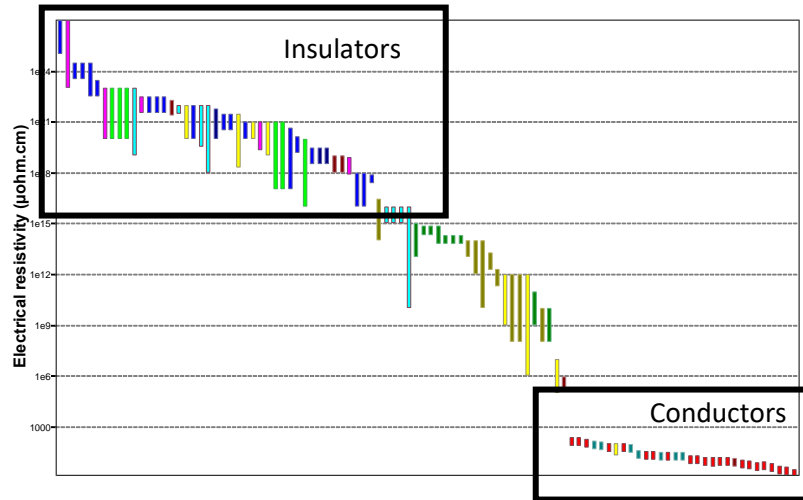


Figure 63: Image of electrical resistivity and search regions of interest, [18].

Closer inspection of these sections can be seen in Figure 63 and Figure 65, with some example materials illustrated.

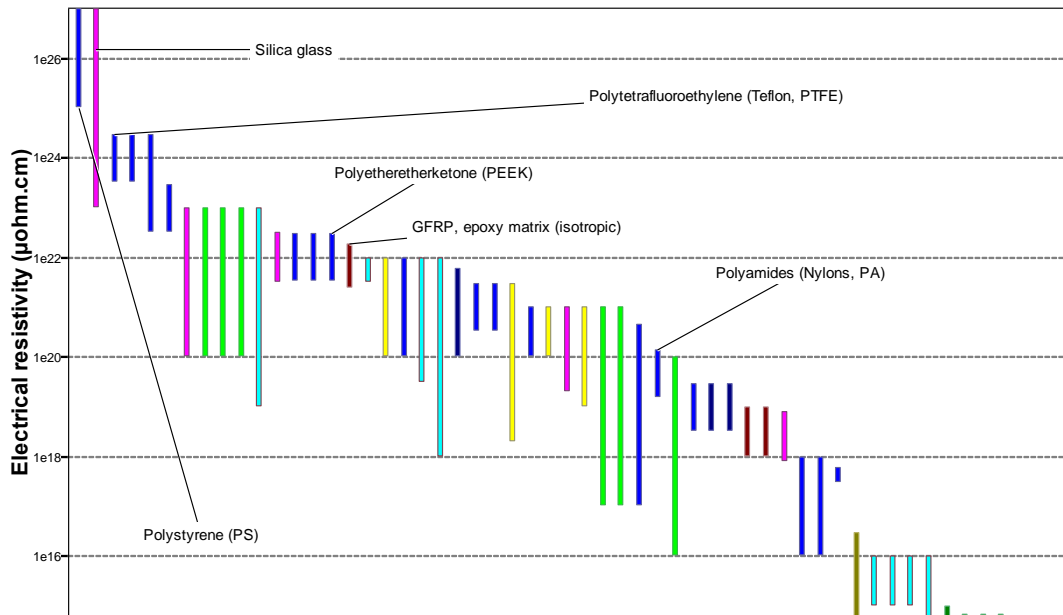


Figure 64: Insulator region of interest, [18].

A number of the insulator materials failed the limit stage, which was a minimum operational temperature of 30K, assuming the worst-case temperature on the surface. Suitable materials were those which could be formed into electrical equipment insulation, with limited gas release when burned and good durability. Any high-performance glasses and ceramics were inappropriate, due to poor formability. The

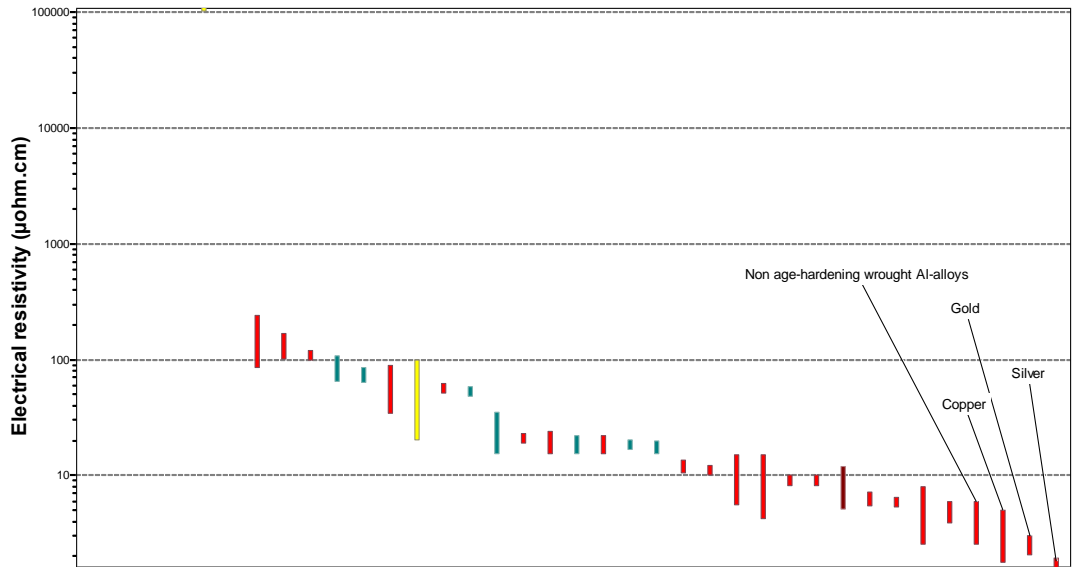


Figure 65: Conductor region of interest, [18].

lunar surface is also rocky with sharp gradients, so cable needs to be able to withstand this having a certain degree of flexibility. It has been stated that polyimide and PTFE are already accepted materials, however polyethylene (PE) also performed well, with good insulating ability and temperature endurance.

Unsurprisingly, the best performing conductors were silver, gold, copper, and aluminium alloy. Various grades of these materials give slightly differing resistive properties, hence the representation using a bar. To reduce the heat loss, due to resistance in the wire, it is imperative that the resistivity is low. The losses could be vast if transmission voltage is kept relatively low and very long cabling lengths are required.

From Figure 66, the trade-off between density and electrical resistivity can be seen. The two objectives conflict, and so there is a pareto front developed, consisting of non-dominated solutions. Considering only these objectives, the ideal solution for metals would be located at the bottom left of the chart, reducing resistivity. The optimal solution for insulators would be located at the upper left, finding the maximum of resistivity. In both cases density is reduced.

Metal foam (aluminium based) is the least dense of the excellent conductors but is very unsuitable for wire creation due to its form. Foam by nature contains air holes and thus it is most appropriately used for cooling due to large exposed surface area, [18]. Other

non-dominated solutions include silver and magnesium alloys. Though it is possible to draw magnesium alloys, they are unsuitable for wiring. Other potential materials included alloys of titanium, and nickel-chromium alloys. These materials have their uses but are again unsuitable for large-scale wiring; titanium alloys tend to be used for compressor blades, and nickel-chromium alloys used for their chemical and corrosion

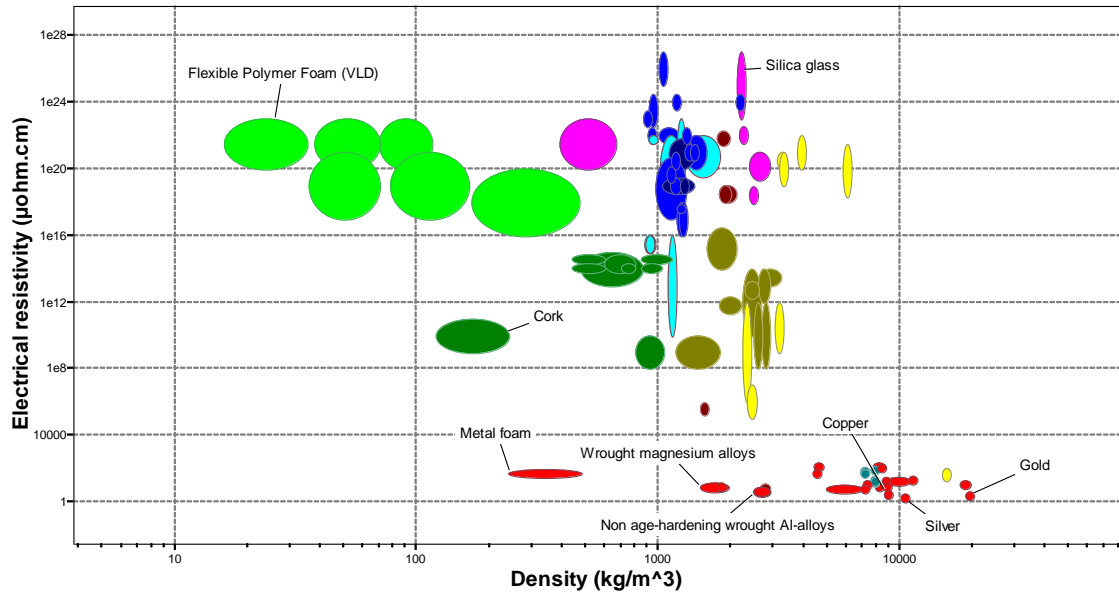


Figure 66: Electrical resistivity against density, showing pareto front trade-off between the two, [18].

resistance, [18].

Amongst the optimal solutions at the bottom right, are aluminium alloys. There is a clear weight saving effect by using these alloys, with a small sacrifice in conductivity. Any mass saving for launch is beneficial when considering missions to space. Cost is lower, but coefficient of thermal expansion is greater, which is undesirable.

For important conductors and contacts in the system, silver and copper should be used. They are higher in density but have superior conductive properties.

It is possible, due to increased standardisation, that the cables required already exist and are currently used in extra-terrestrial operations.

6.1.4. Future materials

Metal matrix composites (MMC) are composite materials with a metal matrix (binder) and various fibre materials and shapes. They can be designed to have desirable properties, such as low resistivity and high dimensional stability. Though not widely accepted as yet, they have had uses of note within the space industry because of their desirable properties; an example is the Hubble telescope. Such materials may one day be engineered to give excellent properties to the cabling and connector components, and research is ongoing.

6.1.5. Lunar Surface Positioning and cable length

It was assumed that the base was located near the Shackleton crater, within the lava tubes under the surface. Several potential locations for solar arrays become obvious when considering the time-weighted illumination, Figure 67. It makes the most sense to position arrays separately, thus reducing the possibility of an event affecting them all.

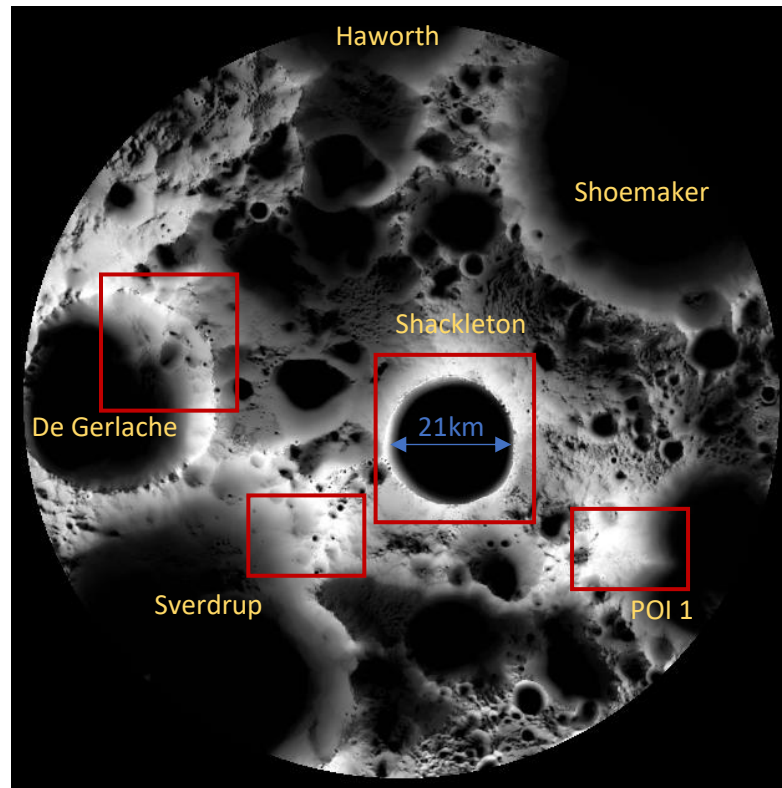


Figure 67: Time-weighted lunar south pole illumination map showing regions of interest, [8].

The rim of the Shackleton crater presents itself as a suitable position for solar arrays, with particularly high predicted illumination potential, [9]. The Shackleton crater itself is 21km across, and therefore almost 66km in circumference. The top right image of Figure 8 shows that even during night time conditions, the region between the Shackleton and Sverdrup craters are lit, at least for part of the year. It is also predicted that these elevated areas will receive the most sunlight during lunar winter. Figure 67 shows various points of interest (POI) located close to the Shackleton crater. Due north of the Haworth crater is Malapert Mountain, some 100km from Shackleton, which could receive light for up to 70% of the year, and so may be a valid choice depending on transmission system and habitat location, [9].

Care must be taken due to the rocky topography and steep slopes of the surface. Around the crater edges slopes may be approximately 20% in gradient (Figure 6) which is significant. Positioning of solar cells within the farms would need to be such that shadows cast would have minimal effect. Safe securing of panel supports may be difficult

because of the nature of the lunar soil. Advanced securing mechanisms involving drilling into rock would likely be required.

Based on potential arrays at the sites indicated, long lengths of cabling would be required; many tens of kms would be needed just to connect the array locations with the habitat. Above this would be the requirements for individual arrays, safety equipment, and within the habitat itself.

6.2. Generation

By developing three separate solar generation methods, the generation team was able to compare their energy outputs in order to assess which designs may be most suitable for the IGLUNA project.

Each design had benefits and drawbacks, with concept 1 providing a design, which enabled experimentation or life support to be housed within its structure. Despite the ability to adjust its solar panel direction in dual axes, manual movement was required making it unsuitable for large scale implementation. The body of the design was heavy and contained a large volume of unnecessary material, making it less cost efficient to transport and lowering its weight to power output ratio compared with concept 2 and 3. The device offered the ability to add mirrors to improve performance, which proved effective in raising output by 3.4% at 30°. This suggested that all utilised devices should hold this ability, as small percentage improvements in efficiency can have a big impact on large-scale deployment of panels. The loss this device incurs due to being fixed was 1.099 x10⁷ kWh/year on a farm of 5000m² compared with a dual axis system, showing the importance of tracking capabilities.

The single axis system delivered the ability to track the sun's movement in one direction autonomously, offering a large improvement of 1.098 x10⁷ kWh/year in solar output compared with a stationary panel. It was able to do so using smaller solar panels, meaning it would not need to draw electricity from the IGLUNA base to power its movement, giving it an energy saving advantage. The system was mechanical in nature and did not require cabling and programming, however this did limit the control and adjustability of the device. The device has a flat packed design allowing it to be transported more easily to the lunar base, which gives it an advantage over concept 1. Overall the weight of the device was lighter than concept 1, however it's weight to power ratio could be improved and the option for scalability of the device was limited compared with concept 3. The device would suffer losses due to its inability to track the sun's movement in the vertical axis, despite the majority of the sun's movement occurring in the horizontal axis at the lunar South Pole. The means of tracking suffered lag due to the angling of the solar panels, meaning it would likely incur further losses due to misalignment.

The dual axis solar tracker offered a further improvement to solar output compared with concept 2. This was attained through a more accurate and adaptable solar tracking system, which enabled perpendicular alignment with the sun at all, times. The weight of each individual device within concept was minimized whilst maintaining adequate strength to support the same 6V 200mA solar panel used by concept 1 and 2. This offered clear advantages over concepts 1 and 2 with regards to power output to weight ratio, providing an added benefit of reducing material transport and construction costs. Concept 3 also offered the ability to adjust the motion of a farm of devices using inputs from one device, reducing the overall complexity of the system and reducing overall maintenance requirements. Drawbacks include the increased number of moving parts with the addition of an additional motor, as well as the need for the motors to draw power from the grid. Relatively speaking the single axis and dual axis trackers offered similar levels of improvement at 1.098×10^7 a kWh/year and 1.099×10^7 a kWh/year, suggesting a single axis solar tracking system may be more cost efficient. This would depend on the energy requirements of the additional motors required for vertical adjustments, however the additional 10,039 kWh/year generated by the dual axis compared with single axis systems, would help alleviate this issue.

6.3. Harvesting

The data obtained during the analysis and the behaviour of the generators must be discussed, showing the strengths and weaknesses of each model.

The higher voltages obtained in the arch-shaped generator are directly related with the stresses obtained. Higher stresses are due to higher deformations in this model, produced by the different stiffeners used in each case. The cantilever generator deformation is constrained by the limit of the steel sheet which is much lower than the PVDF one (due to its flexibility), whereas the stiffener in the arch-shaped generator is the nylon66, a very flexible material that allows much bigger deformations than the PVDF. On the other hand, the output current is bigger in the cantilever generator. The difference is related to the deformation and stress variation velocity; although the velocity is relatively high for the arch-shaped generator, the high frequency in the vibration generator produces even higher speeds, leading to a higher output current and therefore more power than the arch shaped generator.

An important consideration when comparing the two generators is the environment and conditions of each analysis. The cantilever model is very favourable, assuming a free vibration, something not found in a real world, where internal mechanical and electrical resistance of the material occur as well as air resistance and thus the values should be analysed prudently. As mentioned, the cantilever model analysis is very optimistic, leading to results that could be confusing, avoiding a fair comparison with the arch-

shaped generator. To check if this generator is as effective as it seems, another analysis and output power calculation was performed. The new analysis shows that a small deflection produced an output comparable with the arch-shaped generator. The small deflection assumed was 0.624mm in the tip, and the procedure followed was the same as in the previous cases. The harmonic frequency is again the same and the deflection points where stress values are taken for the calculations are displayed in Table 15 and Table 16 .

With the stresses at these points, the output data shown in Table 16 is calculated. The results show that even for small deformation the output power is like the arch-shaped generator for only one cycle. If the vibration of the system is taken into account, the cantilever generator is found to be more efficient.

t	Y
0	-0,624
0,000251	-0,605
0,000503	-0,549
0,000765	-0,455
0,001004	-0,343
0,001253	-0,206
0,001489	-0,065
0,001594	0

Table 15: Calculation points

t	z	V	I	W
0	-0,624	114,75	0	0
0,000251	-0,605	111,31	4,60873E-05	0,00513
0,000503	-0,549	100,98	0,0001381	0,013945
0,000765	-0,455	83,77	0,000220798	0,018496
0,001004	-0,343	49,35	0,000485228	0,023946
0,001253	-0,206	37,87	0,00015497	0,005869
0,001489	-0,065	12,05	0,000368759	0,004444
0,001594	0	0	0,000382736	0
0,0017	0,065	-12,05	0,000382736	-0,00461
0,001936	0,206	-37,87	0,000368759	-0,01396
0,002185	0,343	-49,35	0,00015497	-0,00765
0,002424	0,455	-83,77	0,000485228	-0,04065
0,002686	0,549	-100,98	0,000220798	-0,0223
0,002938	0,605	-111,31	0,0001381	-0,01537
0,003189	0,624	-114,75	4,60873E-05	-0,00529

Table 16: Final results

For the analysis of all the results, the distribution of the stresses for the calculation should be considered. When the electric displacement is calculated, the distribution of the stresses is supposed as perfect, this means that all the compression and tension stresses take place on the same side of the material. This situation is unreal due to the interaction between the stresses in complex zones. Although this will lead to some small zones where the direction of polarization will not be coincident with the one assumed, the dominant bending stresses will lead to the voltage formation assumed. The results of each model will be therefore more reliable when the stress distribution is simpler, thus the cantilever the simpler in this case.

Another drawback for the cantilever model when considering large deflections is the life of the components. After performing a fatigue analysis, the cantilever model is found to last near 20000 complete cycles of loading at a low value for an object subjected to

vibration. Meanwhile the arch shaped generator has a life of more than $10e^7$ cycles. This problem could be solved by increasing the steel sheet thickness. However, if small deflections are analysed (as before), low stress values are found and safety factors lower than 5 are not reached. The advantages of the arch-shaped generator is the underfloor implementation, the long life of the components and the enhanced output due to the triboelectric material. The main advantage of the cantilever generators is the enhanced output values when vibrating.

The space needed for the implementation of the arch-shaped generator is bigger than in the cantilever generator, so less generators will fit.

With the values obtained in every generator analysed, the use of triboelectric material is shown to be unnecessary. The triboelectric materials enhance the output of a piezoelectric generator due to its output voltage, higher than the one obtained by piezoelectric materials. This statement is true when talking about nanogenerators where the deformation is smaller and lower voltage values are obtained; but when the generators are bigger (as it is the case), the voltages obtained are higher than the triboelectric ones.

6.4. Storage

6.4.1. Selection of Solution

Given a review of all potential options, the first stage was to rule out any option which had any characteristics which made them totally unsuitable for lunar implementation. This was not limited to any specific conditions but anything that would stop the solution from operating in lunar environments;

- The pumped hydro is a water-based system which, given the sub-zero conditions wouldn't function adequately on the moon
- Both supercapacitors and vanadium flow batteries simply aren't developed enough to carry out the purpose for which they are required

In order to select a suitable option from the remaining some self-determined basic requirements were created that would allow the removal of unsuitable solutions. The first is a low operating temperature ($<100^{\circ}\text{C}$) that wouldn't require special housing within the habitat.

- MCFC runs at incredibly high temperature that could potentially raise concerns over the safety of the habitat. Along with its slow start up and low power density this fuel cell becomes an unsuitable option.

A minimum efficiency of 40% was another requirement but none of the remaining options failed to meet this criterion. Meeting a minimum capacity requirement was suggested but all storage options can theoretically either be stacked or have more cells added to increase the capacity. A less quantitative and more qualitative review of the potential options was required in order to decide which would be the most suitable storage solution.

Compressed air on paper is a very suitable option but the downside is its requirement of specific geographic formations. Lava tubes pose a potentially suitable space but without further exploration it is impossible to design a system without a full analysis of the space. Non-airtight sections or structural instability are just some of the issues that would make the space unusable.

Nickel-Hydrogen batteries on paper also are a viable option but the development of Li-ion batteries has made them almost redundant. As mentioned previously, the similar cycle life, larger temperature window and high specific energy make the li-ion battery a much more favourable option.

A similar situation unfolds when comparing the PEMFC to the AFC. With similar performance but with no electrolyte (and all the other associated benefits) the PEMFC is undoubtedly more suited.

Comparing the Li-ion to the PEMFC brings about a closer contest. The Li-ion battery is superior in its energy density and efficiency but the reduction in capacity over time is where it presents an issue. In the case of a lunar outpost, storage may need to be operational every day for many years and a significant drop in capacity cannot be tolerated. The risk of thermal runaway is also not permissible from a safety point of view. Battery malfunctions also cannot be fixed meaning there is little contingency if something were to go wrong. PEMFC's on the other hand are basic in their construction and failed components can simply be removed with no further consequence. Much of the weight associated with fuel cells is the fuel itself but the presence of ice on the moon means there is a vast supply of fuel for the system.

The flywheel is the last remaining solution and while it simply wouldn't be feasible to scale it up for a primary storage option, its use as a secondary option is promising. As it is not chemical-based it won't deteriorate when it is not in use unlike many other options. It can store quick energy fluxes well albeit for a short amount of time. For the purposes of a back-up storage, which is to take over for parts of the primary system during malfunction, repair or maintenance, it is well-suited.

6.4.2. Reflections

Before concept generation a brief regarding the basic requirements for the electrolyser was proposed. As this is first and foremost a demonstrator project aesthetics were a high priority. A fully transparent design was decided upon to give those viewing the device an unobstructed view of both the design and the process occurring within. In order to successfully capture the gas at the separate electrodes, it should be channelled upwards independently into two openings. Given that testing of the device was to occur in Switzerland, portability and robustness was a necessity.

The initial single cylinder designs were dropped due to their confined space in which the electrodes would have to be placed. Also, the cylindrical design and requirement for a removable lid raised concerns that the separator would be difficult to seal entirely. Leaks would lead to a risk of mixing gas which is intolerable. The side tanks in one design were made to further separate the gas but further minimised the electrode space and was not suitable for manufacturing.

The two-cylinder designs that allowed storage of one tank inside the other proved both costly and provided little benefit. Ordering different diameters of both discs and tubes was considerably more expensive than ordering identical parts. The design intention was to save space and to keep everything in one piece as a simple package. However, the additional space required to store the second tank was simply wasted space and compromised the function of both the bigger and smaller cylinder by reducing electrode sizes. The benefit of having one unit versus two was small and yet the cost of implementing it was substantial (both financial and regarding features). It was also significantly easier to design two identical cylinders as opposed to ones which would fit together. Given the time sensitive nature of the project, it was decided to pursue the two-cylinder symmetrical design over all others.

The connection between both cylinders was one of the biggest design challenges faced throughout this part of the project. Maintaining transparency meant that all traditional plumbing fittings and fluid couplings could not be used as the majority of these were made from metal or opaque PVC. A custom fitting was the remaining option, but manufacturing introduced further issues. The initial CAD design was a connection piece with flanges at either end and a female housing in both the cylinders.

Magnets placed in both pieces would provide enough force at either side of the connection and gasket to ensure a water-tights seal. Manufacturing the recess proved difficult as a completely flat surface was required to create a seal and the tools to produce this recess were not readily available. Circular recess can be created with flat wood drill bits, but they are only available up to 32mm which was not large enough. As previously mentioned, attempts to remove the materials by heating it and removing pieces with pliers was both time consuming and ineffective. The surface which remained was full of bumps and simply wouldn't be usable (Figure 68). A redesign was devised which would essentially half the connection piece and fix each end to the cylinders. The flanges would protrude from the cylinders and connect to one another. While this was implemented in response to a failure, the design did have some benefits. It reduced the number of separate components from three to two and also the number of non-fixed connections from two to one. The old design required a water tight 'quick release' fitting at either end of the connection piece while the revised design only required one at the connection of the flanges. It also allowed for more magnets to be used creating a more secure connection and lowering the risk of leaking. The only drawback was the protrusion of additional pieces from the cylinder which was initially avoided to lower the risk of damage during transport. Cylinders are predictable and clean shapes and don't require special considerations and any outcrops increases the risk of it catching on something or inducing unwanted stresses on the structure. This change in design also made some other features redundant.



Figure 68: Failed Connection Piece Housing

The increased length in one of the cylinders along with the cut-out from one of the steel plates was to accommodate the connection piece when not in use. The idea was that it

could be stored inside the slightly larger cylinder for convenience. Removing this piece and incorporating a fixed design left these design features without purpose.

Changes to design are often inevitable and another slight variation was the removal of two rods connecting the steel plates. Substituting the singular central rod for the three used in the previous design was in the interest of simplicity and reducing unnecessary work. Fewer threaded rods needed to be cut and twenty fewer holes needed to be drilled into the steel plates. There were also no disadvantages to simplifying the design.

Another change implemented was the removal of the latching mechanism present in the CAD model. The weight of the thick acrylic was heavier than anticipated and provided a large enough force to mitigate the need for a latch. Given that there would be no overpressure in the cylinder and the gas could escape easily unimpeded through the bulkhead fitting there was no need to secure the lid.

The triangular supports present in the CAD model were also substituted for the 120° cylinder supports (Figure 69). This saved the purchasing of additional acrylic and the large surplus of the 34mm diameter tube could be put to use.

Although throughout this section the goal of designing and constructing an electrolyser was achieved it was not without its problems. During the design stage, a lack of forethought for the manufacturing of a component forced serious amendments during construction. Available workshop facilities and staff could have been taken advantage of throughout the practical stages. Heavy reliance on the Strathclyde workshop was avoided as this added risk of delays to the project. However, attempts to manufacture all components without the use of the workshop was met with difficulty. Though challenges were faced, they were overcome, and the electrolyser was constructed on schedule.

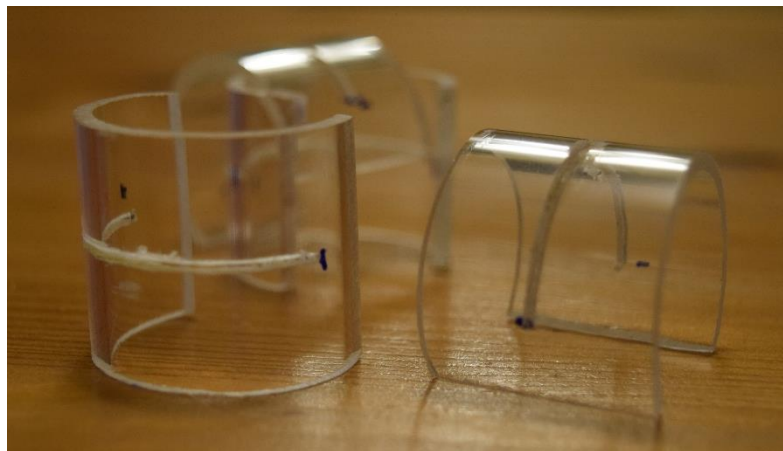


Figure 69: Steel Plate Supports

7. Project Management

7.1. Sub-Team Formation and Structure

7.1.1. Overview

Given the size of the groups, effective project management was imperative for the success of projects across all groups. The first stage was to establish project leaders with the primary functions being to streamline communication between the advisor and the group, lead meetings and take control of organisation and planning. It was suggested by the advisor to nominate one leader from each of the masters-level groups, where one would also take on the role of the overall group leader. Jacob Kent took on the role for the Mechanical Engineering group and Louise Guthrie was both the primary leader role and the EME group leader. Another position responsible for all communication between Strathclyde and the ESA was suggested and Joelle Yu took on this role.

Following the nomination of the leaders, group division was the necessary step before work could begin. The nature of power systems provided four distinct areas into which sub-teams could be formed;

- Generation
- Storage
- Harvesting
- Distribution

In order to divide groups, all members put forward which teams they would and wouldn't like to participate in. Louise then proceeded to divide up the students into the sub-teams that would work together throughout the year. The only other criteria that influenced the formation was to spread students of the same discipline and year group evenly throughout the teams where possible. The reasoning behind this was to ensure that each sub-team had expertise in both Electromechanical and Mechanical and assistance could be provided within the group. Harvesting was the only team without an EME student as two EME students had been placed in distribution. The heavy focus on programming and electronics within distribution justified the need to have an additional student with experience in the subject area. All other teams contained at least one Mech Eng and EME student. Each of the fourth-year students were also divided amongst the groups with one in harvesting, one in storage and the last in generation.

7.1.2. Reflection

One of the challenges encountered was the lack of work for all parties within the distribution team. This wasn't a lack of volume of work but a lack of tasks that could be completed by three separate students. The work within the team following research fell naturally into two separate sections. While this was an inconvenience, there was plenty

of work to in other areas and the third student was reassigned to the generation team. This allowed the generation team to complete more work and develop additional prototypes that previously would not have been possible.

While these groups were designed to best tackle the challenge set by the ESA, the arrangements created significant difficulty when dealing with Strathclyde imposed deadlines and requirements. For fourth year students, this biggest challenge was to carve out a significant individual project within whichever sub-team they were participating in. While this was achieved, (taking the form of a flywheel storage system, solar tracking system and thermocouple harvesting system) there was definitely a compromise with regards to the targets set out by the ESA. As the individual students have to focus on completing their chosen topics in order to fulfil their project requirement (which is understandable), they would naturally be less inclined to assist in areas in which they would not receive credit. This also holds true for the fifth-year students but there is naturally more freedom within a group project as helping one another is encouraged and can also be documented. There exists a conflict of interest for all students between the institution that is responsible for delivering the mark that contributes toward one's degree and the institution which holds little to no influence over academic grading. Little can be done practically to combat this and it is simply the responsibility of the student to do right by all institutions which they are working with.

The lack of work faced by distribution is perhaps not an issue that can be always solved in future projects. Some tasks will often require more or less work than initially anticipated although more research could have been done prior to the division of teams to attain a better understanding of the workload each team with face. The conflict of interest would require a restructuring by one of the institutions to ensure that the goals set for the student were more closely aligned therefore reducing the need for the students to neglect one in favour of the other.

Working with different disciplines is now common practise but experiencing the benefits first-hand showed how useful it can be. Limited knowledge in control and electronics amongst the Mech Eng students were resolved with relative ease by those studying EME. Although the subject are very closely related, different experiences and mindset assist greatly in group discussions. Discussions with students who have studied together for five years often produces a 'echo chamber' effect with few new perspectives being offered. Working with different disciplines and year groups brings a surprisingly fresh feel to group work.

7.2. Communication

Note: Only high-level communication between the supervisor, ESA and leaders is discussed in this section. Inter-team and group communication will be elaborated upon in the Group Working section.

7.2.1. Overview

Effective communication is crucial for management to keeping everyone up to date with developments, managing any changes and ensuring everyone is working toward the same common goal. The communication structure was unusual due to having two independent bodies to report to.

At the request of the ESA, fortnightly video calls were scheduled throughout the two semesters to track progress of the Strathclyde team. Given the number of students involved in the project only two or three students were present at any one meeting. The two team leaders along with the student in charge of ESA communications conducted the majority of these meetings.

Little direct contact was made with the supervisor throughout the semesters, which left much of the project management up to the two leaders. Periodic updates were given to the supervisor as and when they were required. These were either given in the form of group meeting or presentations.

Any and all information received from either of the two sources could then be passed on to the rest of the team at group meetings or through group messages.

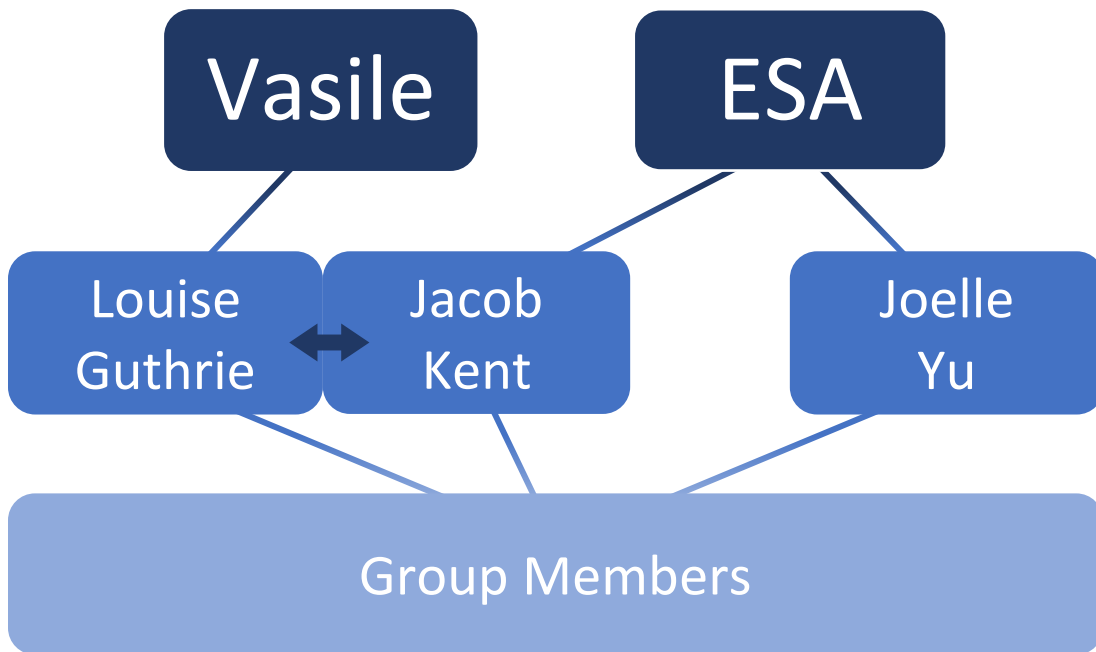


Figure 70 : Communication Structure

7.2.2. Reflection

Initial plans were to schedule the ESA meetings in a conference room in the TIC every fortnight, but this soon became tedious and counter-productive. Irregular meeting times meant that the exact date and time of the meetings was often not known until a few

days prior to the meeting. The room had to be booked in advance which was a slow and cumbersome process that involved emailing individuals as there was no access to an online booking service. Students were also not given access to the required room and thus had to be let in by another member of staff. This process was time-consuming and was dropped in favour of using a laptop in another easily accessible room in the university. Though no revelations were had, an important lesson was learned in not sticking to a system which is not working.

The 'hands-off' approach taken by the supervisor was beneficial as it allowed students to develop project management skills. It also provided the students with greater freedom to complete the work in a time frame that best suited the group. Giving students free reign on planning the final year project has been one of the key learning points of this experience. The perceived lack of a 'safety net' creates an environment more akin to the world of work.

Consistent fortnightly meetings set by the ESA proved to be a successful method of communicating updates. The two-week time frame was not too intrusive and allowed enough work to produce substantial updates to the ESA. It also proved frequent enough that all non-urgent questions could be raised and answered

7.3. Time management

7.3.1. Overview

Projects cannot succeed if any aspects of project management are neglected and time management is no different. Poor time management can have serious repercussions and many projects become delayed for this very reason. Fixed deadlines will dictate the overall schedule which must be adhered to but the freedom between these deadlines is where self-imposed targets must be set and where discipline must be exercised.

The two bodies which governed this project created for unusual scheduling as each had its own set of fixed deadlines entirely independent from one another. To further add to the situation, each department and year group held differing schedules therefore within the larger group, five different schedules had to coexist and be dealt with (4th yr EME/4th yr Mech Eng/5th yr EME/5th yr Mech Eng). On an entire group scale, keeping track of every student deadline was obviously not a realistic option. Therefore, it was decided that the departmental schedule of each student would not be kept track of. Instead, when scheduling deadlines were set in meetings any pertinent information could be raised by individuals. Fixed deadlines set by the ESA were noted by all as these were common for all students.

Within the Mech Eng fifth year group, a Gantt chart was made with key departmental dates along with key ESA dates. A clear visual was beneficial for planning and ensuring work was completed on time. Fortunately, many of the dates for design finalisation and construction were looser than those imposed by Strathclyde. This meant that, for the

most part, ESA deadlines could be ignored, and focus was shifted to the university deadlines. The few ESA specific requirements were highlighted, and attention was given those as necessary. The most important of which was a preliminary design review in late November. This forced the entire group to fast-track some design work prior to the review.

7.3.2. Reflection

The multiple sets of deadlines proved to be one of the largest challenges for the larger group but the system of individuals giving significant forewarning of upcoming deadlines was successful though not ideal. Where members of a group have different deadlines imposed by different parties it becomes very difficult to keep track of everything. Ideally, a group calendar could have been implemented in which all students could input deadlines. Though, there would have been the risk of it becoming too cluttered and losing its usefulness. That remains to be seen but it is a suggestion which could be tested in future projects.

When working in large groups it is easy to lose track of upcoming events so everyone keeping track of their own key dates ensured none of the shared ESA deadlines were missed. Giving the responsibility of scheduling to one person runs the risk of deadlines slipping through the net if that individual makes an error. Making everyone responsible for their own dates significantly reduces the likelihood that large shared deadlines will be overlooked.

7.4. Financial Management

7.4.1. Overview

Budgeting was initially set up as an entire group wide affair in which a document outlining everyone's intended expenditure was created. The idea behind this, was to bring everyone's budget together and allocate it to where it was required. In theory this was the best option but practically it caused some issues. Requests are required to be signed off by a staff member from the department, making cross-departmental budget sharing considerably more difficult. In lieu of this, it was decided to keep within personal or team allocated budgets where possible. Although this was far from the most financially-efficient method it was more time-efficient. When the stage is reached where parts are purchased, time is valuable and spending it waiting for paperwork to be signed off can be costly. Regarding the Mech Eng group, two of the students work was entirely research based which released additional funds for the two practical projects. This significantly eased the financial pressure and the practical projects progressed with the knowledge that they would remain within budget.

7.4.2. Reflection

Having to alter the initial budget plan was far from ideal but it was clear working with budgets across departments was not an option. Constraining everyone to personal

budgets was likely not the optimum solution but with the timeframe provided it was the most appropriate option. If this problem was foreseen, a meeting could have been scheduled with all the project supervisors from both department in order to plan a workaround. If a solution was achieved and a shared budget was implemented it would have given significantly more freedom for the entire group.

7.5. Statement of Work Review

The statement of work (SoW) is a document (located in appendix 7) which states clearly the aims of the project, likely risk and methods of mitigation, a proposed methodology and a definition of the scope of the project. A comparison between the finished project versus the SoW will give shed light on the success of the project with respect to our initial aims and how the project developed and varied from our initial expectations.

The 'Key Objectives' and 'Project Deliverables' outlines the aims of the project back in October which in summary was to 'derive technical requirement for the power system' and produce 'various prototypes for the field test in the alps'. This has been successfully completed by the larger group and the Mech Eng group have contributed heavily to the prototypes within the generation and storage team and research in the distribution and harvesting teams. One of the key objectives was to 'size the power harvesting, generation and storage system' which has not been completed. It is unclear if this was misinterpreted from the outset or whether the focus from the ESA shifted away from this in the early stages. It quickly became apparent that the main focus of the INGLUNA initiative was to develop demonstrator projects that could be displayed in Switzerland. This was not necessarily practical/working models but could also be a display of conducted research into relevant technology. The emphasis on 'sizing' a power system was dropped by the team as efforts were concentrated on the demonstrator projects.

A review of the proposed methodology, though high-level in its description, was followed closely by the team throughout both semesters. Comparison of the Gantt chart with how the project unfolded was also remarkably similar. Often with such early estimations the final schedule is deviates heavily initial plans. In this case the majority was accurate however the design stage started considerably later than thought but the large window of manufacture allowed for delays during the designing.

7.6. Final Reflection

The management of projects is a skill that requires practise to develop and this project has been a learning curve for much of the team. With a sizeable group such as this, problems were inevitable. Attempting to keep everyone focused on the same goal while still meeting the requirements of each individual's course was difficult. Communication was inefficient at times but was refined as the weeks progressed. Keeping to a tight schedule in amongst a variety of other commitments to other classes again presented issues. In the end the goals set out at the beginning were achieved and a great deal was

learned along the way. Specific suggestions for changes and future work have been made throughout this review but an overarching learning point has been made abundantly clear. The undertaking of a large group project is not to be taken lightly. The organisation and attention that needs to be given, to even relatively small projects such as this, is significant. While this may have been known before, the experience has made the need for good project management far more apparent.

8. Team Work

8.1. Overview

As mentioned, it was imperative that such a large team have effective management. Combined with this, communication between sub-teams and departmental groups was crucial. In all, there was an attitude of determination to meet the challenges set, focussing on feedback, staying connected, and trying to make-up for lost time at the project inception. This section is a review of the group working processes with reflections.

Within this section 'full team' refers to the entire cohort involved in this project at the University of Strathclyde; 'sub-team' refers to the 4 main teams at Strathclyde, distribution, storage, harvesting and generation; 'departmental team' refers to the 4 individuals taking part in the project for their masters group project, in Mechanical and Aerospace Engineering; 'IGLUNA projects' refers to any/all of the separate teams spread across Europe.

8.2. Departmental Team Dynamic

8.2.1. Overview

The MAE departmental team originally consisted of 5 members; Sarah, Pedro, Jacob, Jonathon and Laetitia. Laetitia was present for 1 semester and was part of the harvesting sub-team.

The members were assigned based on project preference, rather than forming a team and selecting the project. This was recommended as generally teams function more efficiently if they do not consist entirely of close friends. Each member of the team brought with them experiences of previous group work and individual projects, however none had worked on a university project of this scale before.

During departmental team meetings, discussion was free but always kept on-track. Each individual took notes in the meetings, with documentation uploaded to a shared area when required. The general atmosphere in departmental team meetings was constructive and sociable. In semester 2, team meetings involved review of prototype concepts. Members were free to ask questions regarding design choices and assumptions made, perhaps highlighting overlooked dangers with the designs. This was beneficial for the design of the component and for project overall. It was clear that there was no maliciousness attached to the discussion; the team was merely looking anew at the design, from different perspectives.

8.2.2. Reflection

One particularly good aspect of departmental team meetings was the ability to discuss complex engineering concepts. Hand-drawn diagrams and computational renders were used allowing each member to clearly understand the work of their peers. The

opportunity for feedback from other engineers was invaluable to the design process. It was definitely found that it is better to question decisions, making them better, rather than ignoring concerns.

Improvement was made to departmental meetings during the project period. During reflection for the interim assessment it was decided that more time be allowed each week for discussion. This improved organisation and target setting in semester two. Team-decided deadlines always allowed for a tolerance.

Minor improvement could have been made to the organisation of the meetings, as well as the note taking. Due to the potential for high numbers of meetings required during the project however, too much time may have been spent planning rather than working.

8.3. Project Focus

8.3.1. Overview

The main outputs of the project are the proof-of-concept prototype models for use in the field test. During the project, focus shifted from considering theoretical ideas for the moon to developing these prototype models.

8.3.2. Reflections

These models are a key output of the programme. It could be argued that at times, the moon base and the prototype design were thought of as two separate projects. During second semester this was remedied. More was known about the lunar habitats, and designs were created with relevance to the theoretical space mission and the lunar environment.

8.4. Communications

8.4.1. Overview

Each member of the departmental team was part of:

- Sub-team meetings
- Full team meetings, with all 11 members
- Departmental (MAE) team meetings

Sub-team meetings were used to ensure that each member was making sufficient progress. These allowed for problem solving and clarifications, discussion of ideas and decision making. The frequency of these meetings varied, though generally was 2-4 times each month.

Full team meetings allowed for sub-team progress to be quantified in terms of overall SSC/ESA objectives and deadlines. They also allowed for discussion between the sub-teams to ensure some design overlap, and for resolution of any technical issues. The meetings were kept succinct, with a clear aim and set topics to discuss. These meetings took place up to twice each month, depending on deadlines.

Departmental group meetings were held approximately once each week, decreasing in number during periods with other significant university commitments. These meetings were used to ensure that requirements for the departmental group project were met, such as report deadlines, as well as giving time for discussion of concerns and reflection of processes. They allowed a more personal assessment of progress and quantification of work achieved to date. They also facilitated contact with Jacob Kent, one of the leaders of the project.

Aside from group meetings, communication was facilitated using instant messenger conversations (primarily on Facebook); one for the full group, one for each sub-team, and one for the departmental group. Rapid communications always ensured that laboratory access and sharing of equipment was possible. They also allowed for general issues to be quickly resolved, though more detailed questions were reserved for meetings.

The Swiss Space Centre encouraged use of Slack. This is a cloud-based service, used to communicate with the other IGLUNA project teams around Europe and mentors at the SSC. There are many different channels allowing message exchange on a number of subjects. There is for example the general admin channel, via which the SSC can give small updates and information to every person involved in the IGLUNA project. More specifically for the University of Strathclyde team, there is the 'p18-powermanagement1' channel for direct communication with the SSC. Direct communication with other teams is also possible, for sharing literature or technical results. At the time of writing there have been 3100 messages in total sent using Slack.

8.4.2. Reflection

Sub-team meetings were crucial to the success of such a large project. They ensured that individuals were meeting demands and staying up-to-date with group progress.

It was useful that large full team meetings were generally organised and focussed, as with 11 individuals present it could have been difficult to control the purpose of discussion. In some cases, discussion devolved to separate groups, beneficial when generating ideas but having a negative effect on the overall flow of the meeting and making note-taking impossible. It may have been more beneficial to have one member from each sub-team elected to represent at these large team meetings, requiring the pre-release of a thorough agenda, though this would have been at a creative loss. By all taking part, the team learned to be personally prepared, and keep description of current work precise and informative. It was also important to listen carefully to what others were saying, important in all aspects of life. Overall, team leaders were approachable, affable and helpful.

In general, the team learned the importance of a structured flow of information. This applies particularly to feedback from the SSC during video calls as it could take a relatively long time for this to trickle down to those not at the meeting.

Slack is a useful tool, effectively allowing exchange of knowledge. It was very useful for talking to other project teams and the mentors at the SSC. The communications lead (Joelle) was likely the most active contributor. Overall, it could have been better utilised by the Strathclyde team. For project communications, there are many other options for keeping in touch. It might have been helpful to assign the task of relaying important general updates from Slack to an individual, leaving the communications lead to work more directly with other teams and the SSC.

8.5. Information Sharing

8.5.1. Overview

Documents were shared to all members online using Google Drive. The Drive for the full team had folders for the four sub-teams, integration, and administration. Everyone had access to all of the folders, facilitating the sharing of knowledge. The administration and integration folders held documents, risk assessments and collaborative presentations, for example. The departmental team folder allowed for sharing of information like the statement of work and updating of the Gantt chart.

Laterally, for compilation of the final report OneDrive was utilised via the university email network. Both Google Drive and OneDrive allowed for real-time editing of work from multiple team members.

The Swiss Space Centre ShareFile was used for uploading documents and presentations to be reviewed by mentors. There was a strict naming convention for files. It also allowed project teams across Europe to learn more about the other projects in the initiative. Important introductory and explanatory documentation was also contained in the ShareFile.

8.5.2. Reflection

The use of online sharing of information was very important to the success of the project. It allowed individuals from different sub-teams to share research, even if it was not relevant to their own field. The team collaborated well on presentations, effectively utilising the shared space. Undoubtedly, increased familiarity with the resources on the SSC ShareFile would have benefitted the team.

8.6. Website

8.6.1. Overview

Creation of the project website was a departmental objective. It presented the opportunity to summarise the aims, methods, and deliverables of the project. It will also increase exposure for the IGLUNA project.

The website is an important form of communication, giving information for a general audience as well as technical information and estimations for the lunar habitat. It allows the prototype designs to be showcased and put within the wider context of the challenges of a lunar habitat.

The content on the website involves all four sub-teams working in collaboration. Information is presented covering general IGLUNA project aims, as well as the specific solutions selected by power generation, distribution, harvesting and storage. A wide collection of results, comprising of theoretical moon base predictions, technical drawings, renders, photographs, and videos has been compiled. The progress blog has been used to note significant events along the timeline of the project.

8.6.2. Reflection

The website is an excellent tool for information sharing, but also for team reflection. It is pleasant to see achievements and progress. It showcases the final results (to date) and gives a fine overview of the established power system, based on the work carried out by the MAE fifth year team. Some of the progress blogs were back-dated as they occurred before website creation. For this, note taking in log books has been crucial. Ideally, it would have been constructed at the project inception.

In all, the website is easily accessible and simple to use, clearly presenting each section in an aesthetically pleasing surrounding. Visual depiction can even make the complex concepts involved in prototype and habitat design accessible to children, capturing their attention. Thus, it can be exhibited during outreach activities – a key aim of the IGLUNA initiative is to inspire the next generation of space engineers!

8.7. Final Reflection

Project development needs and working process have been atypical due to the international scope of the project, the number of teams involved and different deadlines with respect to the ones fixed by Strathclyde university; the adaptation to these facts has been a major goal for the group, inflecting its behaviour. This adaptation has been made by means of the group organisation and communication discussed and agreed by all the team members, which has been described along *project management* and *team work* sections. The success of these decisions and the quality of the team work can only be appreciated at the end of the project, checking the achievement of project goals, the quality of the achievements and the cohesion throughout the whole project, reflected in this report. With that in mind, it can be said that although some management decisions could have been better chosen, the overall result is clearly positive, obtaining the satisfaction of all the team.

9. Conclusion

9.1. Distribution

Recommendations have been made for a number of aspects of the distribution system for the lunar habitat. These include establishment of a system hierarchy, assessment of potential distribution mechanisms, assessment of appropriate material choices, and consideration of future technologies.

The system hierarchy focusses on the life support system, making reference to other IGLUNA projects that are concurrently being worked on around Europe. A version of the system hierarchy is implemented in the field-test prototype, which contributes a significant part of project work for other members of the sub-team.

It was decided by the distribution sub-team that the start-up condition should be chosen for the design. This involved over-ground cabling with insulation, though there is the idea to consider wireless power transfer in future. A number of materials have been suggested for connectors and conductors, with some small consideration to the materials of the future which are currently still in research.

Significant examination of the south pole environment was carried out, establishing the range of areas to be considered when assembling the power network. Namely these were the exposure to sunlight, the gradients of the lunar surface, and the potential effects of moon dust. Positioning of the solar panels, fuel cells, and waste-energy generators has been considered, tying the results of the project together into one coherent concept.

9.2. Generation

With the goal of developing a solar power generation system for the IGLUNA project, the three concepts designed offered a range of uses within the IGLUNA project. Key components of an effective power generation system within the lunar environment would be the power output to weight ratio, tracking capabilities, design complexity and scalability. The single axis solar tracking system offered solutions to a number of challenges including horizontal tracking, self-sufficient movement and reduced weight. It however did not compete with concept 3 with regards to design simplicity, tracking accuracy and scalability.

The dual axis solar tracking system (concept 3) offered solutions to the fundamental requirements set by the generation team. These included accurate tracking capabilities, high power output to weight ratio, minimised transport and construction costs and scalability. Both tracking systems offered large improvements to the solar energy output when compared with a stationary panel, where the single axis tracker offered a 1.098×10^7 kWh/year improvement and the dual axis offering 1.099×10^7 kWh/year, for a

5000m² solar panel surface area. The addition of mirrors set at 30° showed a 3.4% increase in output energy, which could further increase annual output by 3.737 x10⁵ kWh/year.

The dual axis solar tracking system offered the largest increase in output, with an additional 10039 kWh/year compared to concept 2. It offered the strongest power output to weight ratio, with improved adaptability through programmable control and scalability. It is therefore clear that the dual axis solar tracking system would offer the most effective solution for developing a robust power generation system for the IGLUNA project.

Future work might include a study into the power requirements of the vertical axis motor of the dual axis tracking system, as well as any increases in maintenance and operational down time arising from the additional machinery. This might have an impact on any decision to choose a single-axis or dual axis system, due to the relatively minute improvement in power output due to the small vertical changes in the sun's movement in the lunar sky.

9.3. Harvesting

The project was focused on the under-floor implementation of the generators where the cantilever generator proved to be the best choice, being able to generate strong output values with small disturbances (the data displayed was obtained with a 20 N force). In this case, the maximum deformation of the generator should be limited to avoid failure problems and consequently its output values will be reduced, being a more effective production system though. Apart from the application discussed along the project, this kind of generator could be used in other places or situations inside the moon base, for example, door and vibrating machines could activate cantilever energy generation. The arch-shaped generator has demonstrated to be easily implemented needing higher working frequencies to increase the output current and therefore its performance; this generator could be as well used in other situations as inside the shoes, under the beds or even in clothes. This last application mentioned, currently under development, is to extract energy from clothes when stretched or touched.

During the analysis unexpected results were found such as the lower output of the arch-shaped generator even when producing higher voltages or the low fatigue resistance of the cantilever generator. This and more unexpected results produced the change in the way of focusing some aspects of the project, leading to the results and conclusions explained.

Piezoelectric generators have shown that interesting power output can be extracted from them, being a good opportunity for energy harvesting in the future due to its efficiency and the large variety of situations where they can be used. During the project

different layouts of generators have been shown and analysed, allowing the comparison of their behaviour and properties. The results obtained are not supposed to be used as categorical and future work must be done to manufacture physical prototypes and compare the results with the ones displayed in this report. This future work will be used to improve and develop this technology, using the work done in this project as a path and a guideline, taking advantage of the tools developed.

9.4. Storage

Identified as a necessity within a power system, storage of energy was thoroughly investigated, and a variety of viable options were identified. Less conventional options including supercapacitors and flow batteries exhibited exceptional performance in certain areas but lacked certain characteristics that would make them suitable for this case. Larger storage options which have had commercial success and positive track records on Earth were found to be considerably less attractive options for lunar implementation. The low temperature conditions (down to 30 K) rendered pumped hydro useless and lack of confirmed geographical suitability meant the risk of implementing CAES was too high. The likes of Li-ion batteries proved to be a good option, but the fuel cell was chosen above all others. Its simple construction, longevity along with the supply of ice on the moon made the fuel cell uniquely suited for lunar applications. The flywheel showed promising characteristics for a secondary option due to its maintenance of performance when not in use and its flexibility for energy storage.

The design and construction of an electrolyser was the following stage of the project. An initial period of brainstorming produced a variety of options, but a final two-cylinder design was soon decided upon. A CAD model was drawn up and materials were purchased. Much of the construction followed the initial CAD model but some variances from the plans took place (as is often the case with practical work). The final model was successfully built despite many challenges faced throughout the construction stage.

Looking forward, though a lot has been achieved there is still significant room for development. A full testing campaign to attain round trip efficiencies along with power outputs would be suggested. Attaining definitive proof that the chosen option would be most appropriate but cannot be completed without comparison. The development of a similar system using competitive storage options such as Li-ion batteries would give more credibility to the use of fuel cells for lunar applications in the future.

9.5. Overall Project Conclusion

A significant contribution has been made to the Project 18 tasks, in partnership with the other engineers at the University of Strathclyde. Considered are the creation of practical prototyping for the field-test and theoretical predictions for the moon habitat; the link between them is very important for this project. There has been cooperation between sub-teams as well as across Europe. Overall, the project has been a success when evaluated against individual expectation, departmental demands, and IGLUNA objectives.

References

- [1] O. Kirchhoff, G. Petit, D. Bass and G. Feusier, "IGLUNA a Habitat in Ice: Starter Package Documentation," European Space Agency and Swiss Space Centre (unpublished), 2019.
- [2] N. Jarvstrat, "A Self-Sufficient Moon-Base Analogue," in *Lunar Settlements*, Boca Raton, CRC Press, 2010, p. 362.
- [3] Z. Khan, A. Vranis, A. Zavoico, S. Freid and B. Manners, "Power System Concepts for the Lunar Outpost," NASA, Albuquerque, 2006.
- [4] NASA, "Lunar Reconnaissance Orbiter," NASA, [Online]. Available: <https://lunar.gsfc.nasa.gov/moonartgallery.html>. [Accessed March 2019].
- [5] NASA, "Lunar Reconnaissance Orbiter Camera: NAC South Pole PSR Mosaic," NASA, [Online]. Available: http://wms.lroc.asu.edu/lroc/view_rdr/NAC_POLE_PSR_SOUTH. [Accessed March 2019].
- [6] NASA, "Lunar Reconnaissance Orbiter Camera: South Pole NAC Mosaic," NASA, [Online]. Available: http://wms.lroc.asu.edu/lroc/view_rdr/NAC_POLE_SOUTH. [Accessed January 2019].
- [7] European Space Agency, "Lunar Lander: human spaceflight and exploration," ESA, [Online]. Available: http://www.esa.int/Our_Activities/Human_and_Robotic_Exploration/Lunar_Lander/Exploring_the_lunar_South_Pole. [Accessed January 2019].
- [8] NASA, "Lunar Reconnaissance Orbiter Camera: WAC Time_Weighted South Pole Illumination Map - WAC_POLE_ILL_TWI_SOUTH_100M," NASA, [Online]. Available: http://wms.lroc.asu.edu/lroc/view_rdr_product/WAC_POLE_ILL_TWI_SOUTH_100M. [Accessed January 2019].
- [9] D. Bussey, J. McGovern, P. Spudis, C. Neish, H. Noda, Y. Ishihara and S. Sorensen, "Illumination conditions of the south pole of the Moon derived using Kaguya topography," *Icarus*, vol. 208, no. 2, pp. 558 - 564, 2010.
- [1] NASA, "Slopes on the South Pole," NASA Goddard, 2011. [Online]. Available: <https://lola.gsfc.nasa.gov/feature-20110705.html>. [Accessed March 2019].
- [1] D. Paige, M. Siegler, J. Zhang, P. Hayne, E. Foote, K. Bennet, A. Vasavada and e. al, "Diviner
1] Lunar Radiometer Observations of Cold Traps in the Moon's South Polar Region," *Science*, vol. 330, pp. 479-482, 2010.
- [1] Copper Development Association Inc., "The Metallurgy of Copper Wire," Copper Alliance,
2] 1997. [Online]. Available:

<https://www.copper.org/publications/newsletters/innovations/1997/12/wiremetallurgy.html>. [Accessed March 2019].

- [1] NASA, "Overview of International Space Station Electrical Power System," November 3] 2016. [Online]. Available: <https://ntrs.nasa.gov/archive/nasa/casi.ntrs.nasa.gov/20160014034.pdf>. [Accessed March 2019].
- [1] National Aeronautics and Space Administration (NASA), "Reference Guide to the 4] International Space Station," NASA, 2015.
- [1] Japan Aerospace Exploration Agency (JAXA), "Research on Microwave Wireless Power 5] Transmission Technology," JAXA, 2013. [Online]. Available: www.kenkai.jaxa.jp/eng/research/ssps/hmi-mssps.html. [Accessed March 2019].
- [1] NASA, "Bizarre Lunar Orbits," NASA, 6 November 2006. [Online]. Available: 6] https://science.nasa.gov/science-news/science-at-nasa/2006/06nov_loworbit/. [Accessed March 2019].
- [1] G. Ramos and J.-S. Yuan, "Wireless Power Transfer for Space Applications," NASA, 7] Orlando, 2011.
- [1] Granta Design, "CES EduPack," Granta Design, 2018. 8]
- [1] European Space Components Coordination, "Polyimide Insulated Wires and Cables Low 9] Frequency, 600V, -100 to +200C," European Space Agency, 2012.
- [2] European Space Components Coordination, "Coaxial, Triaxial and Symmetric Cables, 0] Flexible, -200 to +180C," European Space Agency, 1999.
- [2] European Space Components Coordination, "Wires and Cables, Electrical, 600V, Low 1] Frequency," European Space Agency, 2017.
- [2] NASA, "Systems," [Online]. Available: 2] https://www.nasa.gov/pdf/167129main_Systems.pdf. [Accessed January 2019].
- [2] NASA, "ECLSS," NASA, [Online]. Available: 3] <https://www.nasa.gov/centers/marshall/history/eclss.html>. [Accessed March 2019].
- [2] E. Cameron, "Helium Mining on the Moon: Site Selection and Evaluation," *The Second 4] Conference on Lunar Bases and Space Activities of the 21st Century*, vol. 1, pp. 189- 197, 1992.
- [2] T. Simko and M. Gray, "Lunar Helium-3 Fuel for Nuclear Fusion: Technology, Economics, 5] and Resources," *World Futures Review*, vol. 6, no. 2, pp. 158 - 171, 2014.

- [2 N. Lovegren, "Chemistry on the Moon: The Quest for Helium-3," 21st CENTURY SCIENCE & 6] TECHNOLOGY .
- [2 I. Sviatoslavsky, "Processes and Energy Costs for Mining Lunar Helium-3," NASA, Madison. 7]
- [2 A. Kleinschneider, M. Lamers, L. Hubert, B. Dijk, J. Blange, J. Hogeveen, R. Noomen, D. 8] Overstraeten, R. Reijnst, N. Hoorn and L. Boer, "Feasibility of lunar Helium-3 mining," in *40th COSPAR Scientific Assembly, Moscow, 2014*.
- [2 Astronoo, "Travel photon or random walk," Astronoo, June 2013. [Online]. Available: 9] <http://www.astronoo.com/en/articles/journey-of-the-photon.html>. [Accessed March 2019].
- [3 V. F. Damon Turney, "Environmental impacts from the installation and operation of large- 0] scale solar power plants," *Renewable and Sustainable Energy Reviews*, vol. 15, no. 6, pp. 3261 - 3270, 2011.
- [3 S. Ong, C. Campbell, P. Denholm, R. Margolis and G. Heath, "Land-Use Requirements for 1] Solar Power Plants in the United States," National Renewable Energy Laboratory.
- [3 J. Summers, "5 largest solar farms in the world," Origin, October 2018. [Online]. Available: 2] <https://www.originenergy.com.au/blog/lifestyle/5-largest-solar-farms-in-the-world.html>. [Accessed March 2019].
- [3 L. Chaar, L. Lamont and N. Zein, "Review of photovoltaic technologies," *Renewable and 3] Sustainable Energy Reviews*, vol. 15, no. 5, pp. 2165 - 2175, 2011.
- [3 NASA, "About the Space Station Solar Arrays," NASA, August 2017. [Online]. Available: 4] https://www.nasa.gov/mission_pages/station/structure/elements/solar_arrays-about.html. [Accessed March 2019].
- [3 N. T. T. Program, "High-Efficiency Solar Cell," NASA, [Online]. Available: 5] <https://technology.nasa.gov/patent/LEW-TOPS-50>. [Accessed March 2019].
- [3 MEKS, "Solar Tracker," WordPress, December 2017. [Online]. Available: 6] <https://www.gsenenergy.eu/solar-tracker/>. [Accessed March 2019].
- [3 H. Zhang, Y. Sun, X. Zhang and Y. Xiang, "Tracking mechanism and cosine effect study of 7] Module-Heliostat Solar Collector," in *4th International Conference on Machinery, Materials and Information Technology Applications*, 2016.
- [3 M. Weik, Lambert's cosine law, Boston: Springer, 2017. 8]

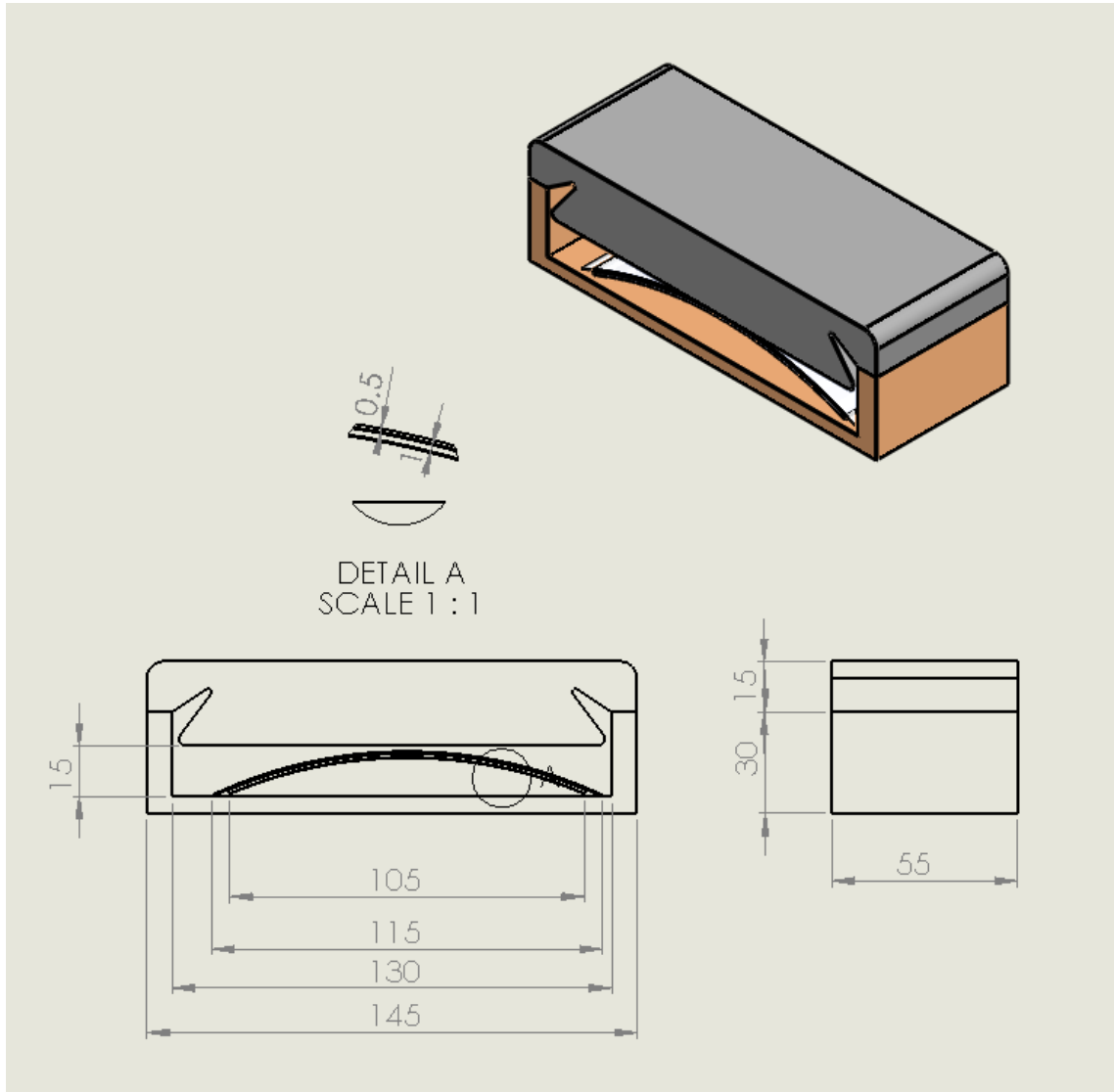
- [3] Z. Fan and Q. Lin, "Reducing reflection losses in solar cells," February 2014. [Online].
 9] Available: <http://spie.org/newsroom/5343-reducing-reflection-losses-in-solar-cells?ArticleID=x106217>. [Accessed March 2019].
- [4] D. Honig and D. Mobius, "Reflectometry at the Brewster angle and Brewster angle
 0] microscopy at the air-water interface," *Thin Solid Films*, pp. 64 - 68, 1992.
- [4] S. Bryant, "Lunar Pole Illumination and Communications Statistics," in *SpaceOps
 1] Conference 2010*, Alabama, 2010.
- [4] Global Sources, "Solar Panel Trackers," Global Sources, 2019. [Online]. Available:
 2] <https://www.globalsources.com/gsol/l/Solar-panel/p/sm/1165057800.htm#1165057800>.
 [Accessed March 2019].
- [4] C. Woodford, "explainthatstuff," 21 August 2018. [Online]. Available:
 3] <https://www.explainthatstuff.com/piezoelectricity.html>. [Accessed 15 march 2019].
- [4] J. M. Hickman, H. B. Curtis and G. A. Landis, "Design Considerations for Lunar Base
 4] Photovoltaic Power Systems," NASA, Cleveland, Ohio, 1990.
- [4] Z. Khan, A. Vranis, A. Zavoico, S. Freid and B. Manners, "Power System Concepts for the
 5] Lunar Outpost: A Review of the Power Generation, Energy Storage, Power Management
 and Distribution (PMAD) System Requirements and Potential Technologies for
 Development of the Lunar Outpost," NASA, Cleveland, Ohio, 2006.
- [4] E. B. Gietl, E. W. Gholdston, B. A. s. Manner and R. A. Delventhal, "The Electric Power
 6] System of the International Space Station-A Platform for Power Technology
 Development," NASA, Cleveland, Ohio, 2000.
- [4] R. Shafiqur, A.-H. Luai M. and A. Md. Mahbub, "Pumped hydro energy storage system: A
 7] technological review," *Renewable and Sustainable Energy Reviews*, pp. 587-596, 2015.
- [4] H. Ibrahim, A. Ilinca and J. Perron, "Energy storage systems—Characteristics and
 8] comparisons," *Renewable & Sustainable Energy Reviews*, pp. 1223-1249, 2007.
- [4] C. Jie, L. Wei, J. Deyi, Z. Junwei, R. Song, L. Lin, L. Xiaokang and S. Xilin, "Preliminary
 9] investigation on the feasibility of a clean CAES system coupled with wind and solar energy
 in China," *Energy*, vol. 127, pp. 462-478, 2017.
- [5] B. Bolund, H. Bernhoff and M. Leijon, "Flywheel energy and power storage systems,"
 0] *Renewable & Sustainable Energy Reviews*, vol. 11, pp. 236-256, 2005.
- [5] A. González, E. Goikolea, J. A. Barrena and R. Mysyk, "Review on supercapacitors:
 1] Technologies and materials," *Renewable and Sustainable Energy Reviews*, vol. 58, pp.
 1190-1202, 2016.

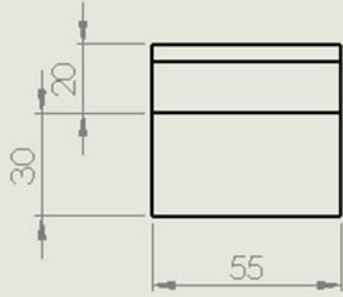
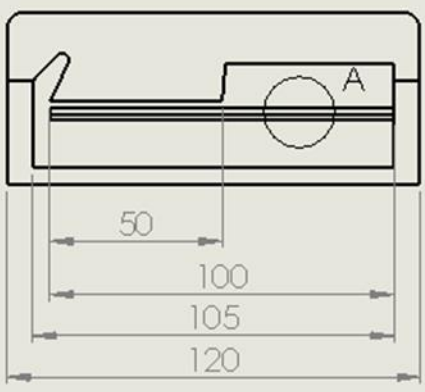
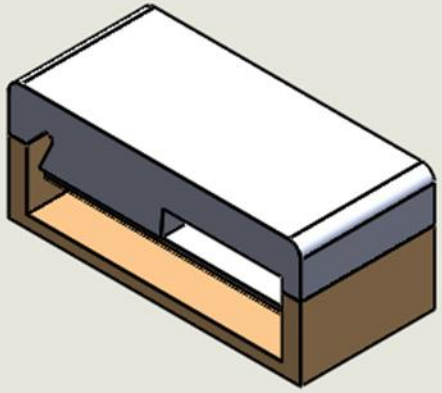
- [5 D. Linden and T. B. Reddy, HANDBOOK OF BATTERIES, Mcgraw-Hill, 2001.
2]
- [5 A. Parasuraman, T. M. Lim, C. Menictas and M. Skyllas-Kazacos, "Review of material
3] research and development for vanadium redox flow battery applications," *Electrochimica Acta*, vol. 101, pp. 28-38, 2013.
- [5 L. Carrette, K. A. Friedrich and U. Stimming, "Fuel Cells: Principles, Types, Fuels, and
4] Applications," *Chemphyschem*, vol. 1, pp. 162-193, 2000.
- [5 *Fuel Cell Technologies Program*, Energy, Energy Efficiency & Renewable, 2011.
5]
- [5 M. Chaplin, "Electrolysis of Water," Isbu, 2 03 2019. [Online]. Available:
6] <http://www1.isbu.ac.uk/water/electrolysis.html>. [Accessed 16 03 2019].
- [5 S. O. R. M. J. Fleming, "Fundamentals of Piezoelectricity," in *Piezoelectric Transducers for
7] Vibration Control and Damping*, London, Springer, 2006, pp. 9-35.
- [5 M. V. R.S. Dahiya, "Fundamentals of Piezoelectricity," in *Robotic Tactile Sensing*, Springer
8] Science+Business Media Dordrecht, 2013, pp. 195-245.
- [5 M. Yamaguci, T. Takamoto and K. Araki, "Present and future of super high efficiency multi-
9] junction solar cells," *SPIE - The International Society for Optical Engineering*, vol. 6889, 2008.
- [6 John H. Glenn Research Centre, "Selenium Interlayer for High-Efficiency Multi-Junctioin
0] Solar Cell," Tech Briefs, October 2016. [Online]. Available:
<https://www.techbriefs.com/component/content/article/tb/techbriefs/energy/25518>.
[Accessed March 2019].
- [6 X. Li, W. Yu, S. Wang, S. Li, H. Tang, Y. Li, Y. Zheng, K. Tsang and Z. Ouyang, "Condition of
1] Solar Radiation on the Moon," in *Moon*, Springer, 2012, pp. 347 - 365.
- [6 SMA Solar Technology AG, "Performance Ratio," SMA.
2]
- [6 NASA, "International Space Station Basics," NASA, 2007.
3]
- [6 A. Wilson and R. Ross, "Angle-of-Incidence Effects on Module Power and Energy
4] Performance," in *21st Project Integration Meeting Jet Propulsion Laboratory*, Pasadena, 1983.
- [6 A. Townley, "semanticscholar," [Online]. Available:
5] <https://pdfs.semanticscholar.org/1609/6bb20967e626f78f6c96eb788309661a848c.pdf>.
[Accessed 19 March 2019].

- [6] C. Q. Choi, "space.com," 27 September 2014. [Online]. Available:
6] <https://www.space.com/27285-astronauts-moon-walking-speed-spacesuits.html>.
[Accessed 10 March 2019].
- [6] Tired Tires, "Technology," Tired Tires, [Online]. Available:
7] <http://dev.nsta.org/evwebs/2014102/news/default.html>. [Accessed March 2019].
- [6] Fab.to.Lab, "Piezoelectric Transducer (with Soldered Wire)," Fab.to.Lab, 2019. [Online].
8] Available: <https://www.fabtolab.com/piezoelectric-transducer-soldered>. [Accessed March 2019].
- [6] P. Acoustics, "acoustics," November 2015. [Online]. Available: www.acoustics.co.uk.
9] [Accessed 20 January 2019].
- [7] D. Nagy, "Solar analysis in Grasshopper," Generative Design, February 2017. [Online].
0] Available: <https://medium.com/generative-design/solar-analysis-in-grasshopper-5dae76c9b6cb>. [Accessed March 2019].
- [7] A. Lechner, "Pumped Storage for the Future," Andritz, 2019. [Online]. Available:
1] <https://www.andritz.com/hydro-en/hydronews/hn32/11-pumped-storage>. [Accessed 16
03 2019].
- [7] I. Bhandari, "Energy Storage for the Grid & Transportation," 25 September 2017. [Online].
2] Available: <https://las493energy.wordpress.com/2017/09/25/off-peak-power-storage-advanced-adiabatic-compressed-air-energy-storage-introduction/>. [Accessed 16 03 2019].

Appendix

Appendix 1: Arch-shaped and cantilever generators details

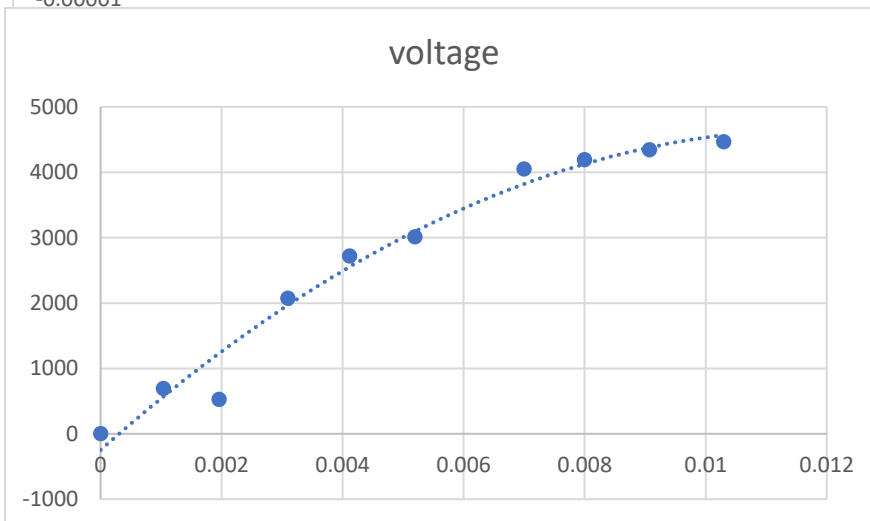
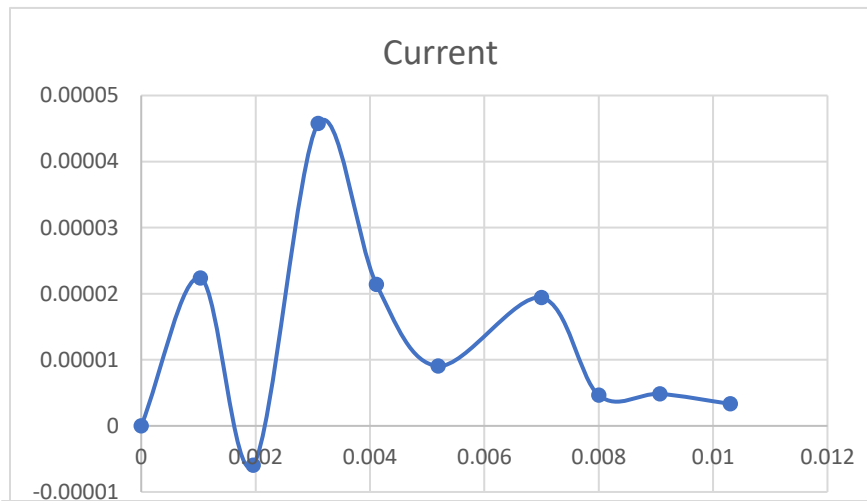
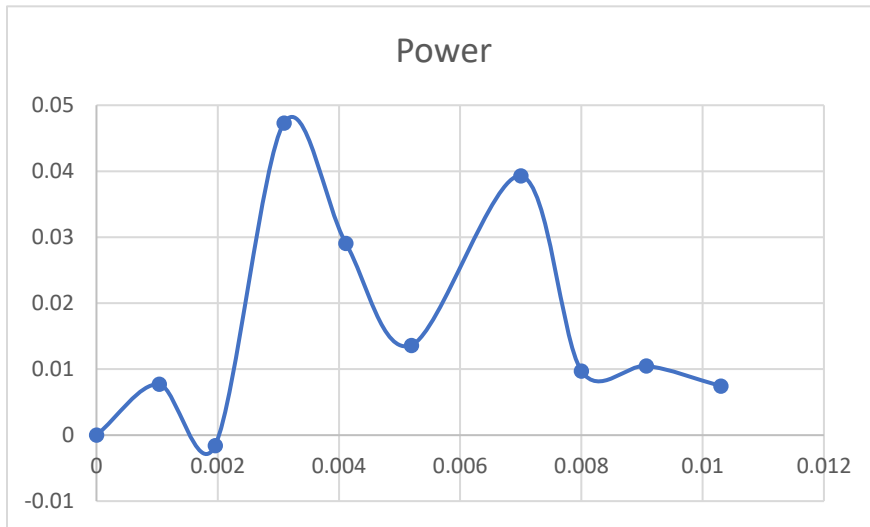




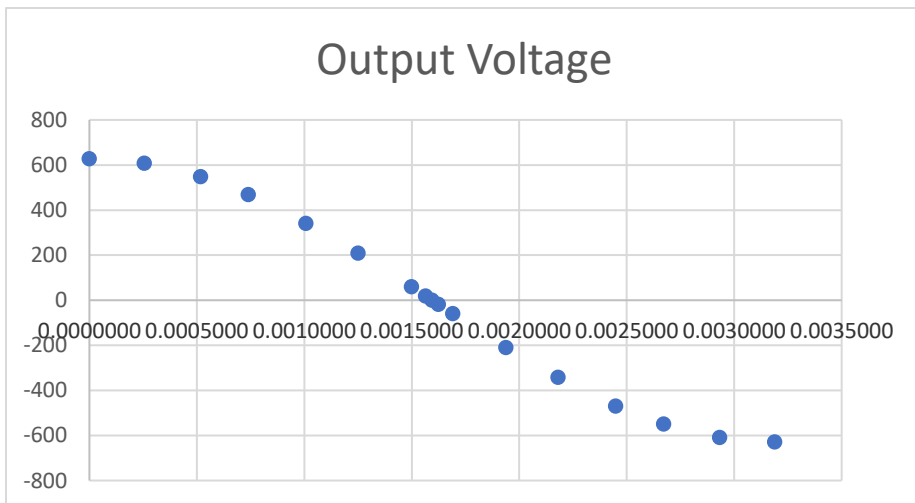
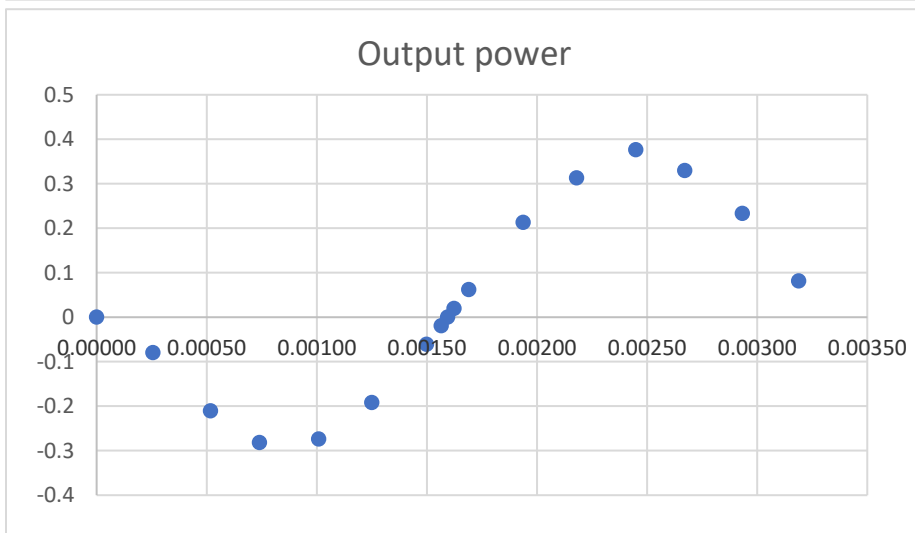
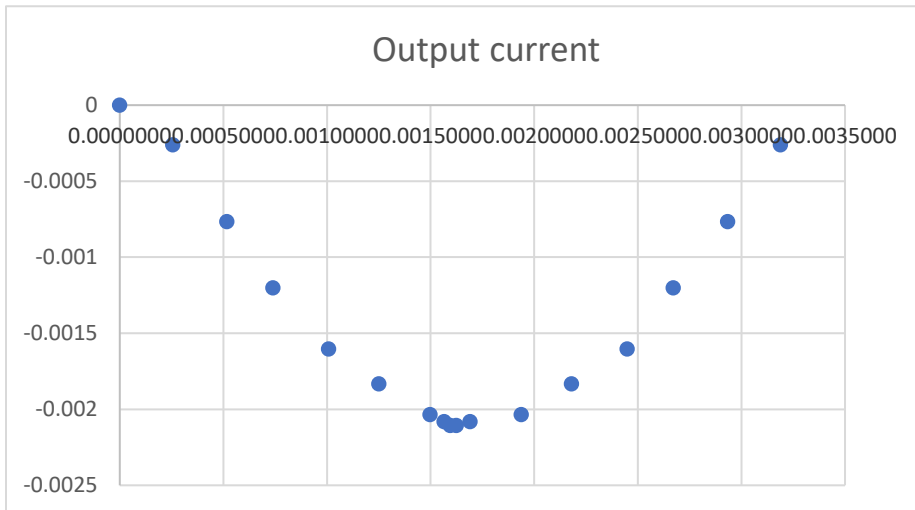
Appendix 2: Electrolyser Bill of Materials

Quantity	Description
4	144mm Acrylic Disc - 5mm Thickness
2	150mm Acrylic Disc - 15mm Thickness
2	52mm Acrylic Disc – 10mm Thickness
2	60mm x 60mm x 20mm Acrylic Block
1	150mm Diameter Acrylic Tube – 3mm Thickness
1	34mm Diameter Acrylic Tube – 2mm Thickness
2	6mm Bulkhead Fitting
1	Rubber Gasket Sheet
2	Rubber Gasket Ring - 200mm Diameter
10	100mm x 100mm Stainless Steel Plates
4	300mm Threaded Stainless Steel Rods – 6mm Thickness
40	Flanged M6 Stainless Steel Washers
20	5mm Diameter Neodymium Magnets – 3mm Thickness
1	Hybrid Adhesive and Sealant

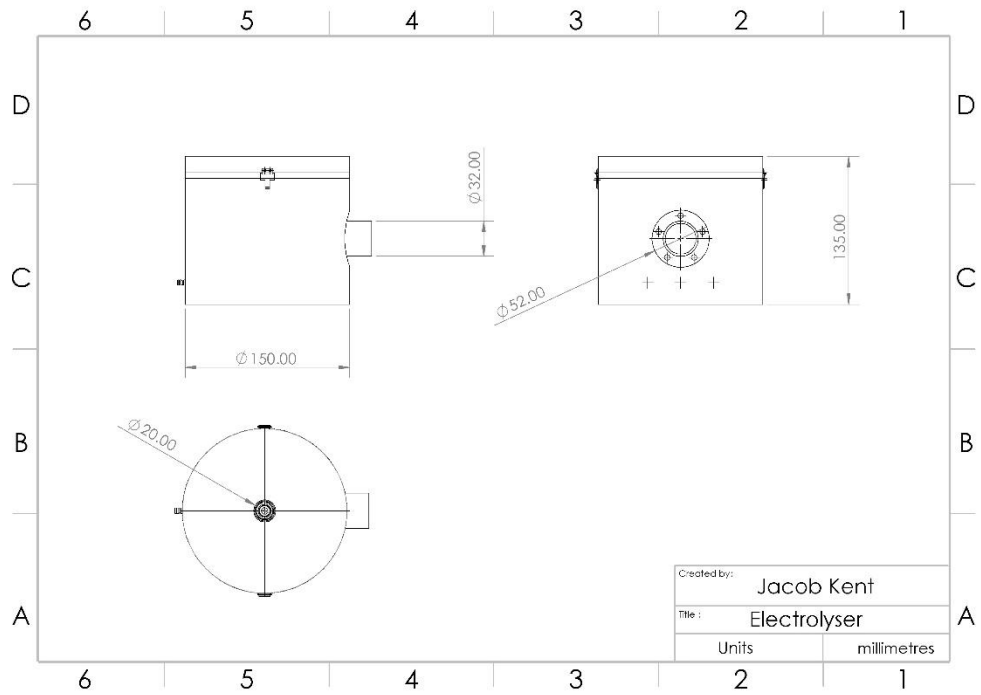
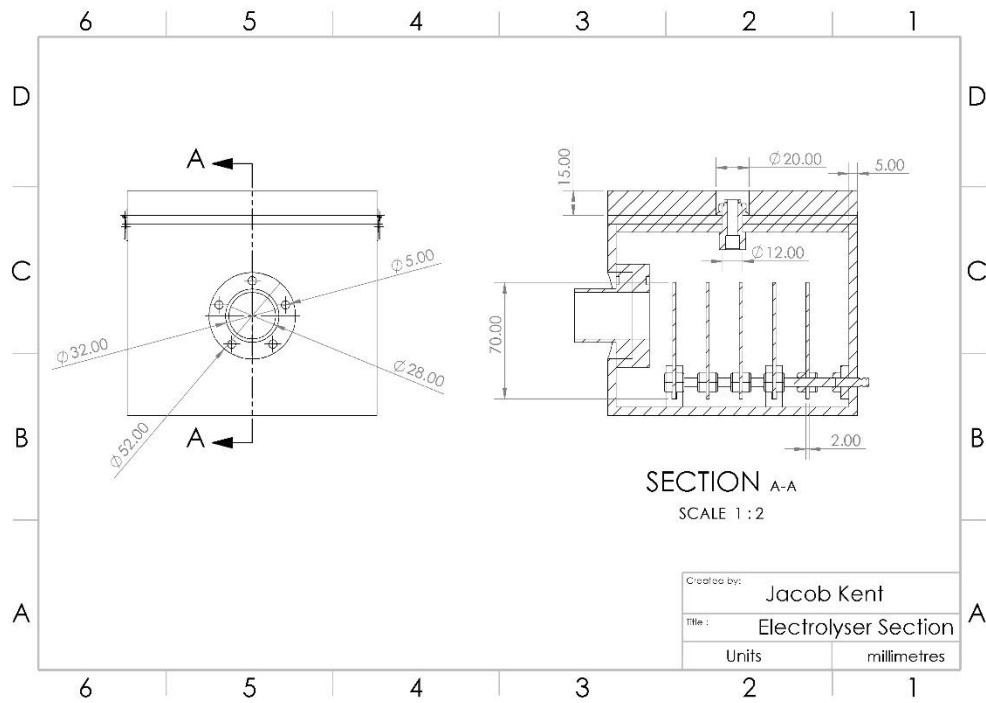
Appendix 3: Arch-shaped generator output graphs



Appendix 4: Cantilever generator output graphs



Appendix 5: Electrolyser Drawings



Appendix 6: Prioritisation of IGLUNA Project Systems

Project	Title	Description	Priority	Connections
01	Autonomous construction robot	Construction robot	High initial, medium - may have own battery. Needed in case of repairs.	
02	Smart Waste-based Agriculture Growing System	Human waste based agriculture; regeneration of oxygen	High; will need atmosphere and temperature control; 230V	05 greenhouse module; 04 algal bioreactor
03	Space Toilet	In context of life support system; waste treatment option	High; electrical power required; must keep base sanitary	Connection to 02?
04	Algal Bioreactor for Space Habitat	Waste treatment	High; heating required, lighting, power for bioreactor system	02, 03, 05?
05	Greenhouse module for food production and water recovery		High	02, 03, 04
06	Habitat concept in lunar lava-tubes			
07	Habitat in ice structure			
08	Digging robot with navigation in ice capability		Medium/Low – unless it serves crucial purpose; 220V max 10A	
09	Oxygen production from native rocks		High; 220V	
10	Human activity and health monitoring clothing		High/medium – depending on functionality; batteries?	
11	Smart adaptable habitat	Concerns a smart energy management system (lighting, climate control, safety, entertainment, work)	High - Smart control of habitat, including safety	10; connected to management system of 19?

12	Development of an Experiment Box		Low; requires power supply	
13	CYCLAMINA – Cybernetic companion pLAnts to Mitigate iNteraction with nAture		Low; needs standard connection to power (PC)	
14	Guidance and Localisation for Astronauts Cooperating in Environmental Roughness (GLACiER)		Medium/High; 230VAC power supply required	
15	Science Lab		Low	
16	Science Project		Low	
17	Hephaestus: 3D – Laser Shock Peening of a High Performance Ice Saw/Drill		Medium; battery powered; needed for water collection?	
18	Power_Hab	Power storage, distribution, generation and harvesting	High;	
19	Smart adaptable habitat		Medium; depends on health risks of not exercising (due to low gravity for example)	P10 and P11

Appendix 7: Statement of Work

Statement of Work			
Project Title		ESA_Lab – Power Hab	
Supervisor	Massimiliano Vasile	Second Supervisor	Edmondo Minsci
Start Date (SSC)	9/10/18	End Date (SSC)	9/7/19
Start Date (UoS)	21/9/18	End Date (UoS)	25/3/19
Project Background	<p>The Swiss Space Centre (SSC) and European Space Agency (ESA) have joined to create an initiative designed to give students the opportunity to develop technologies to sustain life in extreme conditions and beyond the Earth.</p> <p>The challenge posed by the SSC is to design a habitat in ice – a terrain similar to that at the Southern Pole of the moon. Students across Europe (9 institutions, 20 Projects) have been invited to share, discuss and demonstrate ideas that support the realisation of a human habitat in ice as a precursor of a moon base.</p>		
Project Description	<p>This project aims to define and design a power system that will support the human habitat on the moon. The power system will need to harvest/generate energy, distribute energy to a number of loads, and store energy for periods of zero/limited generation.</p> <p>Strathclyde has put forward a large 12-person group that will take on this project. The larger group consists of the following :</p> <ul style="list-style-type: none"> - 5th yr Mech Eng group (5 members) - 5th yr EME group (4 members) - 1x 4th yr EME individual project - 2x 4th yr Mech Eng individual project <p>Key Objectives</p> <ul style="list-style-type: none"> ● Analyse the objective and requirements of the ESA_lab habitat in ice and derive technical requirements for the power system (involves cooperation with other teams across Europe) ● Devise an energy harvesting system that can be used in future planetary exploration missions ● Devise an energy generation system ● Devise an energy storage system ● Devise and design an energy distribution system ● Size the power harvesting, generation and storage systems ● Develop prototypes of select designs for field testing 		
Project Deliverables	<ul style="list-style-type: none"> ● Progress updates (SSC) ● Interim Report (UoS) ● Interim Presentation (UoS) ● Preliminary Design Review Report (SSC) ● Critical Design Review Report (SSC) ● Final Report (UoS/SSC) 		

Group Q

	<ul style="list-style-type: none"> ● Final Presentation (UoS) ● Readiness Review (SSC) ● Various prototypes for field test in the Alps, June 2018 (UoS/SSC) ● Website (UoS)
--	---

Project Scope (General)	In Scope: <ul style="list-style-type: none"> ● A system to collect and store solar energy ● Alternative heat and power sources ● Short-term emergency power sources and storages ● Distribution system including various sources, storages, sinks and users ● Communicating with other teams around Europe to obtain specifications 	Out of Scope: <ul style="list-style-type: none"> ● Any other specialist task designated by the SSC/ESA ● Management of any other separate group
Project Scope (Specific)	Jacob	
	Jonathon	
	Pedro	
	Sarah	
	Laetitia	
Acceptance Criteria	<ul style="list-style-type: none"> ● Designed system fulfils: <ul style="list-style-type: none"> ○ energy requirements of basic needs as detailed by other teams (extend and sustain human activities) e.g. life support, communications ○ energy requirements for exploration e.g. scientific experimentation ● Various reports during reviewing sessions ● Functional UI/ prototypes <p>TBC</p>	
Constraints	<ul style="list-style-type: none"> ● Internal University of Strathclyde (UoS) deadlines (course related) ● External SSC/ESA deadlines ● Working externally with groups across Europe (must work to their specifications) 	

Group Q

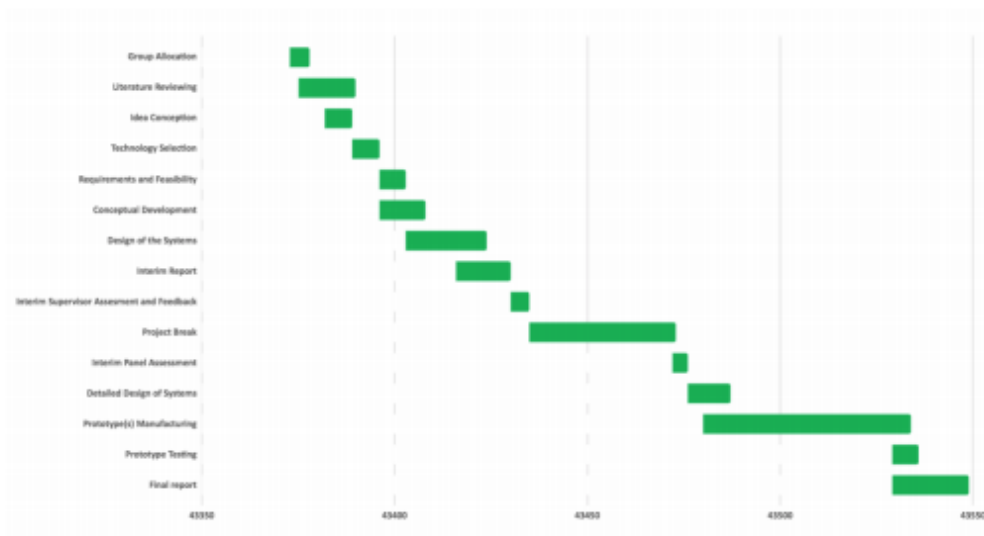
	<ul style="list-style-type: none"> Limited by scale/number of prototypes to be built
Assumptions	<ul style="list-style-type: none"> Full cooperation between teams at all times <ul style="list-style-type: none"> Internal: Fifth year MAE group (5 members); Fifth year EME group (4 members); Fourth year MAE (2 individuals); Fourth year EME (1 individual) No major project changes after Nov/Dec/Jan <p>TBC</p>
Project Structure	Gantt Chart
Proposed Methodology	<ol style="list-style-type: none"> Conception phase <ol style="list-style-type: none"> Literature reviewing Initial ideas Definition of requirements and constraints Peak power requirement Average power requirement Number and type of loads Review 1 (PDR) <ol style="list-style-type: none"> Confirmation of concept feasibility Confirmation of experiment to be carried out in field campaign Identifying external interfaces with other teams Conduct safety assessment Initiate any long-lead item procurement if required Design phase <ol style="list-style-type: none"> Detailed design of systems for generation/harvesting/storage/distribution Review 2 (CDR) <ol style="list-style-type: none"> Final review stage before construction of prototypes Reviewed by IGLUNA project management team – presentation and question session Project break (<i>Christmas holidays</i>) Prototype manufacturing Final Report (UoS) (<i>March 2019</i>) Review 3 and intermediate report (<i>March/April 2019</i>) <ol style="list-style-type: none"> Readiness review – equipment and testing schedule ready for field campaign Presentation and question session Roll-out (<i>May/June 2019</i>) Final Report (<i>June 2019</i>) (less than 30 pages for SSC) IGLUNA field campaign

Group Q

Key Milestones	12 – 14/9/18	Kick-off Event (SSC)
	21/9/18	Project Allocation (UoS)
	2/10/18	Full team meeting
	9/10/18	Video meeting with T. Benavides
	17/10/18	Statement of Work (UoS)
	26/11/18	Interim Report (UoS)
	19 – 30/11/18	Preliminary Design Review (SSC)
	14/12/18 – 14/1/19	Critical Design Review (SSC)
	7 – 11/1/19	Interim Panel Assessment (UoS)
	25/3/19	Final Report (UoS)
	15 – 26/4/19	Final Panel Assessments (UoS)
	29/4/19 – 10/5/19	Readiness Review (SSC)
	17 – 30/6/19	Field Campaign (SSC)
	9/7/19	Final Report
Risks and Mitigation	Risk	Mitigation
	Testing/prototype equipment unavailable	Source alternative equipment/ change experimental plan and schedule/ utilise time for other activities
	Changes being made to design critical projects by other teams	Multiple ideas and concepts/ Stay in contact with relevant teams/ Discuss and assess whether changes can be met; review the change request document and reject if necessary
	Machining/ fabrication not available	Work on other topics/ change construction schedule
	Adverse weather	a) Team members cannot make it to university – other members compensate b) University is closed – use time to work on other topics
	Team members unavailable	Other team members compensate; disciplinary flexibility in team (cross disciplinary skills)
	Decision making in sub-teams delaying work in others	Use time for other tasks/ Use a decision-making method
	Construction of various prototypes (e.g. Hydrogen fuel cell)	Location? TBC

Group Q

Communication Plan	<ul style="list-style-type: none"> • Fortnightly meetings via WebEx with Tatiana Benavides (SSC) • Weekly meetings with Prof. Vasile (either after video chat, or on Wednesday) • Separate Group meetings • Separate Sub-team meetings • Separate university team meetings • Separate ad-hoc video meetings with other project teams 	
Team Members (Project Group)	Member Name	Sub-team
	Jacob Kent	Storage
	Pedro Corujo	Harvesting
	Jonathon Marshall	Generation
	Sarah Davidson	Distribution
	Laetitia Petit (1st Sem Only)	Harvesting
Team Members (Wider group within Strathclyde)	Fraser Scott (EME)	Generation
	Louise Guthrie (EME)	Distribution
	Fraser Bisset (EME)	Storage
	Joelle Yu (EME)	Distribution
	Jonathon Libby (EME 4th yr)	Storage
	Kerr McMaster (Mech Eng 4th yr)	Generation
	James Webb (Mech Eng 4th yr)	Harvesting



Group Q

SISTEMA DE POTENCIA ESA_LAB/IGLUNA

1 CONTENTS

2	Introducción.....	2
3	Distribución del Proyecto.....	2
4	Distribución.....	3
4.1.1	Terreno.....	3
4.1.2	Sistemas de distribución	3
5	Generación.....	5
5.1	Diseño	5
5.1.1	Placa solar estacionaria.....	5
5.1.2	Seguidor Solar Uniaxial	6
5.1.3	Seguidor Solar de Doble Eje	7
5.2	Resultados.....	9
6	Aprovechamiento de Energía.....	10
6.1	Diseño	11
6.2	Análisis	11
6.3	Modificación	13
7	Almacenamiento.....	14
7.1	Diseño	15
8	Conclusión.....	15

2 INTRODUCCIÓN

Este proyecto forma parte del programa internacional *Igluna* organizado y planteado por la *Agencia Espacial Europea* junto con el *Centro Espacial Suizo*. El objetivo de este programa es el diseño y desarrollo de una base lunar donde sea posible la vida humana y se puedan llevar a cabo experimentos; para ello, veinte equipos de estudiantes de universidades europeas trabajaran de forma conjunta. Dentro de este marco de trabajo, la Universidad de Strathclyde se encargará de diseñar y desarrollar los sistemas de potencia capaces de generar, almacenar y distribuir la energía necesaria en el hábitat lunar, así como ser capaces de aprovechar energía residual. La principal dificultad es la falta de luz solar ya que la base estaría situada en el polo sur de la Luna, donde los eclipses solares podrían provocar largos periodos de oscuridad. A demás, en esta localización las temperaturas son extremadamente bajas y debido a la carencia de atmósfera existe la posibilidad de impactos de asteroides.

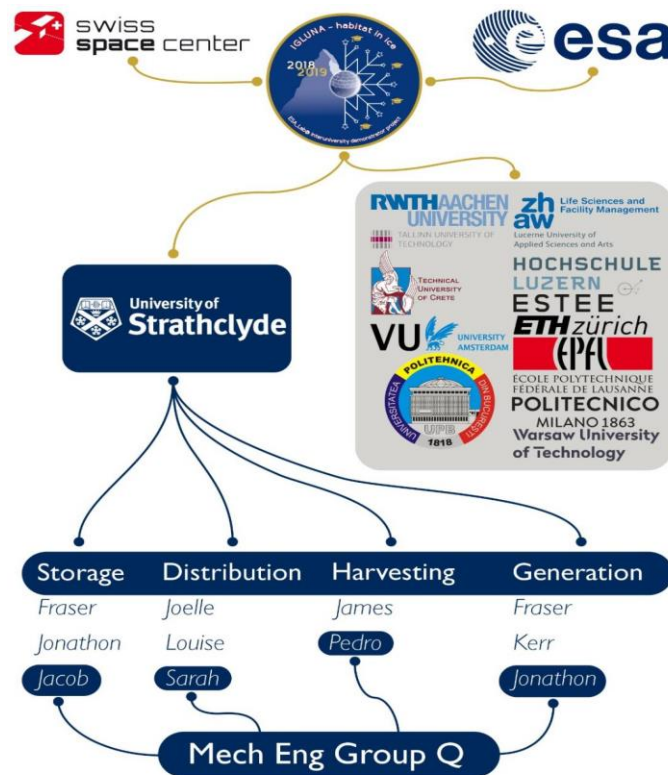


Ilustración 1 Organización del proyecto

3 DISTRIBUCIÓN DEL PROYECTO

Puesto que es un trabajo en equipo y las tareas a realizar son varias, a cada integrante del equipo se le encomendó una tarea distinta. A la hora de dividir las tareas se tomaron como patrón los diferentes objetivos del proyecto, siendo estos: distribución, generación, aprovechamiento y almacenamiento de energía. Dentro de la Universidad de Strathclyde existían varios grupos de estudiantes vinculados al mismo proyecto que realizaban a su vez otras tareas distintas a las descritas en este documento. Para

repartir las tareas dentro de cada división comentada anteriormente se tuvo en cuenta la especialidad de cada estudiante, distinguiendo estudiantes de ingeniería mecánica, electromecánica y aeroespacial. El material recogido en este trabajo es exclusivamente el aportado por los componentes del grupo (Jacob, Sarah, Pedro y Jonathon).

4 DISTRIBUCIÓN

Esta área de trabajo está dedicado a la comunicación de los sistemas de generación y almacenaje de energía entre ellos y el hábitat a su vez. Para diseñar el subsistema de distribución se deberá estudiar tanto el terreno de la superficie lunar donde será implementado como la tecnología y los sistemas que se usarán.

4.1.1 Terreno

El entorno de la superficie lunar se puede considerar vacío ya que la atmósfera es prácticamente inexistente. El lugar de interés es el polo sur, donde las reservas de agua serían mayores debido a los numerosos y profundos cráteres. Los más importantes serían Cabeus, Haworth, Shoemaker, Faustini, Shackleton y Sverdrup. La Ilustración 2 muestra la orografía, destacando en rojo las zonas de mayor elevación y en azul las de menor.

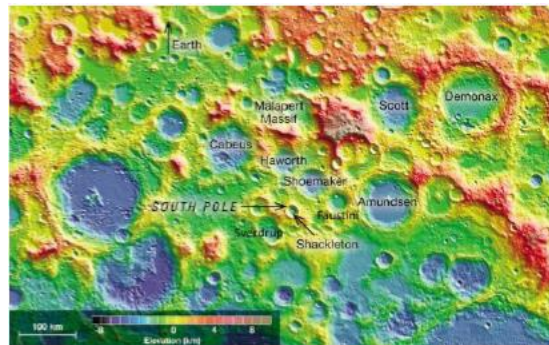


Ilustración 2 Mapa del relieve lunar

A través de esta y otras imágenes donde se muestra el terreno y las zonas en sombra e iluminadas, se puede predecir que la zona cercana a Shackleton (posible lugar para el hábitat) recibirá luz solar el 86% del tiempo en el año 2020.

En cuanto a las temperaturas en esta zona de la Luna, según imágenes tomadas por la NASA, en las partes en sombra la temperatura sería de 40K y en el resto del terreno alrededor de 220K. Estas temperaturas podrían variar a lo largo de los meses en torno a 10K. Esta información sobre las temperaturas se deberá tener en cuenta a la hora de escoger los medios de distribución y los materiales utilizados.

4.1.2 Sistemas de distribución

Mientras que en la tierra la electricidad se transporta a altos voltajes y con corriente AC, en el espacio no es así. En la estación espacial internacional la fuente primaria de energía es la solar, ésta es generada en corriente DC a 160 Voltios y se distribuye manteniendo estas condiciones hasta que es finalmente convertida a 124 voltios para su consumo. Cómo se verá más adelante, la fuente de generación de energía

escogida es la solar, por lo que el sistema principal de distribución estará basado en el descrito anteriormente debido a su similitud.

A demás de la transmisión de electricidad mediante corriente DC, también se ha hecho una investigación sobre la implementación de la transmisión por ondas. Esta tecnología está basada en ondas electromagnéticas de longitud de onda comprendida entre 0.1 y 100mm. La transmisión sin cables se podría utilizar para obtener la energía generada por placas solares situadas en satélites orbitando alrededor de la Luna. Los motivos por los que se podría utilizar este sistema son: la mayor eficacia de las placas fotovoltaicas al situarse en órbita (pudiendo escoger aquella con mayor y mejor incidencia de luz) y el relativamente pequeño radio de órbita necesario en la Luna, facilitando la comunicación transmisión. Puesto que esta tecnología está aún en desarrollo, este trabajo se ha centrado en la transmisión por corriente DC.

Para poder diseñar el sistema de distribución se calculó la potencia requerida por toda la base lunar, teniendo en cuenta las demandas de cada departamento y actividad existente en el hábitat. A demás se creó un sistema jerárquico para dividir las necesidades energéticas según su importancia y aplicarlo al sistema de distribución.

Las tareas llevadas a cabo por este grupo fueron: selección de conductores, selección de aislantes y cálculos de distancias de cableado. Para escoger los materiales se tuvo en cuenta la densidad, las temperaturas de funcionamiento, durabilidad y flexibilidad. Como aislantes, los materiales escogidos fueron la poliamida y el PTFE. Los materiales conductores serán: cobre y plata en las zonas más importantes y aleación de aluminio para el resto.

Estimated moon base power requirement	67kW
Estimated moon base power requirement with electrolysis production	104kW
AC/DC transmission	DC
Distribution system	Primarily over-surface cabling, working toward a wireless system.
Estimated max line voltage	380V DC
Estimated secondary transmission voltage	48V DC
Estimated cabling material	Aluminium
Estimated connector material	Copper/ Silver/ specialist engineered alternative
Estimated insulation material	PTFE/ polyimide/ PE
Estimated length of cabling	10s of km
Location of solar arrays	Various locations, on elevated areas surrounding Shackleton crater
Location of fuel-cell (storage)	Within the base, in temperature-controlled environment (safe distance from personnel)
Location harvesting techniques	Under the floor of the habitat
Potential source of back-up power	Located safe distance from the base in protective environment

Tabla 1 Información de distribución

5 GENERACIÓN

El equipo de generación eléctrica debe ser capaz de producir la electricidad suficiente para abastecer a todo el hábitat lunar, incluyendo los experimentos. El primer paso es la elección de la tecnología más adecuada. Los sistemas habituales de generación de energía basados en combustibles fósiles quedan descartados puesto que su implementación sería muy cara debido al continuo transporte del combustible necesario; por este motivo se optó por un diseño basado en fuentes de energía sostenibles. Considerando las condiciones y tomando como referencia la tecnología usada en la Estación Espacial Internacional, el sistema de generación de energía escogido fue la energía solar.

5.1 DISEÑO

El principal condicionante para la implementación en la Luna de células fotovoltaicas es el coste del material y su transporte. Teniendo esto en cuenta, se decidió que el diseño del sistema de generación de energía debía realizarse en torno a la optimización peso/potencia.

La optimización de la energía solar se puede realizar principalmente de dos formas:

- Mediante seguimiento: Las placas solares se pueden automatizar para que sigan el movimiento del sol a lo largo del día; de esta manera, las placas solares se mantienen siempre en una posición óptima con respecto a la incidencia lumínica.
- Mediante espejos: Colocando espejos en un cierto ángulo alrededor de la célula fotovoltaica se consigue una mayor eficiencia debido a la reflexión de la luz en los espejos.

Aunque en teoría la utilización de cualquiera de estos métodos aumentaría la producción de electricidad, ésta dependerá en mayor o menor medida de la trayectoria del sol. Para demostrar y calcular la mejoría obtenida mediante el seguimiento solar y el uso de espejos, se diseñaron 3 prototipos:

5.1.1 Placa solar estacionaria

Este modelo debía cumplir varios requerimientos del proyecto IGLUNA, incluyendo medidor de temperatura, humedad y voltímetro; ayudando de esta forma a comparar su rendimiento con el del resto de prototipos.

Este prototipo fue diseñado mediante SolidWorks en para ser posteriormente impreso en 3D (Ilustración 3). Está compuesto de tres partes principales:

- Base: Sobre ella descansan el resto de las partes del prototipo. Posee una entrada de puerto USB, una pantalla donde mostrar los datos medidos y una salida para medir el voltaje.
- Rotador: Encaja sobre la base y es capaz de rotar 360° sobre un eje vertical.
- Sujeción de la célula: Encaja en el rotador y permite un giro superior a 180° en un eje horizontal.

Estas tres partes y su movilidad permiten ajustar manualmente la orientación de la célula fotovoltaica. La sujeción de la célula lleva incorporados unos enganches donde colocar espejos, para comparar así el rendimiento con y sin estos.



Ilustración 3 Modelo estacionario

5.1.2 Seguidor Solar Uniaxial

Fue diseñado por ordenador mediante SolidWork y posteriormente construido en contrachapado mediante corte por láser. Los requerimientos técnicos del modelo eran:

- Capacidad de seguimiento autónomo
- Capacidad para sujetar una placa solar de 6V
- Autosuficiencia
- Sencillez para facilitar transporte y mantenimiento

El movimiento es generado mediante un motor acoplado a un engranaje (Ilustración 4); de esta forma se permite la rotación del panel en 360°.

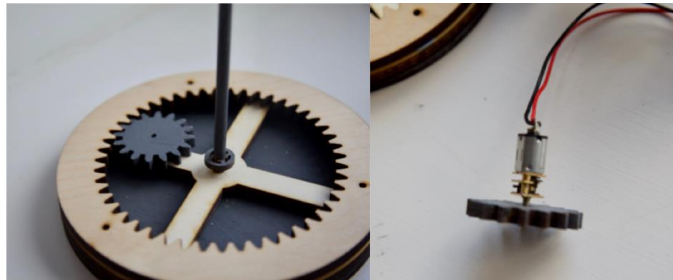


Ilustración 4 Engranajes modelo uniaxial

Para conseguir la autosuficiencia y automatización del sistema se utilizan pequeñas células fotovoltaicas colocadas en cuña como muestra la Ilustración 5. Cada placa está conectada a uno de los polos del motor, de esta manera el motor únicamente dejará de girar cuando ambas placas suministren el mismo voltaje y para que esto suceda, la cuña deberá estar orientada perpendicular al sol, dejando a su vez la placa solar principal orientada hacia el sol.

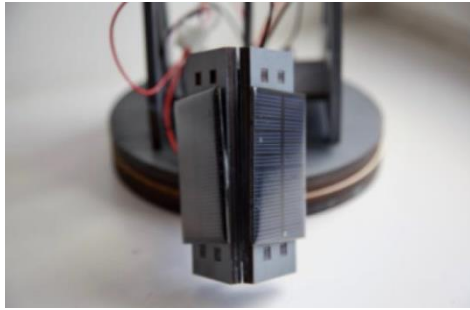


Ilustración 5 Modelo uniaxial (1)



Ilustración 6 Modelo uniaxial (2)

5.1.3 Seguidor Solar de Doble Eje

En este caso el seguidor se utilizará para automatizar una huerta solar. El motivo por el que usa un seguidor con dos ejes es la mayor precisión para posicionar las células fotovoltaicas puesto que en este caso girarán tanto en horizontal como en vertical. El proceso de diseño y fabricación es el mismo que en el prototipo anterior, consiguiendo el modelo mostrado en la Ilustración 7.

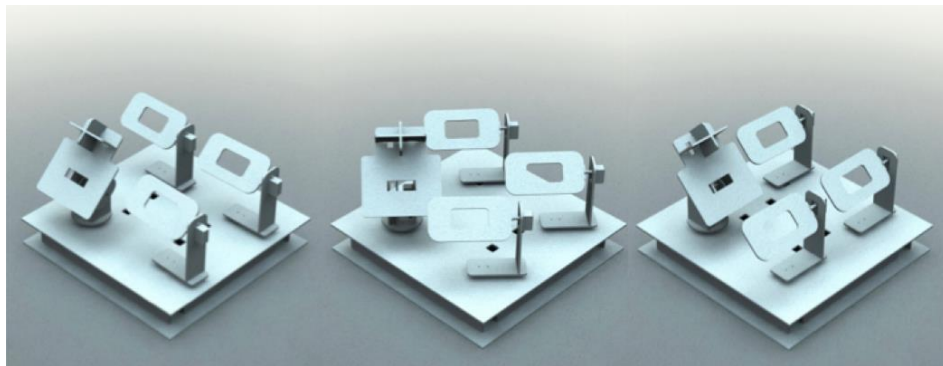


Ilustración 7 Modelo de doble eje

Para automatizar este prototipo se usaron micro-servos en dos ejes de cada panel. Dentro del modelo existe una jerarquía entre los distintos paneles de la huerta solar; uno de los paneles es el principal y el resto son clones que copiarán el movimiento hecho por el principal.

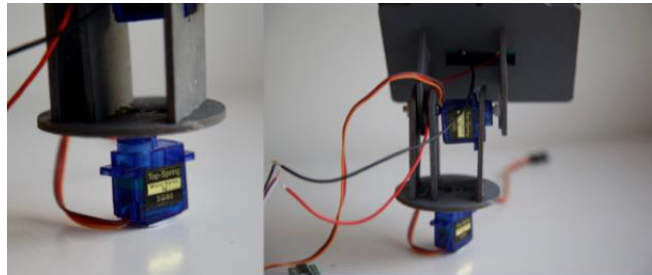


Ilustración 8 Micro-servos, modelo de doble ejes

El sistema de seguimiento se basa en un Arduino y 4 LDRs colocados en el panel principal y separados como se muestra en la Ilustración 9. Cada LDR detecta la cantidad de luz y generan una diferencia de voltaje entre ellos que controla el Arduino. A través de un código y un algoritmo en el Arduino se activan los distintos micro-servos hasta que la luz recibida en los 4 LDRs es igual indicando la posición correcta del panel.

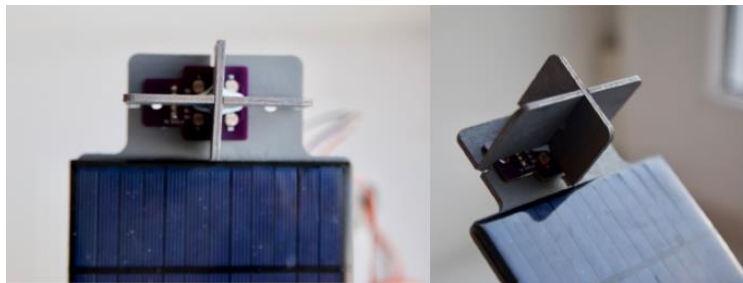


Ilustración 9 LDRs, modelo de doble eje

5.2 RESULTADOS

El primer prototipo probado es el estacionario. El paso inicial es hacer una estimación del voltaje obtenido en función de la alineación entre la placa y el sol, éste es comparado con el valor real obtenido mediante varias mediciones. Posteriormente se mide el voltaje del modelo añadiendo los espejos. Los resultados obtenidos se muestran en las siguientes ilustraciones.

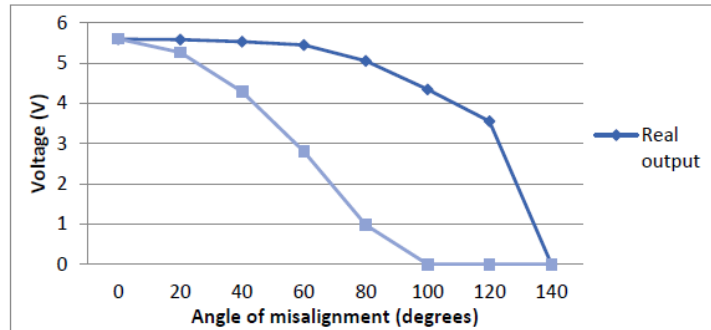


Ilustración 10 Valores del voltaje generado

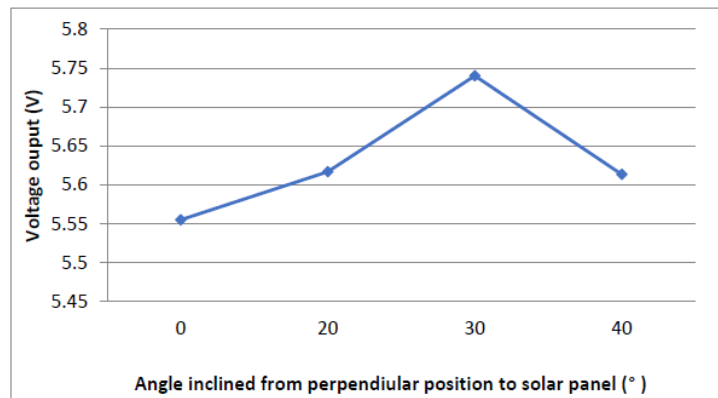


Ilustración 11 Resultados usando espejos

A continuación, se calcula una estimación de la energía obtenida por los distintos modelos estando en la Luna; para ello se utiliza la siguiente fórmula: $E = A * r * H * PR$; donde A es el área de los paneles, r es la eficiencia de conversión, H la irradiación solar y PR el coeficiente de actuación. Además se calculará también la energía perdida debido al desalineamiento de los paneles solares mediante: $\text{Potencia Perdida (\%)} = 1 - \cos(i)$; donde i es el grado de desalineamiento. Usando estas fórmulas y tomando un área de 5000m^2 , una eficiencia del 40%, una irradiación solar de $1.367,3 \text{ kW/m}^2$ (basada en los datos obtenidos en el polo sur de la Luna) y un coeficiente de actuación de 0,8 se obtienen los datos mostrados en la tabla.

Como se puede comprobar el resultado es el esperado, siendo el seguidor de doble eje el que mayor energía obtiene, aunque la diferencia no es muy grande debido a que la trayectoria solar en el polo sur

de la Luna apenas varía su altitud. Dada la escalabilidad del prototipo, su gran proporción potencia/peso y la relativa sencillez de su automatización, esta opción sería la mejor opción en el hábitat lunar.

Device	Loss (Horizontal) kWh/year	Loss (Vertical) kWh/year	Total Loss kWh/year	Effective output kWh/year	Improvement kWh/year
Stationary	1.099×10^7	1.004×10^4	1.1×10^7	5490353.33	0
Single axis	0	1.004×10^4	1.004×10^4	16471066.45	$10980713.12 = 1.098 \times 10^7$
Dual axis	0	0	0	16481105.6	$10990752.27 = 1.099 \times 10^7$

Tabla 2 Resumen de potencias eperadas

6 APROVECHAMIENTO DE ENERGÍA

El aprovechamiento de energía tiene como objetivo obtener energía presente en actividades o situaciones que de otra manera sería malgastada; en este caso la energía se extraerá de los pasos y movimientos de los habitantes de la base. Así, el consumo de la energía proveniente de las placas solare será menor, dando un mayor margen durante los picos de demanda.

En esta situación y teniendo en cuenta las posibilidades de la base lunar, se optó por los materiales piezoeléctricos (PE) y triboeléctricos (TE). Este tipo de materiales obtienen electricidad de las deformaciones y la fricción respectivamente. Para obtener energía mediante estos materiales se utilizará un generador híbrido que unirá los generadores piezo y triboeléctricos habituales.

La Ilustración 12 muestra cómo los materiales PE obtienen energía eléctrica de su deformación. El proceso en los materiales TE es similar, pero en este caso la creación de dipolos se produce mediante la fricción entre el material TE y otro material distinto.

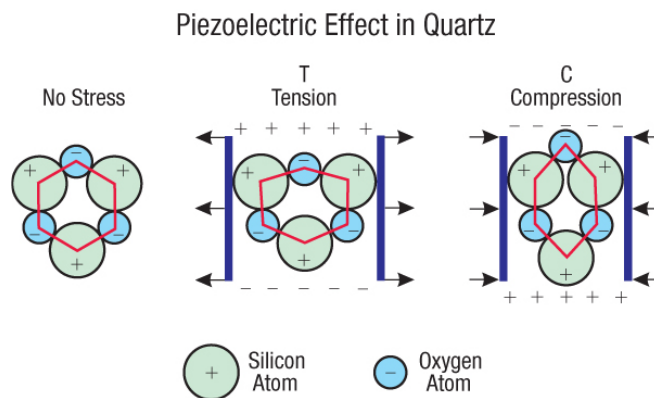


Ilustración 12 Efecto piezoeléctrico

6.1 DISEÑO

Analizando los diseños de generadores híbridos existentes y considerando que deberá ser implementado bajo el suelo, se escogió un generador en arco. Este tipo de generadores están divididos en dos partes:

- Parte piezoeléctrica: Situada en la parte superior del generador, es la parte con forma de arco. Está formada por un film protector, dos electrodos y el material piezoeléctrico. La función del film es reforzar el generador permitir que el material piezoeléctrico pueda volver a su forma inicial tras ser deformado.
- Parte triboeléctrica: Más simple que la anterior, está formada por una lámina de material triboeléctrico y un electrodo inferior.

Al pisar el suelo, este comunicará el movimiento al generador, presionando la parte superior en forma de arco y deformándola (generando energía eléctrica) hasta quedar plana y en contacto con la parte inferior. Al entrar en contacto con el material triboeléctrico se producirá también electricidad y el electrodo inferior de la parte PE se compartirá con la parte TE. Ambos generadores se utilizan simultáneamente para obtener altos voltajes debidos al material TE y las altas corrientes producidas por el material PE.



Ilustración 13 Distribución de capas

El modelo en arco descrito hasta ahora será posteriormente analizado mediante elementos finitos y modificado para conseguir un generador que aproveche de la mejor manera posible la energía de las pisadas.

6.2 ANÁLISIS

Debido al alto coste de los materiales necesarios para construir el generador, se optó por realizar un modelo virtual con ayuda del software ANSYS. El modelo (Ilustración 14) fue diseñado en SoidWorks y exportado a ANSYS. Está formado por un polímero esponjoso y flexible que forma el suelo, el generador y una base que da cabida al generador y soporta el suelo. El material piezoeléctrico elegido es el PVDF, la placa protectora es de nylon 66 y para ahorrar espacio, la base está hecha de acero. Para realizar las simulaciones se utilizaron elementos laminares para simplificar el proceso y porque de esta manera se adaptarían mejor a las grandes deformaciones a las que estarían sometidos.

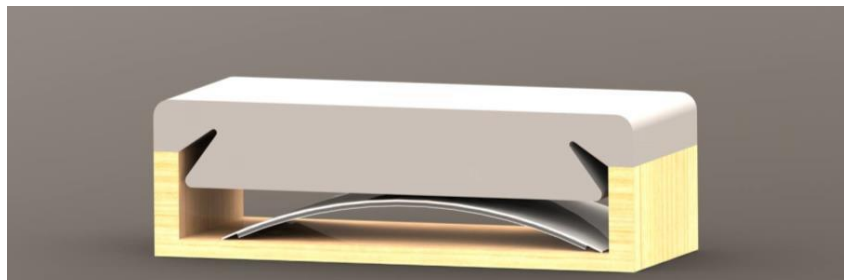


Ilustración 14 Generador en arco

Como se puede apreciar en la Ilustración 15, solo se están usando tres elementos; esto se debe a que los electrodos son despreciables si se considera su rigidez puesto que el grosor es menor a un milímetro. La parte triboeléctrica del generador no se simulará puesto que no depende de deformaciones o fuerzas, sino del contacto con el electrodo y este valor es considerado constante. Por lo tanto, los elementos que se consideran son la base, el film protector y el material piezoeléctrico. De esta manera se supone que el contacto entre la parte del suelo y el generador es perfecto.

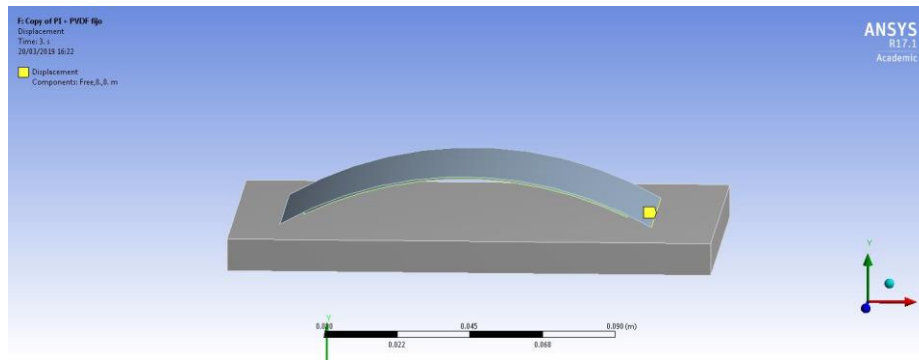


Ilustración 15 Modelo de ANSYS

La fuerza ejercida sobre la parte superior del generador es el peso de una persona de 70kg en la luna. Para extraer los valores del voltaje y corriente obtenidos por el material piezoeléctrico se utilizan las constantes piezoeléctricas del material se relacionan con los datos del estrés obtenidos en ANSYS. El cálculo se basa

$$\begin{bmatrix} D_1 \\ D_2 \\ D_3 \end{bmatrix} = \begin{bmatrix} d_{11} & d_{12} & d_{13} & d_{14} & d_{15} & d_{16} \\ d_{21} & d_{22} & d_{23} & d_{24} & d_{25} & d_{26} \\ d_{31} & d_{32} & d_{33} & d_{34} & d_{35} & d_{36} \end{bmatrix} \begin{bmatrix} \sigma_1 \\ \sigma_2 \\ \sigma_3 \\ \sigma_4 \\ \sigma_5 \\ \sigma_6 \end{bmatrix} + \begin{bmatrix} e_{11}^\sigma & e_{12}^\sigma & e_{13}^\sigma \\ e_{21}^\sigma & e_{22}^\sigma & e_{23}^\sigma \\ e_{31}^\sigma & e_{32}^\sigma & e_{33}^\sigma \end{bmatrix} \begin{bmatrix} E_1 \\ E_2 \\ E_3 \end{bmatrix} .$$

Ilustración 16 Ecuaciones piezoeléctricas

en las ecuaciones piezoeléctricas en forma matricial que se aplican a diferentes momentos para obtener de esta forma el voltaje presente en el generador a lo largo de la deformación del material.

A demás de obtener la progresión del voltaje con la deformación, se debe calcular también con respecto al tiempo, ya que los materiales piezoeléctricos se asemejan a condensadores y la corriente obtenida se calcula con la variación del voltaje con respecto del tiempo. Por lo tanto, se consideró que la velocidad de la deformación igual a la velocidad de un paso en la luna, 5 km/h. Los datos obtenidos se muestran en la Ilustración 17.

t	z	sub-step	V	I	W
0	0	0	0	0	0
0,001036	0,00145	17	688,9901	2,238E-05	0,007710603
0,001957	0,00274	23	525,565	-5,97E-06	-0,00156814
0,003093	0,00433	30	2069,304	4,573E-05	0,047318539
0,004114	0,00576	31	2718,664	2,139E-05	0,029076053
0,005193	0,00727	32	3009,011	9,057E-06	0,013626824
0,007	0,0098	33	4050,814	1,94E-05	0,039286014
0,008	0,0112	34	4189,119	4,653E-06	0,009746771
0,009071	0,0127	37	4342,955	4,831E-06	0,010490163
0,0103	0,01442	last	4464,737	3,335E-06	0,007445271

Ilustración 17 Resultados generador en arco

6.3 MODIFICACIÓN

Tras analizar los resultados obtenidos en el generador en arco, se decide diseñar un nuevo generador basado solamente en materiales piezoeléctricos. El motivo de esta elección son los altos voltajes conseguidos y que hacen prescindible el uso de los materiales triboeléctricos. La base y el suelo son muy parecidos al modelo en arco, pero en este caso el generador está formado por una lámina de PVDF pegada a una lámina de acero en voladizo (Ilustración 19).

Puesto que la corriente depende de la variación del voltaje, el nuevo generador se basa en las vibraciones; de esta manera las variaciones de voltajes serán mayores y el generador podría continuar funcionando durante más tiempo. El principio que rige su funcionamiento se muestra en la Ilustración 18.

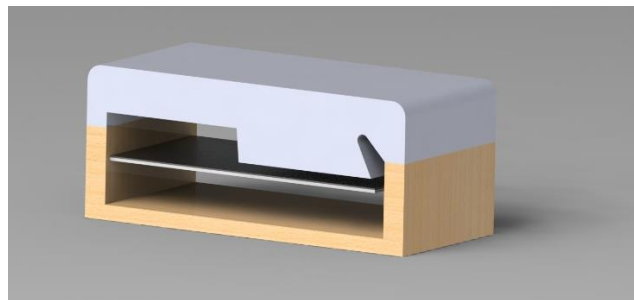


Ilustración 18 Principio de funcionamiento, generador en voladizo

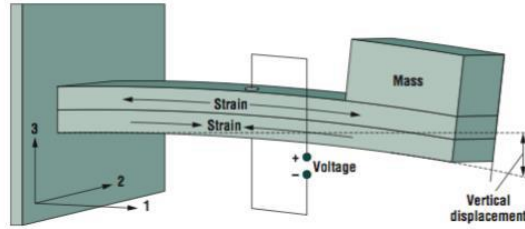


Ilustración 19 Generador en voladizo

Utilizando el mismo procedimiento que con el anterior modelo y unas dimensiones muy similares, los datos obtenidos fueron los siguientes.

t	z	V	I	W
0	-0,624	114,75	0	0
0,000251	-0,605	111,31	4,60873E-05	0,00513
0,000503	-0,549	100,98	0,0001381	0,013945
0,000765	-0,455	83,77	0,000220798	0,018496
0,001004	-0,343	49,35	0,000485228	0,023946
0,001253	-0,206	37,87	0,00015497	0,005869
0,001489	-0,065	12,05	0,000368759	0,004444
0,001594	0	0	0,000382736	0
0,0017	0,065	-12,05	0,000382736	-0,00461
0,001936	0,206	-37,87	0,000368759	-0,01396
0,002185	0,343	-49,35	0,00015497	-0,00765
0,002424	0,455	-83,77	0,000485228	-0,04065
0,002686	0,549	-100,98	0,000220798	-0,0223
0,002938	0,605	-111,31	0,0001381	-0,01537
0,003189	0,624	-114,75	4,60873E-05	-0,00529

Ilustración 20 Resultados generador en voladizo

Como se puede comprobar, aunque el generador en voladizo obtenga menores voltajes debido a una menor deformación, la potencia obtenida es similar a la del generador en arco. Puesto que necesita menores deformaciones, es más sencillo que se produzcan y su funcionamiento perdurará durante segundos hasta que el sistema deje de vibrar, convirtiéndolo en la mejor opción para ser implementada bajo el suelo de la base lunar. Este generador podría a su vez colocarse en otras zonas como puertas o en las camas, aprovechando pequeños movimientos para generar electricidad.

7 ALMACENAMIENTO

Para plantear la solución al almacenamiento de energía en la base lunar se recurrió previamente a leer distintos documentos de la NASA que trataban el mismo tema. De estos documentos se extrajo la conclusión de que todos ellos apuntaban a que el medio de almacenamiento de energía óptimo en las circunstancias esperadas en la luna son las celdas de combustible de hidrógeno.

El desarrollo y fabricación de esta tecnología es relativamente complicado y sobre todo tedioso ya que depende a parte de otros factores como son la obtención y almacenamiento de hidrógeno y oxígeno. Por lo tanto, este grupo se centró en diseñar y desarrollar un electrolizador mientras que otro grupo de la universidad se dedicaría a fabricar las celdas de hidrógeno.

7.1 DISEÑO

Los electrolizadores pueden tener diversas formas y diseños, pudiendo estar formados por dos partes o una. Los electrolizadores con sólo una parte poseen una de las cámaras dentro de la otra (normalmente cilindros concéntricos), mientras que los consistentes en dos partes se basan en dos cilindros diferenciados (uno para cada cámara) y comunicados por un puente. Condicionado por la dificultad en el diseño y construcción, se eligió un modelo de dos partes. El diseño final de una de las cámaras se muestra en la ilustración 21.

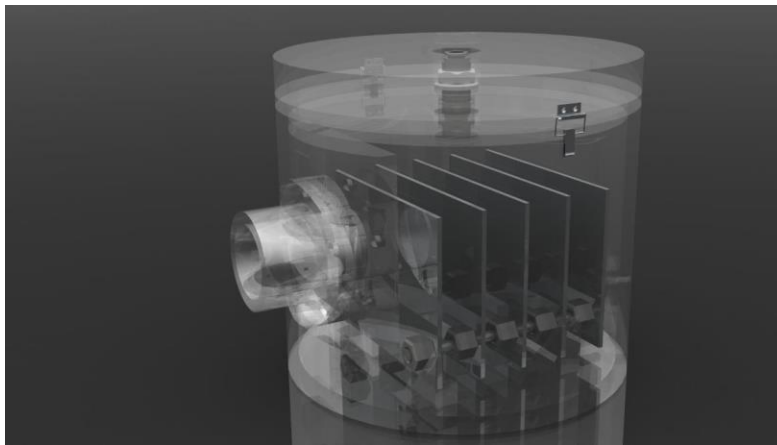


Ilustración 21 Electrolizador

El motivo por el que el electrolizador se construyó usando materiales transparentes es el de permitir ver los procesos que se van desarrollando en su interior cuando está en funcionamiento. El prototipo está formado principalmente por dos cilindros principales y otros dos más pequeño para comunicarlos. Estos cilindros poseen imanes para facilitar su unión y garantizar el sellado. Cada uno de los cilindros grandes posee una base instalada mediante adhesivos y una tapa superior asegurada mediante tuercas y formada por distintas capas para evitar fugas. En el interior de cada cilindro hay una barilla metálica con rosca que atraviesa cinco electrodos de acero inoxidable asegurados en la barilla mediante una tuerca en cada cara.

8 CONCLUSIÓN

La aportación hecha al proyecto global y los resultados obtenidos han sido muy satisfactorios, completando con éxito todas las necesidades y requerimientos que exigía el programa. Observando todos los diseños y el trabajo desempeñado por los alumnos (en colaboración con otro grupo de estudiantes) se observa que en conjunto forman un sistema de potencia completo y viable. De esta forma, el trabajo desempeñado en este proyecto sienta las bases para que las siguientes generaciones de este programa puedan mejorar lo conseguido hasta ahora y obtener prototipos completamente funcionales.